4. SEA ICE AND SNOW MEASUREMENTS

Polona Itkin[1], Dmitry Divine[2], Marcus Huntemann[3], Matthias Jaggi[4], Arttu Jutila[3], Christian Katlein[3], Daniela Krampe[3], Vishnu Nandan[5], Ian Raphael[6], Martin Schnebeeli[4], Igor Sheikin[7], Egor Shimanschuk[7], Julienne Stroeve[5], Rasmus Tage Tonboe[8], Marcel Nicolaus[3] (not on board), Don Perovich[6] (not onboard), Gunnar Spreen[9] (not on board)

[1]UiT/CSU
[2]NPI
[3]AWI
[4]WSL/SLF
[5]U Manitoba
[6]Dartmouth
[7]AARI
[8]DMI
[9]U Bremen

Grant-No. AWI_PS122_00

A comprehensive summary of the sea ice and snow measurements during all 5 cruise legs can be found in Nicolaus et al., 2022.

Sea and snow measurements on leg 2 were done by a team of 14 scientists. In addition to the 13 members that were planned for this work, Ian Raphael volunteered to extend his stay from leg 1.

The team followed closely the suggested weekly plan. There were several occasions with bad weather, when the working time on the ice was reduced. In such cases the team allocated time to office work (mainly data work and maintenance). In total there was one day, when the team took a complete rest day on a leg that was extended by about two weeks due to delayed crew exchange.

The observational plan foresaw the creation of a approx. 700 m diameter safe zone, maintained by the logistic team. However, this zone never realized, so about 30% of the scientific work force of the team was spent on bear-guarding. It was also impossible to work for more than 3 h outside for many of the tasks (e.g. snowpit) with the clothing provided by AWI-logistics. Taking these circumstances into account we are very satisfied with the achievements of our team.

References

Nicolaus, M, Perovich, DK, Spreen, G, Granskog, MA, Albedyll, LV, Angelopoulos, M, Anhaus, P, Arndt, S, Belter, HJ, Bessonov, V, Birnbaum, G, Brauchle, J, Calmer, R, Cardellach, E, Cheng, B, Clemens-Sewall, D, Dadic, R, Damm, E, de Boer, G, Demir, O, Dethloff, K, Divine, DV, Fong, AA, Fons, S, Frey, MM, Fuchs, N, Gabarró, C, Gerland, S, Goessling, HF, Gradinger, R, Haapala, J, Haas, C, Hamilton, J, Hannula, H-R, Hendricks, S, Herber, A, Heuzé, C, Hoppmann, M, Høyland, KV, Huntemann, M, Hutchings, JK, Hwang, B, Itkin, P, Jacobi, H-W, Jaggi, M, Jutila, A, Kaleschke, L, Katlein, C, Kolabutin, N, Krampe, D, Kristensen, SS, Krumpen, T, Kurtz, N, Lampert, A, Lange, BA, Lei, R, Light, B, Linhardt, F, Liston, GE, Loose, B, Macfarlane, AR, Mahmud, M, Matero, IO, Maus, S, Morgenstern, A, Naderpour, R, Nandan, V, Niubom, A, Oggier, M, Oppelt, N, Pätzold, F, Perron, C, Petrovsky, T, Pirazzini, R, Polashenski, C, Rabe, B, Raphael, IA, Regnery, J, Rex, M, Ricker, R, Riemann-Campe, K, Rinke, A, Rohde, J, Salganik, E, Scharien, RK, Schiller, M, Schneebeli, M, Semmling, M, Shimanchuk, E, Shupe, MD, Smith, MM, Smolyanitsky, V, Sokolov, V, Stanton, T, Stroeve, J, Thielke, L, Timofeeva, A, Tonboe, RT, Tavri, A, Tsamados, M, Wagner, DN, Watkins, D, Webster, M, Wendisch, M. 2022. Overview of the MOSAiC expedition: Snow and sea ice. *Elementa: Science of the Anthropocene* 10(1). DOI: https://doi.org/10.1525/elementa.2021.000046

4.1 Ice Coring

Dmitry Divine[1], Giulia Castellani[2], Patric Pereira[2], Egor Shimanchuk[3], Lasse M. Olsen[4], Adela Dumitrascu[5], Mats Granskog[1] (not onboard), Sonke Maus[6] (not onboard)

[1]NPI
[2]AWI
[3]AARI
[4]UiB
[5]SE.GU
[6]NTNU

4.1.1 Objectives

Within the general coring objectives (8.2 Objectives for General Coring.), the ICE team is responsible for the ice physics properties analysis (salinity, density, microstructure).

4.1.2 Work at sea

Following the general coring event, upon return from the field, the CT samples are centrifuged, and imaged using x-ray computed tomography (CT) technique within half a week. Cores for archive, backup, plastic and the upper part of the CT core are sealed in plastic sleeves and stored at -20 °C. Density is measured at -15 °C by densitometry in paraffin in the freezer lab using a Kern EMB-V scale. Salinity is then measured on the melted samples with a conductivity probe Voltcraft LWT-100 from team ICE. Within 1 day, melted salinity samples are bottled for future isotope measurement, before bulk salinity is measured on the remaining water using a conductivity probe YSI 30 from team ECO. According to the initial work plan, texture cores were supposed to be processed into horizontal and vertical thin sections onboard. However, due to time constraints, this was implemented for only once core from FYI Dark Site during leg 2.

4.1.3 Preliminary (expected) Results

The ice coring team of leg2 successfully continued the coring activity on remote FYI and SYI sites (“Dark Site SYI” and “Dark Site FYI”). Due to a lacking capacity of EGO and BGC groups in sample processing as well as substantial logistical resources required for maintaining activity on two sites in parallel, both sites were scheduled for visiting alternatively every second week.

The ice dynamics however led to inaccessibility of the SYI site twice throughout the leg2 time period. As a result, of eight weekly coring session the FYI coring site was visited five times, whereas the SYI coring site three times. Additional SALO18 core on SYI site was collected during the first visit on 23.12.2019 after finishing the work on FYI coring site. Table **4.5.1** presents a list of cross-disciplinary coring sessions together with a total number of recovered ice cores.

Table **4.1.1** Cross-disciplinary ice coring events on Darks Sites SYI and FYI during leg 2

Date/Activity week	Site	N recovered cores	DSHIP entry
23.12.2019 / 2_17	FYI; SYI	24; 1	20191223-PS122-2_17-3
06.01.2020 / 2_19	FYI	20	20200106-PS122-2_19-7
13.01.2020 / 2_20	SYI	20	20200113-PS122-2_20-5
20.01.2020 / 2_21	FYI	22	20200120-PS122-2_21-13
27.01.2020 / 2_22	SYI	20	20200127-PS122-2_22-7
03.02.2020 / 2_23	FYI	23	20200203-PS122-2_23-3

10.02.2020 / 2_24	FYI	11	20200210-PS122-2_24-8
17.02.2020 / 2_25	SYI	18	20200217-PS122-2_25-15

Basic ice core physical parameters resemble results obtained during leg1 with correction for the observed ice growth on both study sites.

At the FYI coring site, over 7 weeks between the first (23.12.2010) and last (17.02.2010), the ice grew from 80 to 115-120 cm (depending on the actual core). This makes a total FYI ice growth since the last leg 1 visit in 02.12.2019 of 45-50 cm over 9 weeks. The ice structure is similar to the one observed during leg 1 with an upper layer of granular ice, about 15 to 20 cm thick, with columnar growth underneath.

At the SYI coring site, ice consists of a refrozen melt pond about 70 cm to 120 cm thick with a new ice that formed below. With a 20 cm ice columnar ice growth at the bottom estimated during leg 1, preliminary analysis of the retrieved SYI salinity profiles suggest another 40 cm growth during 8 weeks of leg 2 period between the first and last visits to the site. The longest core recovered on SYI site on 17.02.2020 (activity week 25) was found to be around 190 cm long.

Figure **4.1.1** below shows the evolution of the salinity, temperature and density profiles acquired for leveled and undeformed sea-ice for the FYI and SYI site.

Growing FYI displays the expected C-shape salinity profiles, while the salinity value for SYI profiles mirrors the observed stratigraphy (Figure 4.5.1, bottom) with low salinity values (0-1 ppt) in the upper 70 cm, and high salinity values at the bottom (5 ppt) increase in the lowermost section (8 ppt). High variability in the thickness of remnant ice before the onset of ice growth season is apparent from Figure 4.5.1 with the longest recovered SYI core exhibiting about 1.2 m of ice with the low salinity values.

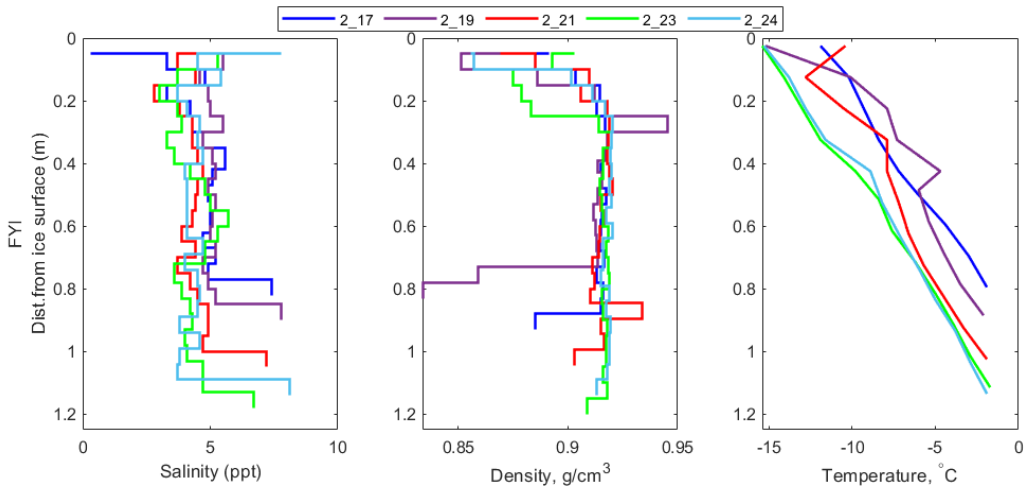

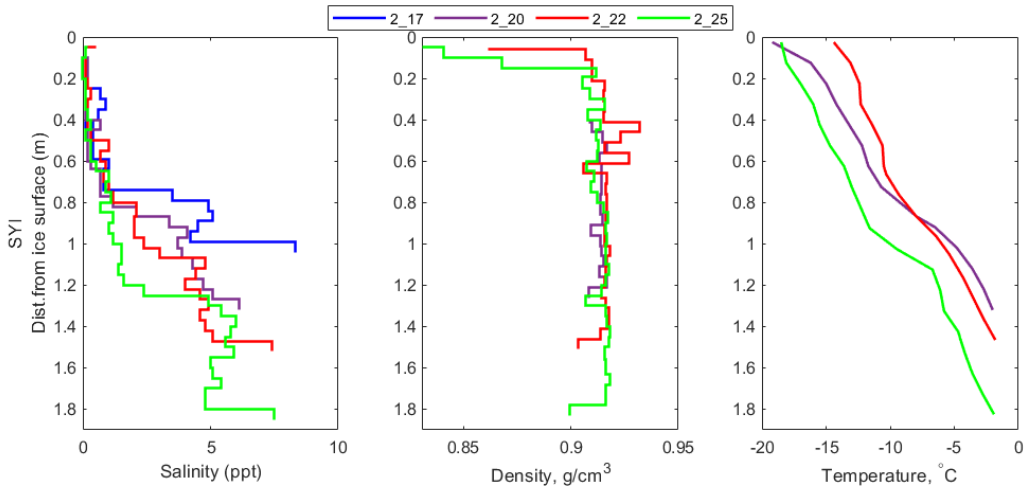

Figure **4.1.1** – Evolution of salinity, temperature and density profiles over a 7-week (8-week) period of observations during leg 2 for first-year ice (second-year ice). Legend shows DSHIP activity week corresponding to a particular coring session.

In the framework of the MOSAiC HAVOC project coring on the ridge of the Sea Ice Ridge Observatory (SIRO) - 'Fort Ridge', was conducted twice during the activity weeks 2_19 and 2_21. The goal for the coring was to identify the age/type of ice the SIRO ridge is formed of and obtain key ecological parameters crucial for the study of ridges as harbors of life. During activity week 2_18 the level ice on the flanks of SIRO ridge was also cored and analyzed in order to establish its physical characteristics and establish the baseline values for major ECO parameters relevant for ridge studies. Preliminary results demonstrate that SIRO ridge has formed of mainly FYI with some inclusions of remnant ice. Figure **4.1.2** below shows the respective salinity profile of the two of three cores recovered from the ridge. Other details of work at ridges is described in **Section 4.9**.

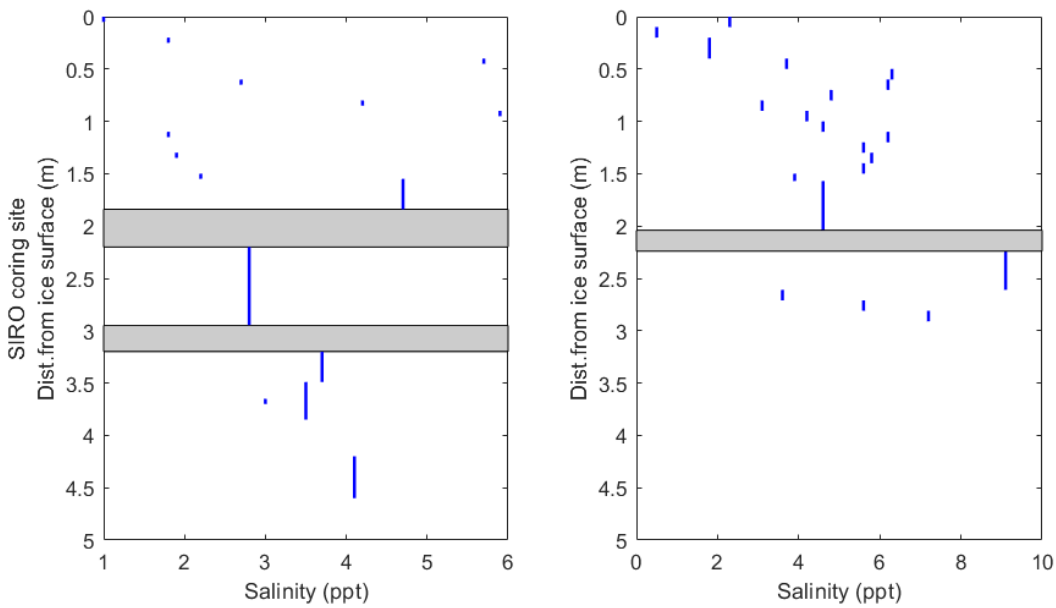

Figure **4.1.2** - Salinity profiles of 2 cores recovered from the SIRO ridge during activity weeks 2_19 (left panel) and 2_21 (right panel). Note that during the week 2_21 coring the bottom of the ice was not reached. Grey shading denotes the locations of water filled voids inside the ridge.

4.1.4 Data Management

All data are handled, documented, archived and published following the MOSAiC data policy (see APPENDIX). All data related to a coring event are collocated on the MCS within the folder

of the device operation corresponding to the deployment of the corer Kovacs Mark II, 9cm. A scanned copy of the field note and laboratory book will be uploaded. The exhaustive list includes:

Primary data for each ICE and ECO core transcribes into a spreadsheet (section depths, ice thickness, ice draft, weather, date and time…)

Salinity and density measured on board within 2-5 days of the coring

Vertical and horizontal thin sections photographed on board during the leg (single core only from leg 2).

Tomographic imagery of two bottom-most 5-cm ice sections of microCT cores together with 0-5 cm and 15-20 cm depth sections of density cores are available on the MCS within a separate subfolder contained in the folder of the X-ray tomographer Scanco90.

4.2 Snow

Martin Schneebeli[1], Matthias Jaggi[1], Daniela Krampe[3], Ian Raphael[2], Polona Itkin[4], Stefanie Arndt[3] (not onboard), Ruzica Dadic[1,6] (not onboard), Glen Liston[5] (not onboard), Amy Macfarlane[1] (not onboard), Chris Polashenski[2] (not onboard)

[1]WSL/SLF

[2]Dartmouth

[3]AWI

[4]UiT/CSU

[5]CU

[6]VUW (Victoria University, Wellington, New Zealand)

4.2.1 Objectives

The overarching goal of the snow measurements is to characterize this spatially variable and changeable porous medium in view of improved snow models and in support of all MOSAiC inquiries from ATMOS, BGC and ECO and Remote Sensing. We refer for details to the report of leg 1.

4.2.2 Work at sea

Conducted snow work can be structured in the following sub-tasks:

1. Snow pits and snow transects
2. Snow sampling
3. Terrestrial Laser Scanning (TLS) of the snow surface
4. Snow lab work

We restructured the MCS-raw data into a more readable and correctable tables, rewrote and revised the SOPs and field tasks. All field note books were scanned and stored on MCS. To improve consistency of the field measurements, protocol sheets for all snow pit - types were created. Detailed documentation is all in the MCS/workspace/snowpits directory.

Snow pits

We continued with the snow sampling sites and -pits established during leg 1. The sites are shown in Figure 4.1.1. In addition we started new measurements at Fort Ridge (A-pit and transect), and a specific snow property transect in Snow1 (Snow1-Transect). The snowpit at the remote sensing site had to be relocated due to instrument relocation (named during leg 2 $RS3$).

We measured no B-pits, as a B-pit was not substantially faster under the logistical constraints . So most snow pits were measured bi-weekly. The spatial variability within a meter-scale was not too large. However, on a 5 m scale substantial changes were observed, although the surface and relief appeared homogenous. This was one reason to extend the A-pit with 5 additional SMP measurements on each side parallel to the profile with a 1 m-spacing (cf. Logbook A+ snowpit, 2020-02-12).

We did not use and suggest to skip the following measurements in A-pits: SLF-density and wetness sensor (salinity affects readings), InfraSnow (prototype not available). We suggest that snow wetness (once the snow is melting) is estimated traditionally.

Snow surface SSA is spatially very heterogenous, and NIR-box surface imaging may result in more consistent and relevant results than point sampling. Micro-CT sample in the 48 mm diameter sample holder with a resolution of 16 µm of the surface layer were sufficient to resolve most snow types, except very new snow.

In total, 67 main snow pit events were realized. Of these events 37 were A-pits and 18 C-pits. On the remote sensing transect 40 pits were measured. These pits included SnowMicroPen (SMP), Snow-Water Equivalent (SWE), snow temperature at the surface and the snow-ice interface, salinity, and BC-surface samples.

The newly created transects were of the C-type pit, the eight Snow1-transect measurements include each between 60-80 SMP measurements, the 8 Fort Ridge transects each 24 SMP measurement. In addition, event specific C-type measurements were realized during the lead event, and on the FYI-runway transect, as well as in the EMIRAD-footprint.

All events are documented in DSHIP as device "snowpit".

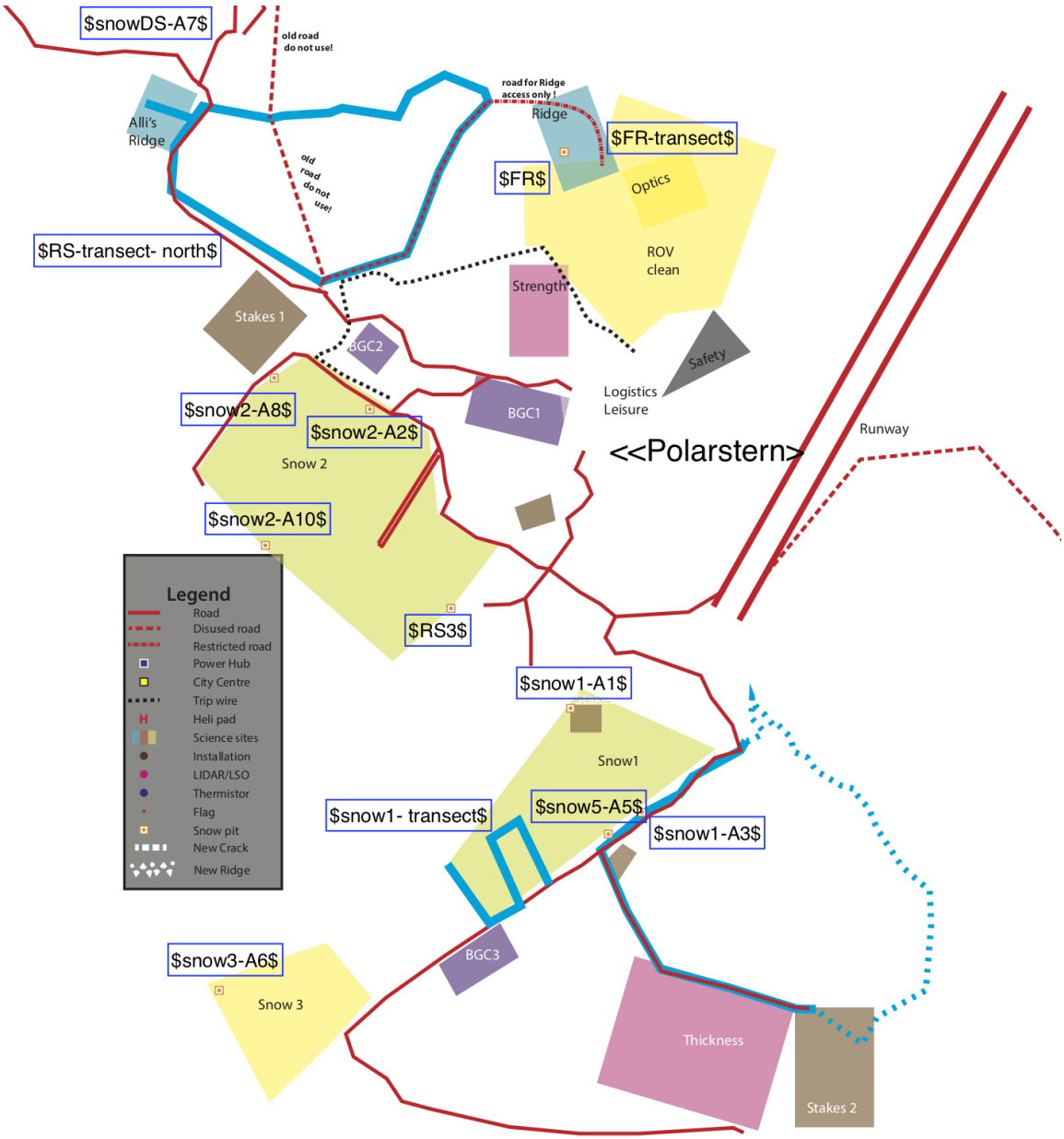

Fig. 4.1.1: Floe map (state 2020-02-25) with locations of the maintained snow pits and snow transect. All sites have a uniquely defined location identifier that can be used to extract site location without the transient GPS-coordinates.

The remote sensing transect North was re-flagged at the end of leg 2, and a detailed SOP is available in the Logbook (Fig. 4.1.2).

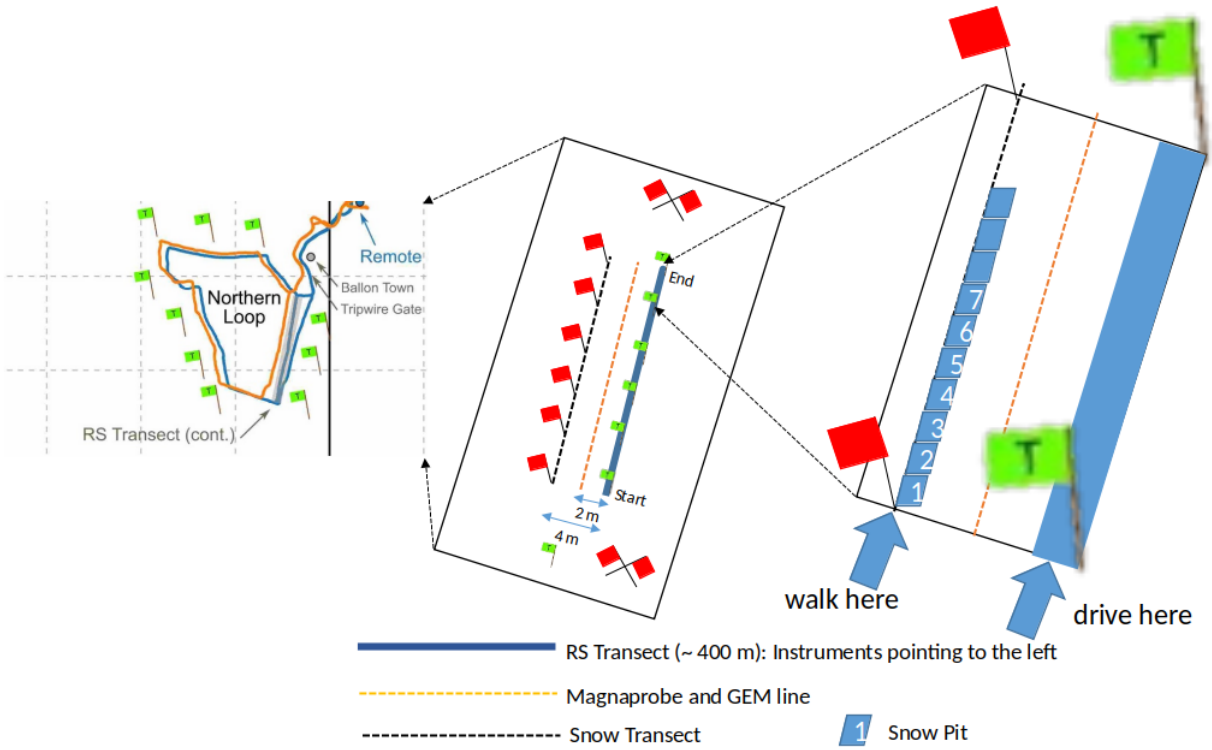

Fig. 4.1.2: Setup and use of the RS-transect after re-flagging. The last snowpit locations is marked by a bamboo stick. This setup improves co-locating remote sensing measurements with the snowpit measurements, and avoids measurements in disturbed area.

Chemical and physical Snow Sampling

Each week, at an A-Pit location, we conducted several sampling tasks. Due to time, personnel and weather/ice constraints we could not fulfil all requests as listed. Furthermore, some sampling was requested only for e.g. 2-weekly, monthly ore only after snowfall. However, we took snow samples for the following purposes (in parentheses: sample coordinator)

- Black Carbon (AWI/Daniela Krampe)
- Halocarbons (BGC/Katarina Abrahamsson)
- Ice Nucleating Particles (INPs) (Jessie Creamean)
- Iodide (Uni Grenoble/Hans-Werner Jacobi)
- Major Ions and Water Isotopes (AWI Glaciology/Maria Hörhold)
- Major Ions, Bromide, INPs, 34S (SO4), Salinity, S-Isotopes (BAS/Markus Frey)
- Major Organic Compounds (PSI/Julia Schmale)
- Microplastics (AWI/SLF)
- Salinity (ICE)
- Sugars (TROPOS)
- micro-CT samples

Beryllium sampling (contact: David Kadko) has mostly conducted by the BGC group by Mark Stevens. Water isotopes were sampled by Ellen Damm (BGC), in addition frozen snow samples for diverse analysis were taken. The melted snow for salinity measurements was also used for d18O samples (NPI).

The rocket traps at MET city for BAS/Markus Frey were mainly checked by the MET group and samples put into the BAS-storage boxes.

Samples which not already had a label have been labelled (or pre-labelled) by us and for each sample the corresponding snow pit and location within the profile has been documented.

After sampling, the bags and vials were stored either in the -20°C freezer in the F-Deck or in the -20° AWI sea ice physics freezer at the bow - either in prepared boxes by the institutes who conducted the sampling requests or in one of the WSL skufa boxes.

Terrestrial LiDAR Surveys (TLS)

This snow-related task is described separatelly in Section 4.3.

Snow Lab

We processed samples cored in the field for micro-CT analysis (about 9 m total snow profile length). For details on the coring procedure we refer to the SOP snow coring and the SOP / cheat sheet for the micro-CT 90 on MCS. The partial reconstruction of images could be corrected by an update of the micro-CT software, and missing stacks in the ISQ-images of leg 1 and 2 were all post-processed.

No samples were cast in the field or in the laboratory, as there was no time left for this time-consuming task, and due to the excellent performance of the micro-CT

The computing and control computers for the micro-CT were moved to Trockenlabor 3 in mid-January 2020 to improve working conditions.

All data are stored on MCS semi-automatically in the correct folder using a script.

We measured snow salinity in Trockenlabor 3, with the salinity sensor provided by U. Fairbanks, the same as used for the physical measurements of the ice cores. As the 20 ml sample vials for d18O from NPI are more suitable for the melted volumes of snow from salinity measurements, we used these since 2020-xx-xx.

4.2.3 Preliminary (expected) results

We could measure all core parameters for snow regularly, at least weekly.

All key devices for measurements of snow on the ground such as SMP, NIR worked without major issues even at experienced temperatures down to -40°C. Additional heating was necessary for the NIR-box. Thermometers, balances, Garmin GPS and cameras had to be kept above about -25°C to be usable before handling at these very low temperature. The reliable measurement of snow density with the density cutter was difficult or impossible in the thin and very fragile depth hoar layers, and in the very hard (knife) recrystallized "snow-ice" depth hoar.

Because snow accumulation maps could not be calculated at the time of leg 2, the implementation of the stratigraphy-based directed sampling was not possible. To cover spatial variability we created snow specific transects in a relatively open field (Snow1-transect) and across a ridge (Fort Ridge transect). In addition, we added to the A-profiles a 10 m transect.

4.2.4 Data management

All data are handled, documented, archived and published following the MOSAiC data policy (see APPENDIX). All device operations were logged in DSHIP and all sensor raw data files are stored in platforms/packice/snowpit section of MCS. Final geophysical parameters will be made available via the workspace section of MCS and archived in the PANGAEA data repository according the MOSAiC data policy.

***Tab. 4.1.1**: Overview on all measured parameters for the three defined snow pit types during leg 2.*

Type A: Parent snow pit Every other week	Type B: Quick snow pit	Type C: SnowMicroPen

Complete sampling of physical and chemical properties	"quick pit"	Super quick measurements
• 10 m - SMP transect, 1 m spacting All Type B measurements • Pictures for snow surface and ice surface roughness (SfM) • MicroCT sampling • Density (volumetric) • Temperature • Salinity • Snow samples for chemical and physical properties	• SnowMicroPen (SMP) • NIR photography (SSA) • SWE (ETH tube) • Site overview photos	C: • SnowMicroPen (SMP) C: Remote Sensing Transect • SMP • SWE • Salinity • Snow surface and bottom temperature

Tab. 4.1.2: Overview for device operations of snowpits
NOT AVAILABLE

4.3 TERRESTRIAL LASER SCANNING

Ian Raphael[1], Polona Itkin[2], Matthias Jaggi[3], Martin Schneebeli[3], Chris Polashenski[1,4] (not on board), Don Perovich[1] (not on board), David Clemens-Sewall[1] (not on board)

[1]Dartmouth College
[2]UiT/CSU
[3]SLF
[4]USACE/CRREL

4.3.1. Objectives

Terrestrial Lidar Scanning (TLS) was used to measure weekly surface evolution in the CO at cm precision. We are primarily interested in snow accumulation and redistribution, especially during high wind events and storms. The data will also be used to evaluate surface roughness, document ice dynamics.

4.3.2 Work at sea

At the end of Leg 1, two scan fields had been established: Snow1 and Snow2. They covered roughly the corresponding original snow plots and surrounding measurement sites (e.g. ROV, MET, RS in Snow1, Stakes1 in Snow2). Snow1 was established first, and has been the longest and most consistently measured site. It is also the primary snow measurement/sampling plot, and intersects the Snow1 Transect and the Southern Transect Loop. It has experienced continuous major deformation at its margins, minor deformation in the center, and extensive shearing/translation relative to the ship and other ice pans. Snow2 was a secondary measurement site, with fewer measurements made in the same area (they include some A-type snow pits, flux-chamber measurements). After deformation during the November shearing event, we were able to link Snow1 and Snow2 into one large scan field, which we called

Snow1b. We did not scan the linked field frequently, since the CO was reconfigured shortly following its establishment. At the beginning of Leg 2 the ROV site was moved to the Northwest corner of the LOG area due to continued deformation at the original site. This meant that the Northern Transect, new ROV site, and the new ridge observatory were all in roughly the same area. We established a new scan field covering primarily those sites, which we called ROV. We discontinued regular measurement at Snow2 to prioritize scanning at the ROV scan field. **Fig. 4.3.1** illustrates the location of our reference reflectors and scan positions within the CO.

We planned to scan the Snow1 and ROV fields weekly during Leg 2. We were able to scan Snow1 eight times, and ROV six times. We additionally scanned Snow2 at the beginning and end of Leg 2, and in flex time, at Egon's Corner, an event site sampled during the late January floe deformation. We conducted TLS much more consistently and successfully during Leg 2 than Leg 1, primarily due to stable ice conditions and a flexible scanning schedule. Moderate winds (>7m/s) and accompanying drifting snow sometimes prevented scanning. We accommodated this by shifting TLS to calmer days whenever flex time and scheduling allowed.

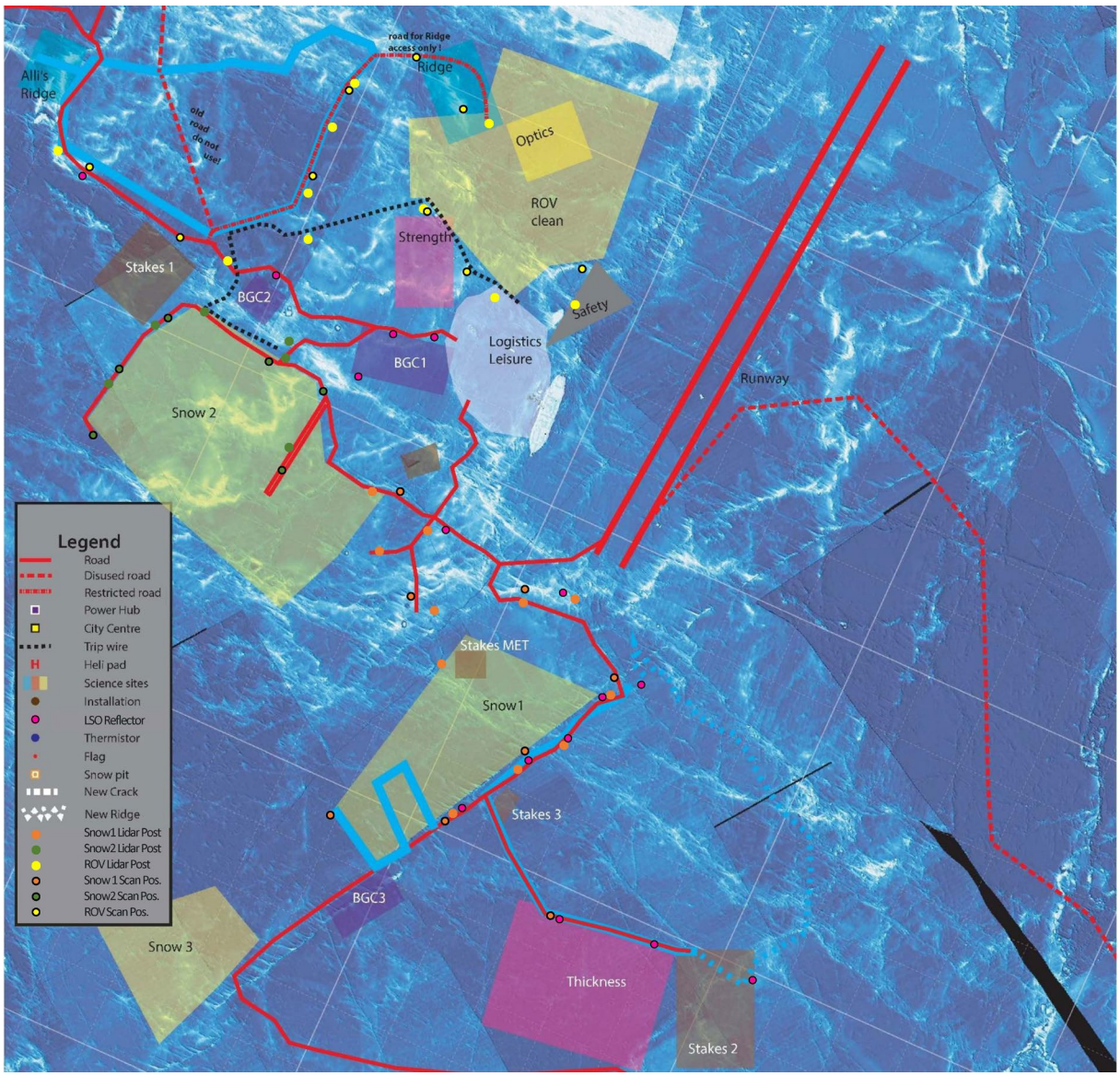

Fig. 4.3.1: Map of Lidar Fields and Features as of 2020.02.28 against an ALS basemap of the CO. Each Scan Position indicates a single scan in its respective scan field. All of the scans in a scan field are registered together using the fixed reference points (Lidar Posts) to create an integrated scan product. The footprint of a single scan is a ~350m radius around the scan position. Each of the scan fields covers ~1300x800m.

4.3.3 Preliminary (expected) results

After wind events, we consistently observed massive snow accumulation in drift aprons behind ridges and other snow traps, e.g. transition rubble and upwind lead-edges. These sometimes evolved or disappeared between wind events, while some features (usually a set of features formed during a single event) sintered and remained unchanged throughout the campaign. We were able to distinguish at least four sets of depositional features associated with four distinct wind events in the final scans from Leg 2. Erosional features on flat, scoured pans generally did not evolve, and snow height in those areas similarly remained unchanged.

4.3.4 Data management

All data are handled, documented, archived and published following the MOSAiC data policy (see APPENDIX). All device operations were logged in the AWI sensorweb portal and all sensor raw data files are stored in platform section of MCS. Final geophysical parameters will be made available via the workspace section of MCS and archived in the PANGAEA data repository according the MOSAiC data policy.

4.4 AIRBORNE SEA-ICE SURVEYS (HELI)

A. Jutila[1], M. Huntemann[1,2], G. Birnbaum[1] (not on board), N. Fuchs[1] (not on board), S. Hendricks[1] (not on board), G. Spreen[2] (not on board)

[1]DE.AWI

[2]DE.UNI-Bremen

4.4.1 Objectives

The objectives for the helicopter-borne sea-ice surveys during PS122.2 have been closely described in the Helicopter Observational Plan, the Expedition Programme and the cruise report for PS122.1, so we only provide a short summary here:

1. Overarching MOSAiC Science Plan question we mainly contribute to: How does sea ice formation, drift, deformation and melting couple to atmospheric, oceanic and ecosystem processes?
2. What is the spatial distribution of snow freeboard and surface roughness within the DN? How does these parameters evolve with the thermodynamic and dynamic forcing in polar winter?
3. What is the surface roughness downwind of the meteorological installation at the CO?
4. How does the sea ice surface deform in response to storms and other dynamic forcing?
5. How does snow precipitation and snow redistribution by wind change the snow freeboard distribution?
6. How does the surface temperature of different ice classes (classified by their snow freeboard) change during the polar winter?
7. How does the lead distribution (open water and thin ice leads) change through polar winter?

4.4.2 Work at sea

4.4.2.1 Sensors

Due to polar night conditions, we operated only the airborne laser scanner (ALS) and the infrared camera (IR) during the entirety of PS122.2. For detailed description of the sensors, please refer to the previous cruise report PS122.1. The instrumentation in the helicopter D-HARK remained as it was at the end of PS122.1, except a new, exactly similar laser scanner (S/N s9997784) replaced the faulty sensor (S/N s9999057).

4.4.2.2 Mission types

Two main mission types determined during PS122.1 remained

1. Grid surveys following a mow-the-lawn or a double-loop pattern centered over the CO with a target side-length of 5 km.
2. Surveys using the three L-sites in the DN as waypoints including the sides and the spokes (connection between *Polarstern* and L-Site) within three triangles.

Figure 4.4.1 shows two exemplary flight lines of the aforementioned mission types at the end of PS122.2. In addition, we commenced also a third mission type

3. Event surveys, including smaller grid surveys over the three L-sites and a lead, which was the target of intense sampling by all MOSAiC teams.

We carried out almost all surveys according to the standard flight parameters of 1000 ft altitude above ground level and 90 kn ground speed. During one of the event surveys, we successfully attempted 500 ft and 60 kn to enable even higher-resolution gridded product.

Between 24 December 2019 and 17 February 2020, we accomplished the predefined aim for weekly small and large-scale surveys and concluded 23 survey flights, out of which 11 were small-scale CO floe grid surveys, 6 were large-scale L-site surveys and 6 were event flights (**Table 4.4.1**).

4.4.3 Preliminary (expected) results

Airborne laser scanner

We continued the routine workflow and quick-view processing of the airborne laser scanner data during PS122.2. We were able to speed up the workflow by enabling parallel processing, therefore the processing the data all the way to the final level-4 gridded product regularly took less than 24 hours. The weekly CO floe grid survey's merged product was the basis and background for the annotated and constantly updated floe map of the CO, but served also as a tool for scouting suitable runway locations.

During PS122.2, the airborne laser scanner surveys of the CO coincided several times with the surveys of the ice underside using the multibeam sonar of the ROV (see chapter 4.5 Sea ice and water properties based on ROV surveys), enabling us to take a full three-dimensional look at the sea ice (**Figure 4.4.2**).

Infrared camera

We operated the infrared camera on each flight together with the airborne laser scanner. Since the observation angles are similar, the coverage of the grid flights and the L-site is the same for airborne laser scanner and the infrared camera. With the acquisition rate of 4 per second, the overlap of individual images is ensured for the purpose of mosaicing in order to create a geographic map. We established a processing chain based on a set of merging and resampling routines developed at the University of Bremen, for the processing of the CO grid based maps running on the virtual machine of the team ICE. As input, the INS data from the laser scanner, as well as the location data from the FloeNavi base stations for the given day is required for orientation and drift correction, respectively. We created a preliminary SOP for the processing of the data and handed it over to leg3. Processing time for the infrared combined map is five minutes to one hour depending on the number of images (requested accuracy) on the team ICE's virtual machine. **Figure 4.4.3** shows an example of a merged mosaic from the infrared camera data.

4.4.4 Data management

All data are handled, documented, archived and published following the MOSAiC data policy (see APPENDIX). All device operations were logged in the AWI sensorweb portal and all sensor raw data files are stored in platform section of MCS. Final geophysical parameters will be made available via the workspace section of MCS and archived in the PANGAEA data repository according the MOSAiC data policy. Data from the data acquisition system of Polar Research Aircraft (DMS) can be accessed after registration at https://dship.awi.de/exportdisplay/.

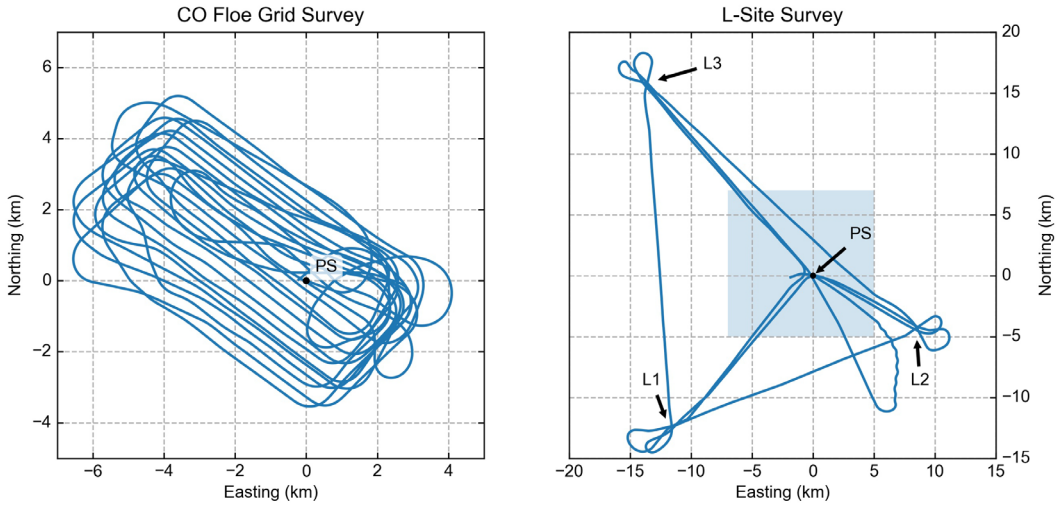

Fig. 4.4.1: *Example flight lines for the two main sea-ice mission types at the end of PS122.2: (left) Grid survey of the CO close to Polarstern and (right) L-Site survey in the DN. The light blue square in right panel marks the spatial extent of the panel on the left. Note that the scale of the axes differ between the panels, but in both the origin (0,0) is set to Polarstern at the start of the survey.*

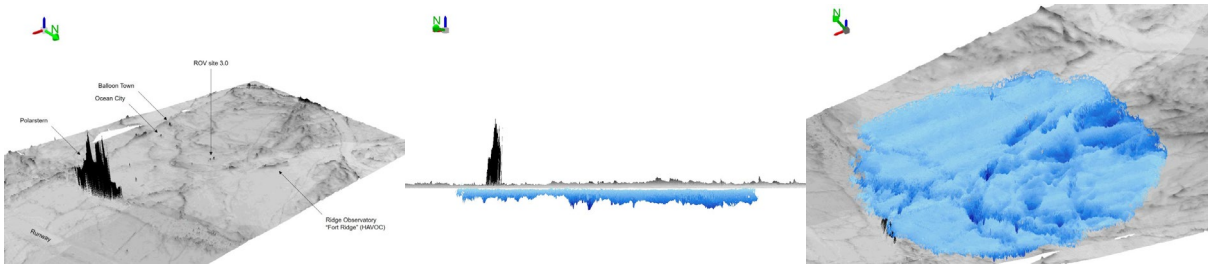

Fig. 4.4.2: *Screenshots from an animation where the ALS data (greyscale) has been laid over the ROV multibeam data (blue colors) to demonstrate the now acquired capability to fully describe the sea-ice system in all three dimensions.*

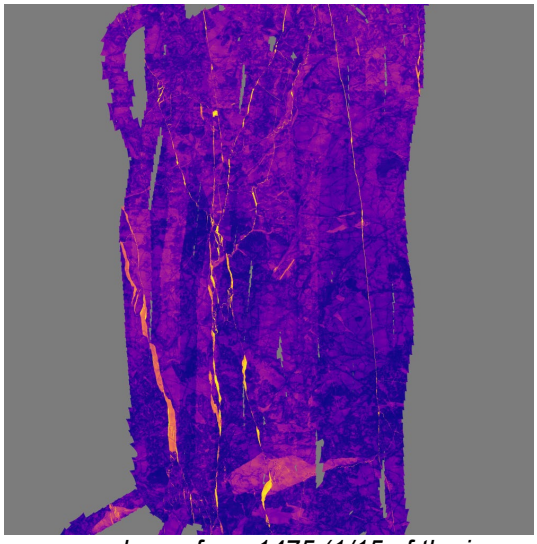

Fig. 4.8.3: *Infrared camera merged map from 1475 (1/15 of the images is used) individual images. Central observatory on 2020-01-07, North is up, Polarstern is in the center, entire patch is 10x10 km.*

Tab. 4.8.1: *Overview of all helicopter sea ice surveys from Polarstern during PS122/2. (TO and LDG designate take-off and landing times in UTC respectively)*

Flight ID	Device Operation	TO	LDG	Aircraft	Sensors	Mission Type
20191224_01	PS122-2_17-98	07:29	09:21	D-HARK	ALS, IR	CO Floe Grid Survey
20191225_01	PS122-2_17-99	14:05	15:44	D-HARK	ALS, IR	CO Floe Grid Survey
20191228_01	PS122-2_17-101	06:57	08:25	D-HARK	ALS, IR	CO Floe Grid Survey
20191230_01	PS122-2_18-7	07:59	09:37	D-HARK	ALS, IR	L-Site Survey
20200107_01	PS122-2_19-44	09:18	10:59	D-HARK	ALS, IR	CO Floe Grid Survey
20200107_02	PS122-2_19-45	12:05	13:54	D-HARK	ALS, IR	L-Site Survey
20200108_01	PS122-2_19-46	07:30	09:05	D-HARK	ALS, IR	L-Site Grid Survey
20200108_02	PS122-2_19-51	N/A	N/A	D-HARK	ALS, IR	L-Site Grid Survey
20200108_03	PS122-2_19-52	09:37	10:30	D-HARK	ALS, IR	L-Site Grid Survey
20200108_04	PS122-2_19-53	11:49	13:44	D-HARK	ALS, IR	L-Site Grid Survey
20200116_01	PS122-2_20-52	06:29	08:01	D-HARK	ALS, IR	CO Floe Grid Survey
20200116_02	PS122-2_20-53	09:14	10:53	D-HARK	ALS, IR	L-Site Survey
20200121_01	PS122-2_21-41	10:30	12:37	D-HARK	ALS, IR	CO Floe Grid Survey
20200123_01	PS122-2_21-77	10:11	12:16	D-HARK	ALS, IR	L-Site Survey
20200123_02	PS122-2_21-78	13:09	14:18	D-HARK	ALS, IR	Lead Event Grid Survey
20200125_01	PS122-2_21-122	12:42	14:26	D-HARK	ALS, IR	Lead Event Grid Survey
20200128_01	PS122-2_22-16	06:30	08:13	D-HARK	ALS, IR	CO Floe Grid Survey
20200202_01	PS122-2_22-97	06:32	07:19	D-HARK	ALS, IR	L-Site Survey
20200204_01	PS122-2_23-14	07:11	09:16	D-HARK	ALS, IR	CO Floe Grid Survey
20200209_01	PS122-2_23-109	11:01	12:41	D-HARK	ALS, IR	L-Site Survey
20200212_01	PS122-2_24-31	08:46	10:36	D-HARK	ALS, IR	CO Floe Grid Survey
20200217_01	PS122-2_25-7	06:45	08:23	D-HARK	ALS, IR	L-Site Survey
20200217_02	PS122-2_25-8	08:57	10:53	D-HARK	ALS, IR	CO Floe Grid Survey

4.7 Sea ice and water properties based on ROV surveys

Christian Katlein[1], Daniela Krampe[1], Arttu Jutila[1], Giulia Castellani[1], Lasse Olsen[2], Dmitry Divine[3], Julienne Stroeve[4]

[1] AWI
[2] Uni Bergen
[3] NPI
[4] UCL

Objectives:

Objectives for ROV based work during PS122.2 have been closely described in the ROV Observational Plan, the expedition booklet and the report for PS122.1, so we only provide a short summary here:

The remotely operated vehicle (ROV) is the main tool to investigate spatial variability of the ice-ocean interface and its physical and biological properties on the scale of the MOSAiC Central Observatory floe. This includes in particular:

1) High resolution studies of ice bottom topography and roughness achieved by extensive multibeam sonar surveys.
2) Vertical and lateral variability of physical (temperature, salinity) and bio-optical (fluorometry, UV and VIS absorbance spectroscopy) water properties
3) Zooplankton vertical distribution in the direct vicinity of the ice using the ROV towed net
4) General tasks of ice documentation (photography), as well as under-ice manipulation and installations (e.g. Sediment traps)
5) Preparations for work related on vertical and horizontal variability of sea ice optical properties and the underwater light field to be conducted once daylight returns.

Work at sea

During PS122.2 we were able to conduct a total of 18 successful ROV diving surveys covering more than 80 hours and a total transect length exceeding 106 km.

Data acquisition was only hampered by the fact, that during handover from PS122.1 on Dec 16 the ice floe cracked right underneath the ROV tent. Due to the limited general strength and stability of that location, we decided to move the ROV site to a more stable location which in addition provided better access to ice types of particular interest such as a ridge observatory and a large sheet of first year ice. The site was thus moved in a joined effort to its current location at the northern edge of the Central Observatory, providing ROV access also to Ocean City and the northern transect (Figure 4.7.1). This site choice proved to be a good selection, as the entire area around the previous location suffered from further deformation during entire Leg 2, whereas the new site remained completely stable allowing for uninterrupted fully functional twice-weekly ROV operations starting 30 Dec 2019 until and beyond the end of Leg 2. As the set-up of the ROV site with control cabin, tent and power line and LBL positioning system was nearly identical to previous setups e.g. during the AO18 Expedition of icebreaker Oden in 2018 we could build on these experiences to ensure continuous high quality data acquisition. During re-setup of the ROV site, we also added a 5cm thick isolation filling to the ROV control cabin which significantly improved pilot comfort during the up to 7 hours long surveys and avoided problems with the control electronics.

According to the dive plan agreed by the ROV task team, the dive time was split into the following tasks that were completed according to their respective schedules:

- A complete multibeam sonar survey of ice draft in 280m operation radius around the ROV hole at 20m depth using a line spacing of 25-30m was conducted at least every two weeks.
- Smaller high resolution studies of the ridge observatory using multibeam sonar and photographic documentation
- Weekly deployment of the towed ROVnet Zooplankton net at 10m depth and slightly below the ice interface
- Vertical profile of water properties in the upper 100m
- Photographic and video documentation of the ice-ocean interface, as well as installations at the various deployment sites.
- Deployment of a pair of sediment traps underneath the ridge observatory 160m away from the ROV hole (conducted three times) as well as a vertical reference trap mooring in the ROV hole (traps at 50m, 15m and 5m depth)
- Deployment and preparation for the optical transect work in spring including slinghook deployments underneath the ridge observatory as well as 300m of marked transect covering second and first year ice.

Further detailed records of all conducted ROV operations can be found in the D-Ship event log, as well as the MOSAiC Logbook and shall not be repeated here. Detailed information about the ROV system can be found in *Katlein et al., 2017* [1].

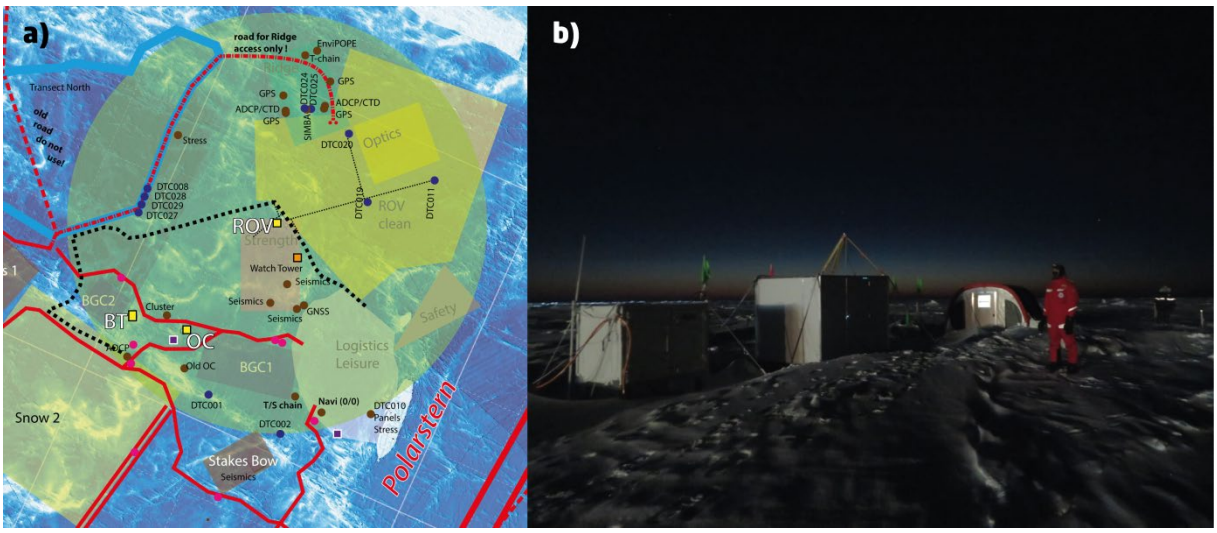

Fig 4.7.1: (a) Overview of the ROV operation radius at the new site (green shaded area), including optical transects, installations at the ridge observatory, the northern transect loop as well as Ocean City (OC). Map: Benjamin Rabe (b) ROV site in February 2020 with the appearance of the very first twilight. From left to right: Power distribution hub, ROV control cabin with surface reference sensor on the roof, ROV tent covering the deployment hole.

Preliminary results

Two factors guaranteed successful operation during the entirety of Leg 2:

- The well proven continuously improved system building on experiences from numerous previous expeditions with almost the same operational setup
- A site choice according to the MOSAiC ROV observational plan which assigns stability as the main criterion for site selection

As expected, the acoustic LBL positioning system with up to 6 transponders provided accurate vehicle position estimates in the entire operational range where acoustic shadowing of transponders was avoidable. Thanks to a real-time overlay of the floe map in the diving computer, it was relatively easy to reach targeted positions even at the maximum extent of the tether reach. For increased accuracy in the upcoming optical work and closer to the ice we deployed additional LBL transponders in the survey area. Calibrated transponder positions were measured using the terrestrial laser scanner to achieve the maximum accuracy. Absolute position accuracy depends on location and vehicle attitude ranging between 0.1-5m.

Visibility under water was mostly limited by ROV lighting due to the polar night, but measured Secchi-depths of more than 20m indicate extremely clear waters.

A main preliminary-result of the winter under-ice ROV work on PS122.2 is that ROVs allow us to see a great deal of things that would stay occluded to our eyes without them, clearly justifying the logistical challenges of ROV operations in the harsh Arctic winter:

- While hook and net catches did not reveal any specimen of fish underneath the MOSAiC floe, ROV camera footage can prove that in particularly the ridges provided shelter to a significant population of polar cod, even sustaining local predators – namely a ringed seal (Figure 4.7.3.d) underneath the ice.
- Similarly ROV footage revealed a significant and widespread cover of locally formed platelet ice at the ice bottom which has not been reported in the literature before.
- ROV based multibeam surveys provided us with a unique view of the underside of our study subject and photographic surveys improve the understanding of sea-ice as a non-plane-parallel medium.

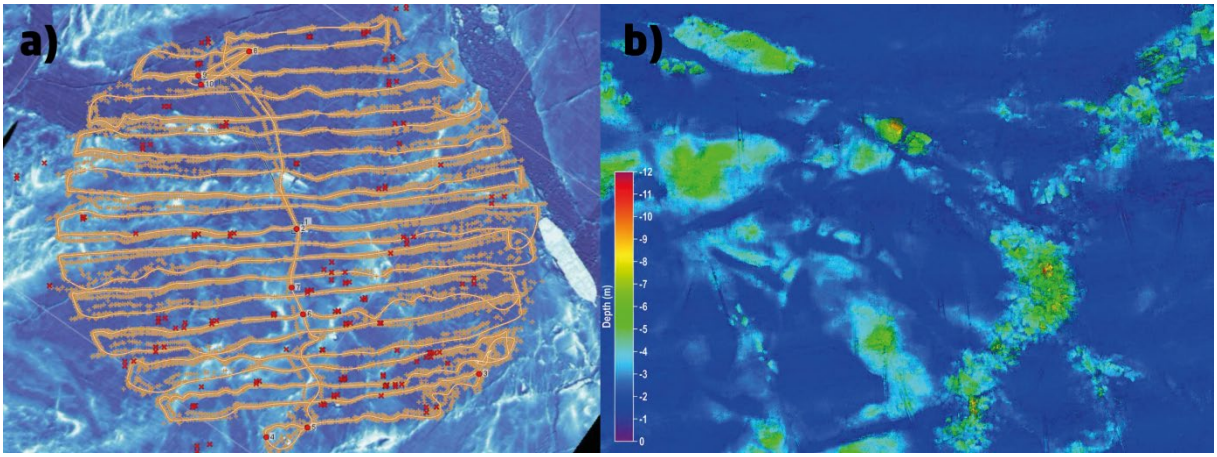

Fig 4.7.2: *Results from the multibeam dive on 21 Jan 2020: (a) Filtered dive track (orange line) overlaid above ALS surface elevation map (by A. Jutila) and accepted (orange + signs) and rejected LBL fixes (red x signs). Polarstern can be seen at the right edge of the image for scale. (b) Quicklook processing of the respective multibeam sonar derived ice draft map.*

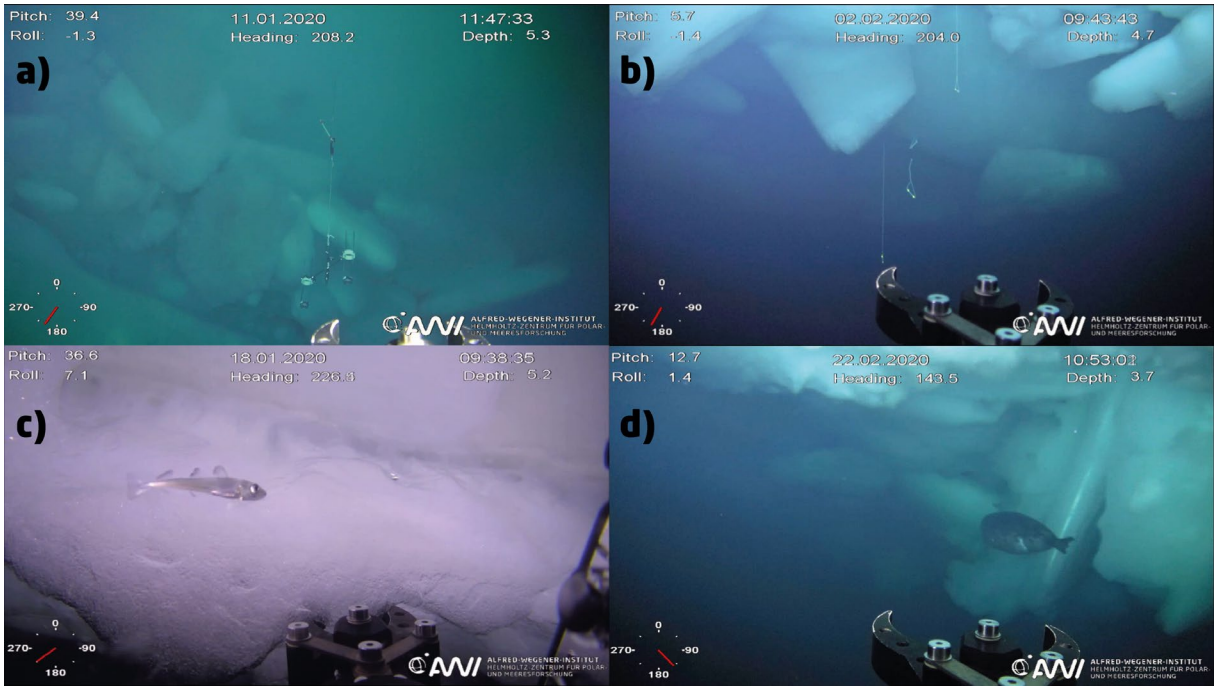

Fig 4.7.3: *(a) Sediment trap deployed in a slinghook underneath the ridge observatory (b) Slinghook transect prepared across the observatory ridge for optical sensor deployment during leg 3 (c) Polar Cod in a ridge cavity (d) A ringed seal diving along the instrumented ridge.*

Data management

All data are handled, documented, archived and published following the MOSAiC data policy (see APPENDIX). Data recorded on the dives on PS122.2 is stored in the Mosaic Central Storage in the “exdata” folder under the vehicle id “BEAST”. The dive data is stored in separate folders for each device operation (Appendix A). Easy data access has been described in the MOSAiC Logbook.

References

Katlein, C., M. Schiller, H. J. Belter, V. Coppolaro, D. Wenslandt, and M. Nicolaus (2017), A New Remotely Operated Sensor Platform for Interdisciplinary Observations under Sea Ice, *Frontiers in Marine Science*, *4*(281), doi:10.3389/fmars.2017.00281.

4.6 Stakes

Ian Raphael[1], Polona Itkin[2], Matthias Jaggi[3], Arttu Jutila[4], Christian Katlein[4], Mario Hoppmann[4] (not on board), Don Perovich[1] (not on board)

[1]Dartmouth
[2]UiT/CSU
[3]WLS/SLF
[4]AWI

4.6.1 Objectives

The point measurements of ice and snow mass balance (IMB) encompassing a full seasonal cycle from freeze-up to the melt are very rare. Likewise, despite large horizontal variability of the snow and ice cover such observations are rarely collected in clusters (more than one observation point). The MOSAiC IMB observations are designed in way to address these challenges. The IMB measurements are also necessary for interpretation of ice dynamics (Section 4.8), ROV (Section 4.6) and others, including cross-disciplinary topics (e.g. heat

fluxes between ocean-ice and atmosphere). The devices used for the point IMB observations on MOSAiC are shortly referred to as ‘stakes’ and include:

- IMB buoys
- digital thermistor chains (DTC)
- ablation stakes and hot wires

4.6.2 Work at sea

4.6.2.1 IMB buoys

On leg 2 we deployed 2 IMB buoys (type SIMBA): one at Fort Ridge and one at Alli’s Ridge. Both have long chains (6.1 and 7 m) and are deployed into the partially consolidated ridge body. More details on both deployments can be found in Section 4.9. The SIMBA’s deployed on leg 1 were all operating autonomously.

4.6.2.2 DTC network

On leg 2 we deployed 6 DTC stations. In total with the units surviving from leg 1, we had at the end of February 17 to 18 working and regularly visited DTC units. The unit RS009 was not working, but it was still accessible and possible to trouble-shoot. Also, there were 4 deployment-ready units left to be deployed at later stages of MOSAiC. The overview of all deployed units is given in **Table 4.6.1** and **Figure 4.61.**

Tab. 4.6.1 *List of DTC units that were operational during leg 2. The units deployed on leg 2 are shaded.*

MCS/DSHIP name	Unit name, map name	Deployment date	Deployment site	Status
DTC05_256	RS012	11/11/2019	Stakes 2 (close to S transect loop)	data downloaded on 7.1.2020 and 26.2.2020
DTC06_256	RS013	11/11/2019	Stakes 2 (close to S transect loop)	data downloaded on 7.1.2020 and 26.2.2020
DTC08_256	RS011	28/1/2020	ROV site at the Fort Ridge T1	clock re-set on 4.2.2020
DTC09_256	RS019	28/1/2020	ROV site at the Fort Ridge T3	data downloaded on 4.2.2020
DTC10_256	RS020	28.1.2020	ROV site at the Fort Ridge T2	data downloaded on 4.2.2020 and 27.2.2020
DTC11_416	RS001	5/11/2019	Old remote sensing site, on a ridge between ocean, city bow stakes and BGC1	data downloaded on 26.2.2020
DTC12_416	RS002	5/11/2019	Old remote sensing site, on a ridge between bow stakes and BGC1 (close to the road)	data downloaded on 21.1.2020 and 26.2.2020
DTC15_416	RS009	7/11/2019	Old(-er) remote sensing site, now 600 m south-eastwards of the ship	data downloaded on 7.1.2020, not working since
DTC16_416	RS010	7/11/2019	Stress panes close to ship	data downloaded on 7.1.2020 and 26.2.2020

MCS/DSHIP name	Unit name, map name	Deployment date	Deployment site	Status
DTC20_416	RS008	11/22/2019	Transect North (4 deployed together)	data downloaded on 4.2.2020 and 27.2.2020
DTC22_416	RS022	12/8/2019	Remote Sensing site 2	data downloaded on 7.1.2020 and 26.2.2020
DTC23_416	RS023	12/10/2019	Remote Sensing site 2	data downloaded on 7.1.2020 and 26.2.2020
DTC24_416	RS024	8/1/2020	Fort Ridge	data downloaded on 4.2.2020 and 27.2.2020
DTC25_416	RS025	8/1/2020	Fort Ridge	data downloaded on 4.2.2020 and 27.2.2020
DTC26_416	RS021	5/2/2020	Alli's Ridge	power connector broken during transport to deployment, fixed and clock reset on 7.2.2020
DTC31_512	RS027	11/22/2019	Transect North	data downloaded on 7.1.2019
DTC32_512	RS029	11/22/2019	Transect North	data downloaded on 7.1.2020
DTC33_512	RS028	11/22/2019	Transect North	data downloaded on 4.2.2020

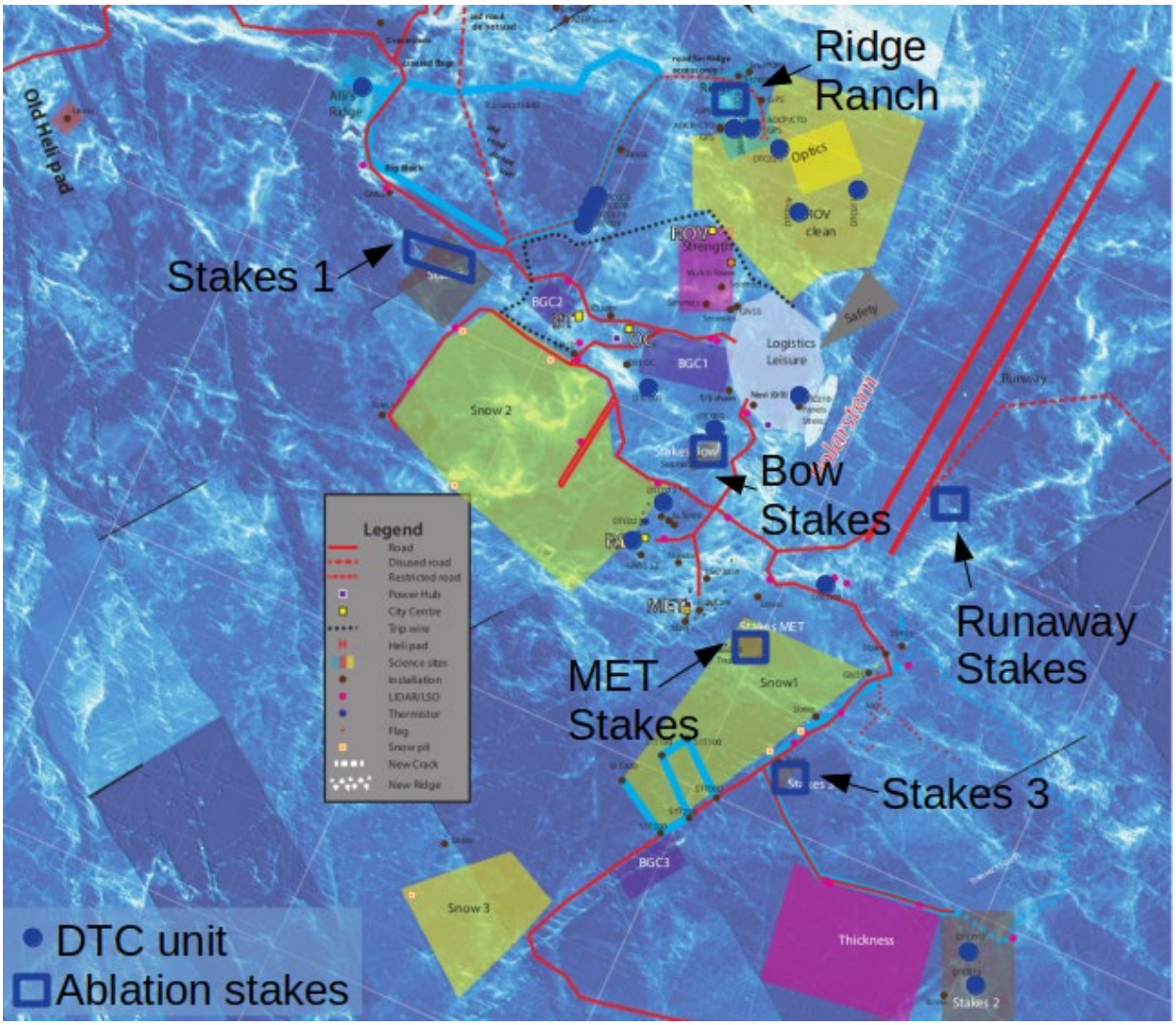

Fig 4.6.1*: Map of of CO with locations of DTC units and ablation stakes fields operational during leg 2. Fort Ridge Stakes are not marked on this map. They run accros the ridge just south of Ridge Ranch Stakes.*

4.6.2.3 Ablation Stakes and Hot Wires

The stakes sites are manual ice mass-balance measurement sites. A 'stake' is actually a paired ablation stake and hotwire thickness gauge. The ablation stake gives the position of the ice and snow surfaces, while the thickness gauge indicates the position of the ice bottom. From these measurements we can determine total change in ice and snow thickness. At each site, we installed several stakes as either transects or grids, measuring local spacial variability of ice thickness over time.

We installed eight stakes sites over Leg 1 and Leg 2 with a total of ~100 individual stakes in order to capture the floe's diverse ice types, as well as take advantage of collocated measurements, e.g. the Transect, ROV, and MET observations:

- Stakes 1
- Stakes 2
- Stakes 3
- ROV stakes
- Bow Stakes
- Ridge Stakes
- Ridge Ranch Stakes

- Runaway Stakes

Several stakes sites have been partially or fully destroyed by ice deformation. We have reestablished or moved some of the affected sites, and at the end of Leg 2 have six operational sites with a total of 77 individual stakes (**Fig. 4.6.1**). We installed an additional transect of seven ablation stakes without hot wire gauges across the ridge at Fort Ridge Observatory (see Section 4.9).

A portion of the hotwire crossbars have either frozen in due to too-short wires, or lost their crossbars entirely. The majority of the affected gauges are in sites installed during Leg 1. Approximately 70% of all hotwires are still intact. We hope that the frozen gauges will become operable again after melt-onset.

4.6.2.3.1 Stakes 1

Established on leg 1, Stakes 1 was originally installed on second year ice in a refrozen melt pond. During the mid-November shearing event, most of the original stakes were destroyed. The rest were translated several-hundred meters to the East, stopping directly in front of Polarstern. The transported stakes became the basis for Bow Stakes. None of the original stakes remain at Stakes 1. The site was reestablished late in leg 1, now on a refrozen lead which had formed right next to the original Stakes 1 location. The site continued to experience deformation after installation, and several of the reinstalled stakes were destroyed. There are now 7 operational stakes at the site, which span the marginal zone from SYI to FYI into the middle of the refrozen lead.

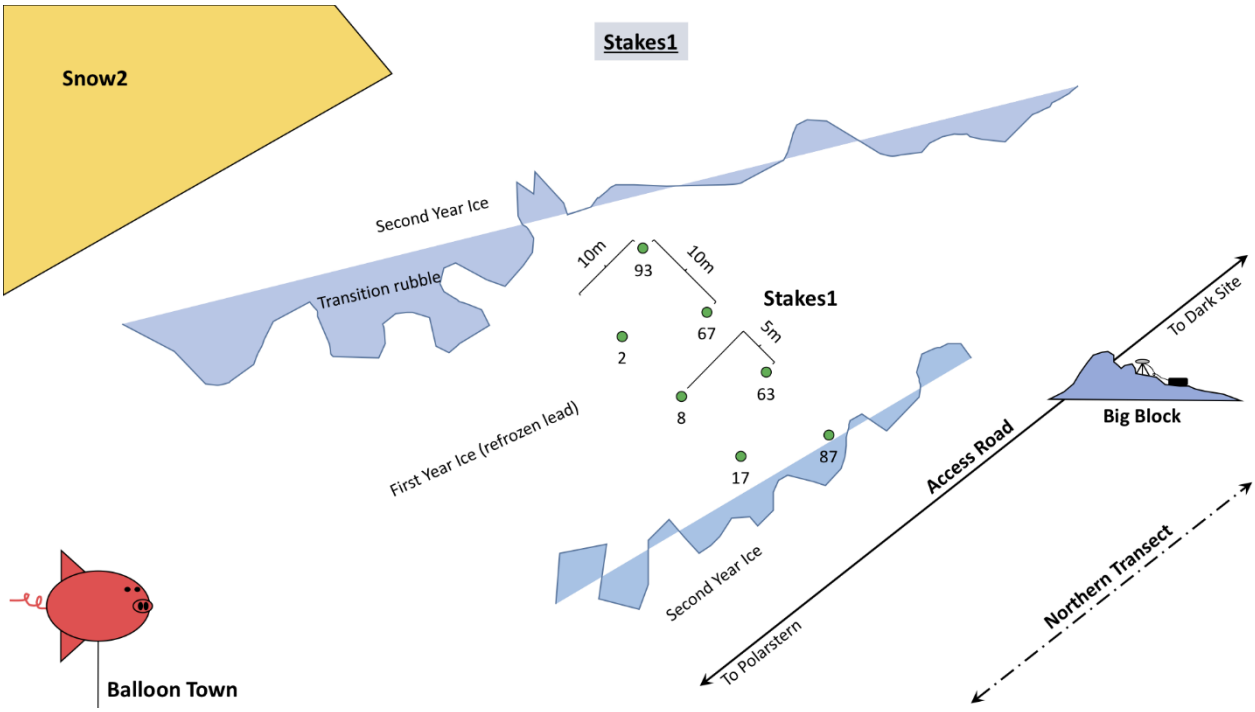

***Fig. 4.6.2.**: Diagram of Stakes1 and features as of 02.20.2020. The plot is located on a refrozen lead that formed during the mid-November shearing event. It crosses from second year ice/first year ice marginal rubble into the middle of the refrozen lead, with large snow dunes extending parallel to the stake lines into the lead. Not to scale.*

4.6.2.3.2 Stakes 2

Stakes 2 was established on leg 1 on SYI. It originally crossed a small ridge, and additionally covered level ice and ponded ice. This site was destroyed during the mid-November deformation event, and is no longer operational.

4.6.2.3.3 Stakes 3

Stakes 3 was established on leg 1 on SYI, and is collocated with the Southern Transect loop. The site crosses a ridge and otherwise densely covers level SYI. The site has 15 operational stakes.

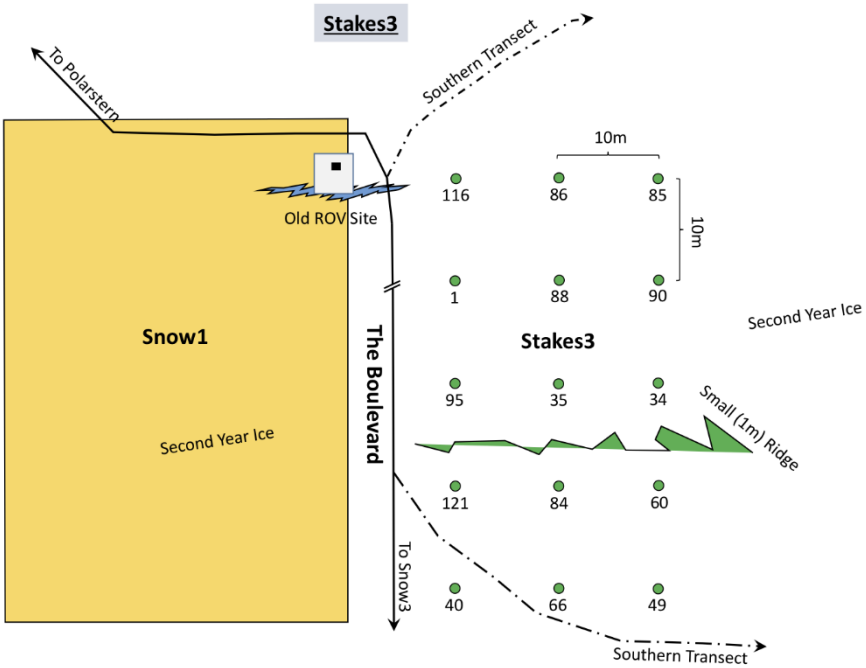

***Fig. 4.6.3**.: Diagram of Stakes3 and features as of 02.20.2020. The plot was installed crossing a small, young, unconsolidated ridge, and otherwise level second year ice. The southern transect loop crosses through the plot in the lower left corner. Not to scale.*

4.6.2.3.4 ROV Stakes

ROV Stakes was established on Leg 1 on SYI, and was intended to be collocated with the Southern Transect Loop and the ROV survey area. This site was destroyed during the mid-November deformation event, and is no longer operational.

4.6.2.3.5 Bow Stakes

Bow Stakes was established on Leg 1, incorporating the surviving stakes from Stakes1, which were transported several-hundred meters towards Polarstern during the mid-November deformation event. The site now transitions from a large ridge into a level SYI area and a ponded SYI area. The site is bordered by medium and large ridges. There are 17 operating stakes.

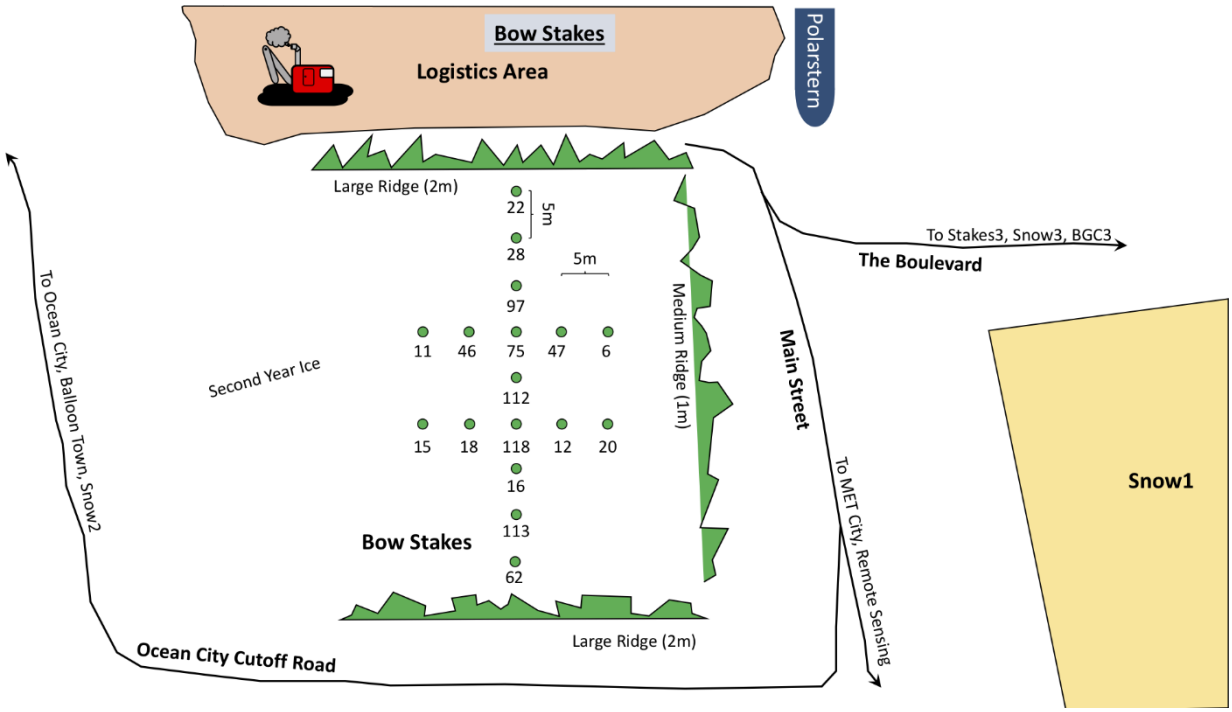

***Fig. 4.6.4**: Diagram of Bow stakes and relevant features as of 20.02.2020. This plot was initially installed on undeformed second year ice and refrozen melt pond. It was then mostly destroyed in mid-November, and reinstalled at the end of Leg1. Stakes 22, 28, and 97, 75, 112, and 118 are part of the original installation, while the rest were installed later. The site experience significant deformation, and is now bordered closely by medium-large ridges on three sides. Not to scale.*

4.6.2.3.6 MET Stakes

MET Stakes was originally installed late in leg 1, directly underneath the 30m flux mast, 'The Noodle.' It was destroyed during the late December deformation event, with none of the original stakes remaining. We reestablished the site at the beginning of leg 2. The site covers an area of level second year ice, crosses small ridge, and reaches the margin of a large, multiyear rubble field. The site is collocated with the MET observations as well as an A-type snowpit in Snow1. The site has 9 stakes.

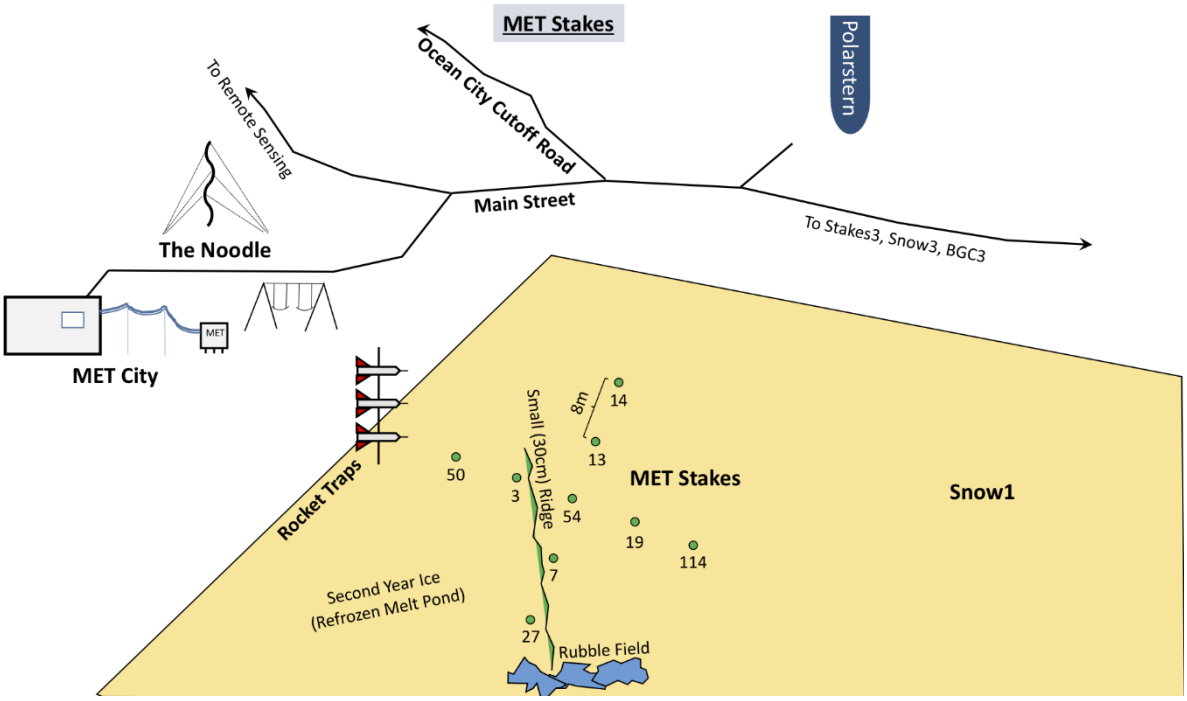

***Fig. 4.6.5**: Diagram of MET Stakes and relevant features as of 20.02.2020. The site was originally installed directly under the noodle, but was destroyed in mid-November. Both the MET Stakes site and the Noodle site have been moved. The MET Stakes sit in the Snow1 field and are directly next to an A-type snow pit, as well as the rocket traps. Not to scale.*

4.6.3.6 Ridge Ranch and Fort Ridge Stakes

Ridge Ranch was installed during leg 2, on level first year ice. The site is adjacent to Fort Ridge (the ridge observatory). In addition to the hotwire gauges, the Ridge Ranch plot has measuring tape on the underside of the stakes, which is readable by the ROV. The stakes are also within the regular ROV multibeam sonar survey area. There are 9 stakes at the site.

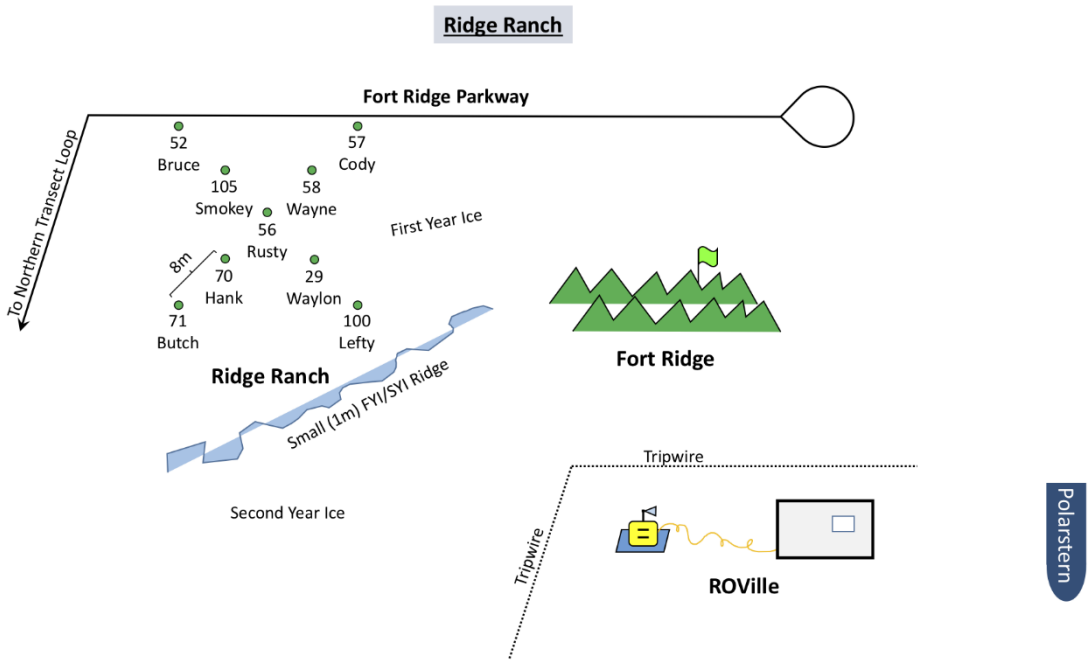

***Fig. 4.6.6**: Diagram of Ridge Ranch stakes and relevant features as of 20.02.2020. The site was installed on level first year ice and barely reaches a small ridge on its southwest (bottom right in diagram) corner. Not to scale.*

4.6.2.7 Runaway Stakes

Runaway Stakes was installed during leg 2, on first year ice. The site is directly next to the Polarsten runway. It covers level first year ice, crosses a small ridge, and on one end borders a larger ridge. There are 14 stakes at this site.

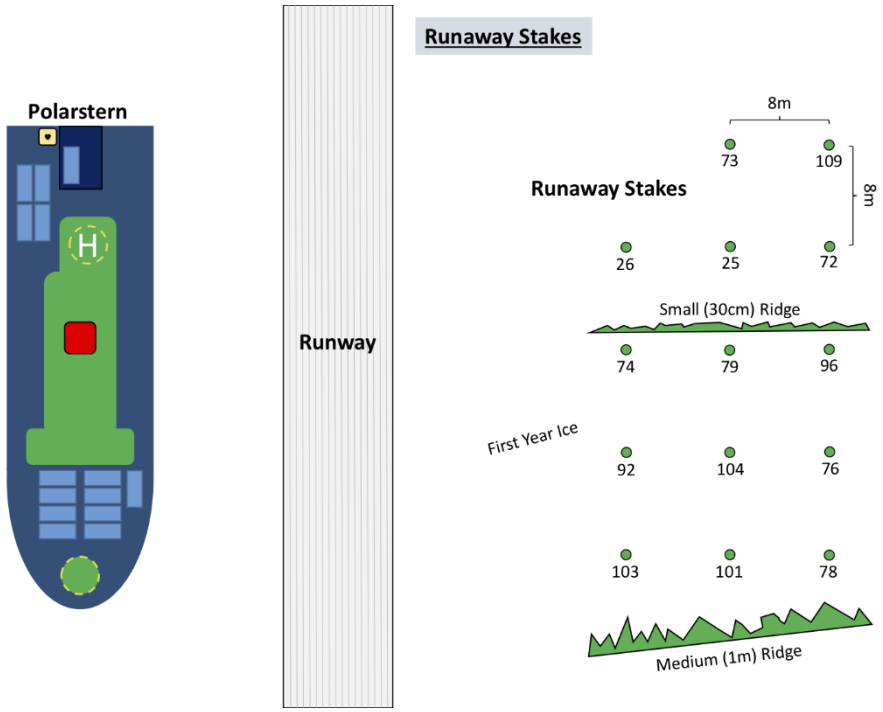

***Fig. 4.6.7**: Diagram of Runaway Stakes and relevant feature as of 20.02.2020. The site was installed on mostly level first year ice, crossing one small ridge and bordering a larger ridge on its southern (bottom in diagram) end. The runway has since been widened almost to the stakes plot, and has significantly changed the snow accumulation pattern on the left margin of the stakes. Not to scale.*

4.3.3. Preliminary (expected) results

The SIMBA data is transmitted to mainland over Iridium. The data from all operating DTCs was downloaded at least once per leg. On average we read the ablation stakes every 2 weeks.

4.6.4 Data management

All data are handled, documented, archived and published following the MOSAiC data policy (see APPENDIX). All device operations were logged in the AWI sensorweb portal and all sensor raw data files are stored in platform section of MCS.

4.7 Transect

Polona Itkin[1,2], Matthias Jaggi[3], Martin Schneebeli[3], Daniela Krampe[4], Marcus Huntemann[4], Julienne Stroeve[5], Vishnu Nandan[5], Rasmus Tage Tonboe[6], Ian Raphael[7] Arttu Jutila[4], Christian Katlein[4], Stefan Hendricks[4] (not on board), Glen Liston[2] (not on board), Gunnar Spreen[8] (not on board), Carolina Gabarró[9] (not on board)

[1]UiT, [2]CSU, [3]SLF, [4]AWI, [5]U Manitoba, [6]DMI, [7]Dartmouth
[8]U Bremen, [9]ICM-CSIC

4.7.1 Objectives

The snow depth and total sea ice thickness measurements in transects are the only direct spatially distributed snow and ice mass balance (IMB) measurements at MOSAiC. Such data has been collected in most of the Arctic expeditions since SHEBA and we need to secure the continuity of such measurements also at MOSAiC. The transect of sea ice and snow depth measurements cover the spatial variability on a kilometer scale (CO scale). In addition, the data on the snow structure and snow and ice microwave properties were collected at sub-

kilometer scale. The spatial diversity of these measurements will help establishing linkages between the snow and ice cover depth and structure and their passive and microwave properties.

Although a part of the full seasonal cycle observations, the post-freeze up, mid-winter phase measurements collected during leg 2 of MOSAiC will also help the specific process-related research topics such as:

- accumulation of snow in the ridges and leads
- re-distribution of snow by drifting snow events - especially with combination with data collected by the TLS (see Section 4.3) and ALS (see Section 4.4)
- ice growth/heat fluxes under spatially patchy snow cover
- consolidation of the ridges
- microwave properties of the leads and frost flowers

4.7.2 Work at sea

The work for the transect task was done on a regular weekly base, normally on Thursday afternoons. All the instruments involved in transect are listed in **Table 4.7.1**. The work was distributed between three separate groups, each advancing at its own pace:

- Collocated observations of sea-ice thickness and snow depth on sea ice along transect lines that are representative for ice conditions in the CO. Measurements were done using a combination of a broadband electromagnetic induction sensors (Geophex GEM-2) and a MagnaProbe. The GEM-2 was towed in a pulk and measuring the total (ice + snow) thickness, while the MagnaProbe measures snow depth by means of a sliding disc on a rod that stays on the top snow surface along a rod that is pushed down to the snow/ice interface.
- Towing of remote sensing sensors along segments of the transect lines with a snow-machine. The towed payload consisted of two sleds, one with two pairs of radar transmitter/receiver antennas for the polarimetric Ku and Ka-Band scatterometers in nadir configuration (see Section 4.10) and the side-ward looking Balamis ARIEL L-Band microwave radiometer (see Section 4.10) configured for measurements at a 45-degree incidence angle.
- Snow pits and collecting of snow samples in regular intervals along a designated short part of the transect line. The observations included measurements with a Snow Micro Penetrometer (SMP) to estimate the vertical profile of snow density and specific surface area (SSA), as well as in-situ observations of snow water equivalent and taking samples to measure snow salinity in the lab afterwards.

The leg 2 ICE team continued the regular sampling at the transect lines established in the form of two main loops on different ice types. The loops were named for the original location in the CO.

1. Northern loop: located on thick and deformed remnant ice. This loop includes a 200-m-long snow structure transect.
2. Southern loop: located in an area of undeformed remnant ice, which however, was dominated by a large fraction of melted through and now refrozen melt ponds with thin ice (i.e. similar to first-year ice). This loop experienced significant deformation in the mid-November shear event.

The location of the two loops is illustrated in **Figure 4.7.1**. Observations were also made on the connecting roads between the two loops.

On leg 2 the remote sensing transect was extended by including the entire northern transect loop and as much of the southern transect as feasible (i.e. over level ice = road access). The instruments were towed by ski-doo along both loops. While snow information is extremely

relevant of the interpretation of this data, snow pits were only collected along a short line at the northern transect loop. To supplement, weekly snow pits were done close to the RS site, where the RS instruments were deployed during the reaming time. On the morning of the transect, the RS instruments were mounted to their sleds and towed to the logistics area for the afternoon transect. Calibration of the Ariel Balamis was performed after the transect at the RS hut. GEM-2 and Magnaprobe were operated by a separate transect group and the GEM-2 was calibrated at the logistic area instead. In the beginning of February the KuKa radar broke down and it was not longer able to take part in the transect. After the first quality checks of Ariel Balamis data, we realized that the measurements are not satisfactory and also the use of this sensor was stopped. To make the best use of the time allocated to the transect task then we did several transect with alternative instruments: IR visual camera with surveillance camera (regular), see also sec 4.10. and SSMI (one time).

Apart of the regular transect we also performed a several other transects under tasks such as 'Snow pits', 'Ridges', 'Events' etc. Specifically these were:

- **Ridge Transects:** Transects of snow depth, ice thickness and snow structure were also done at Fort Ridge and Alli's Ridge. The locations of of these transects are described in Section 4.9.
- Transect of Snow 1: This type of transect was established to monitor the development of the ice and snow cover in the Snow 1 snow pit sampling area. It is supplementing the regular TLS survey, but it is less weather limited (can be done at high winds). Instruments involved were: GEM-2, Magnaprobe, SMP and GPR. GPR broke in February as was no longer used.
- Long/event/special transect: This is a transect that was done occasionally and typically not repeated. Usually this is an event sampling that is part of the FLEX time. On leg 2 such transect were done towards L2 (approx 8 km), as part of the runway survey, several occasions of the transect on the FYI along the emergency runway, at the FYI and SYI coring locations at the Dark Site, transects along the lead etc.

In total there were 27 days with transect activities and 31 device operations for GEM-2 (a device that was most commonly used in transect). The availability of data in form of device operations is listed in the **Table 4.7.2**. The table includes some device operations that are listed in DSHIP as leg 3.

***Tab. 4.4.1**: Overview of sensors used on sea ice transect*

Sensor	Description	Device URN	Geophysical Parameter
GEM-2	Geophex GEM-2 Broadband Electromagnetic Induction Sensor	pack_ice:ice_ps:gem2-556	Total (sea ice + snow) thickness
MagnaProbe	GPS snow depth probe	pack_ice:ice_ps:magnaprobe-anja pack_ice:ice_ps:magnaprobe-bruce pack_ice:ice_ps:magnaprobe-kathrin	Snow depth on sea ice
KuKa Radar	Dual-Band KuKa scatterometer	pack_ice:ice_ps:kuka_radar	KuKa Band radar backscatter
Balamis	Balamis L-Band radiometer	pack_ice:ice_ps:BALAMIS_Rad	L-Band brightness temperature
SMP	Snow Micro Penetrometer	pack_ice:snowpit:SN_SMP49, pack_ice:snowpit:SN_SMP31	Snow density Specific Surface Area
SWE	Snow Water Equivalent Samples	pack_ice:snowpit:SN_SWE	Snow water equivalent
Snow Salinity	Snow Salinity Samples	pack_ice:snowpit:SN_SAMPLER	Snow salinity

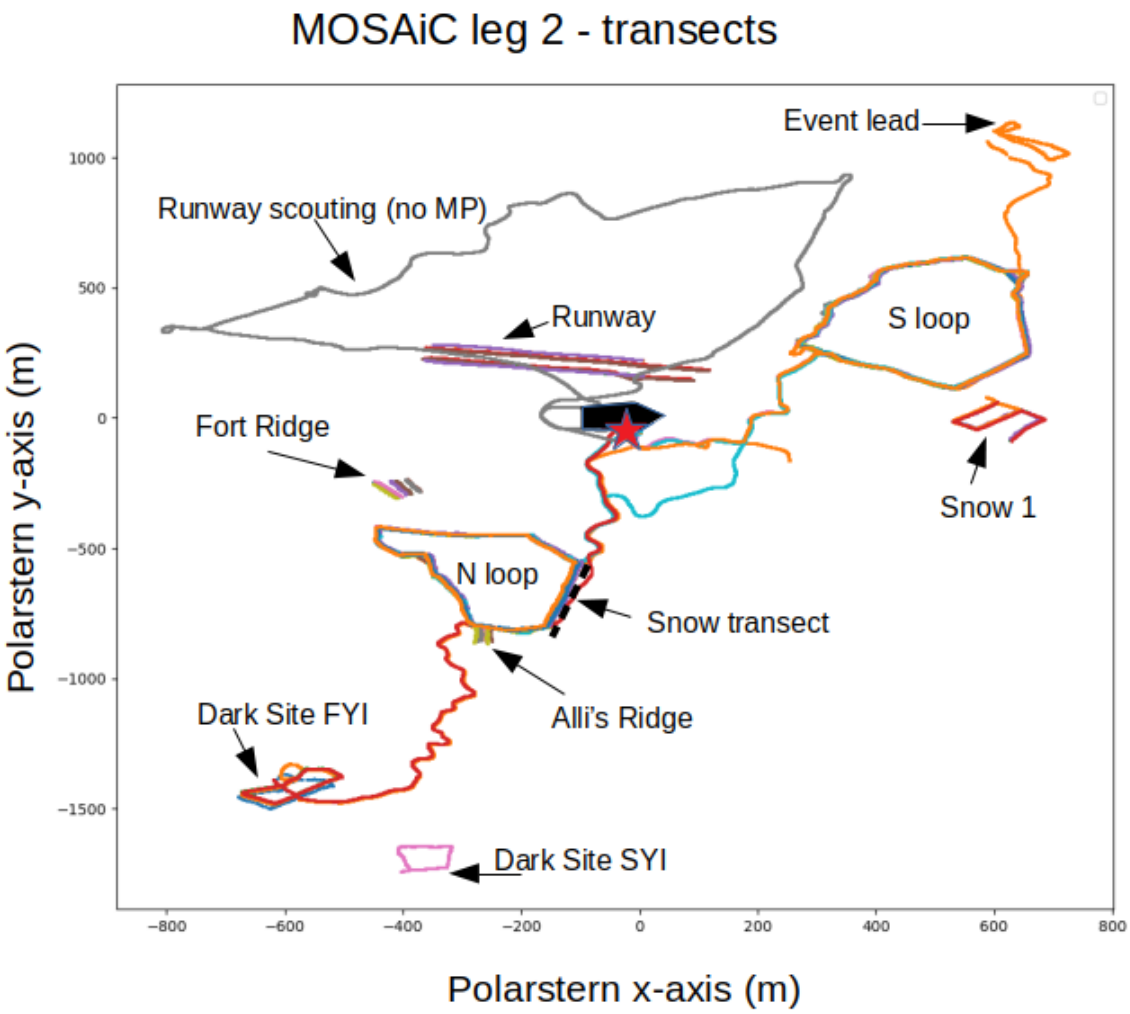

Fig. 4.7.1: Location of the transect lines in the CO during leg 2. Only the named locations/loops have MagnaProbe snow depth measurements. Other lines are GEM-2 only. The calibration site for GEM-2 at Polarstern is marked by a red star. The snow structure transect is approximated by a black dash line. Coordinate reference system is defined by Polarstern location and heading.

Tab. 4.7.2: *Overview of device operations of the mass balance work on the sea ice transects*

4.7.3 Preliminary (expected) results

Quickview total (ice + snow) thickness from the GEM-2 results were produced after each transect activity for the purpose of quality control and initial evaluation of ice conditions. An exemplary quickview products at full sensor resolution are shown in **Figure 4.7.2**. During leg 2 there was a gain in total thickness of about 0.5 to 1 m for level ice (thinnest ice in the figures) along all transect lines.

During leg 2 there we also observed a major change in the snow cover (**Figure 4.7.3**). Due to several strong wind events that also brought some snowfall, there was a small increase in mean snow depth (6-8 cm) and the development of probability density functions (PDFs) of snow depth from uni-modal to more bi-modal shapes.

The remote sensing sensors provide (a) Ku/Ka-band radar backscatter and based on that the range distance to the main scattering horizons in the snow and ice and (b) L-band microwave

brightness temperature, which are primarily related to the snow and ice microwave emissivity. The data from the instruments will be referenced to the FloeNavi CRS together with the locations of the snow pits. Analysis of the remote sensing data and snow structure data however requires extensive data processing, which will be done at home.

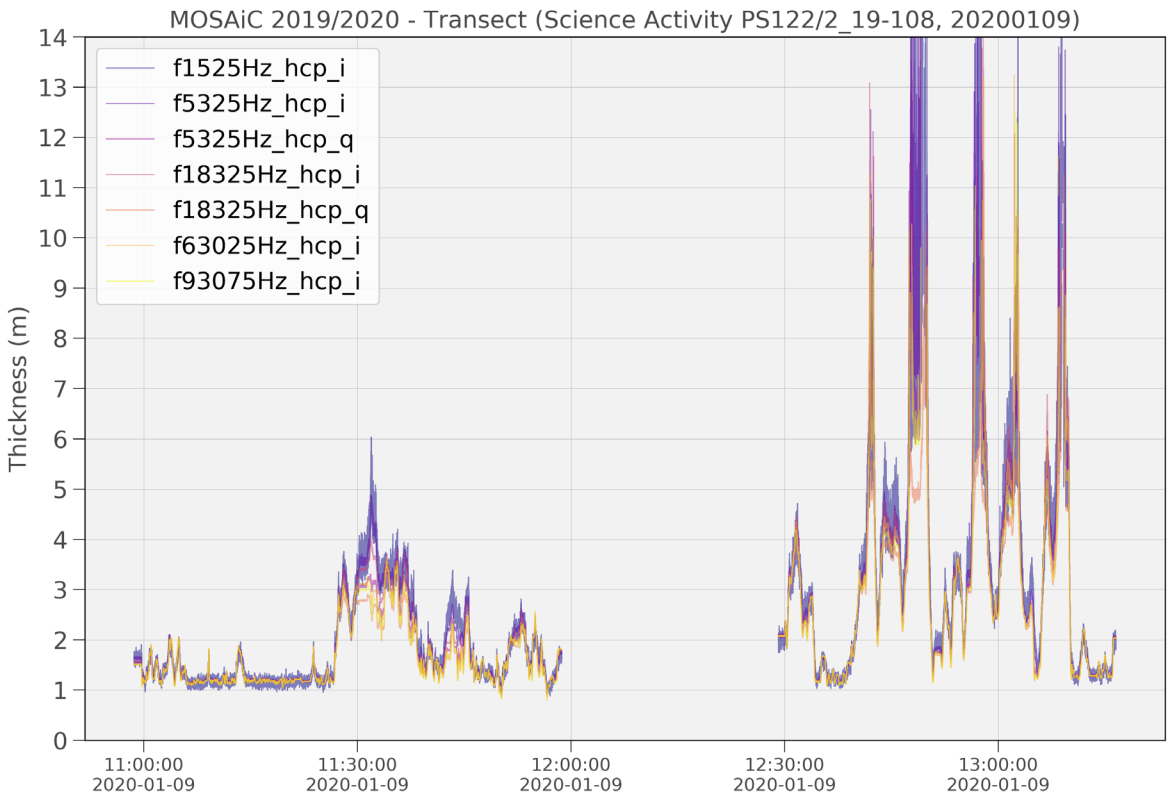

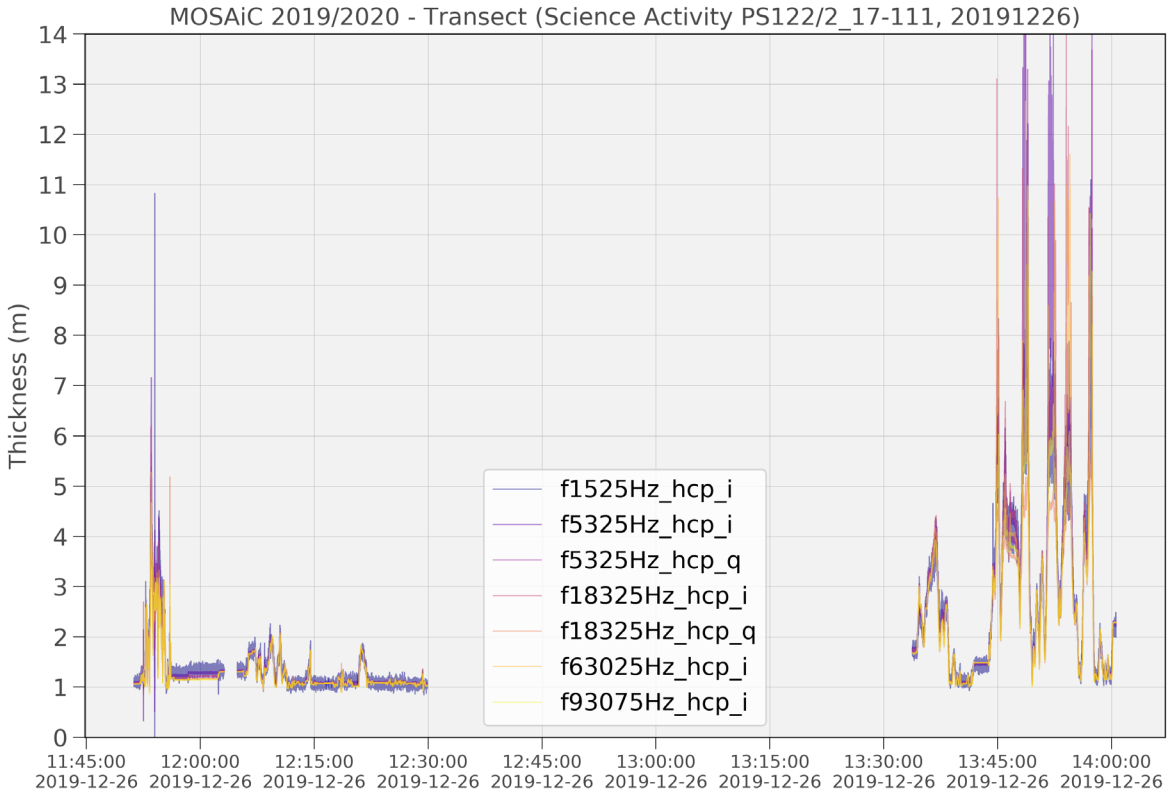

***Fig. 4.7.2**: Quick looks of total sea ice thickness (snow+ice) from GEM-2:examples from one of the earlier (1. Jan 2020) and end (27. Feb 2020) of leg 2. The results are not corrected for different walking speeds or periods of the sensor without moving.*

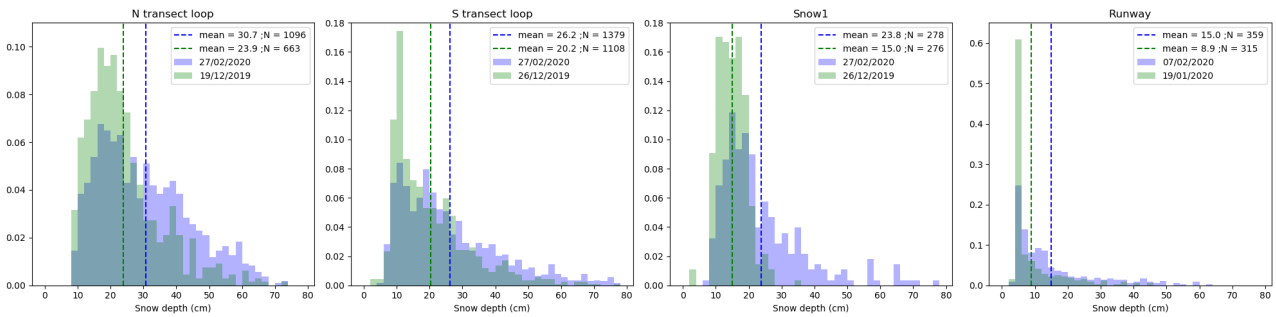

***Fig. 4.7.3**: PDFs of all repeated transects of leg 2. For S and N transect loops the mean increase of snow depth is modest (~6 cm), but obvious for all locations. The increase is slightly larger (~8 cm) for level ice type (Snow1 and Runway) than for the locations with combined ice types (level and deformed ice in N and S transect loops). Likely this is due to re-distribution at those locations: more removal from level ice than accumulations in the ridges. Also note the development of uni-modal distributions into bi-modal for all the cases.*

4.7.4 Data management

All data are handled, documented, archived and published following the MOSAiC data policy (see APPENDIX). All device operations were logged in the AWI sensorweb portal and all sensor raw data files are stored in platform section of MCS. Final geophysical parameters will be made available via the workspace section of MCS and archived in the PANGAEA data repository according the MOSAiC data policy.

4.8 Ice dynamics

Polona Itkin[1], Ian Raphael[2], Igor Sheikin[3], Egor Shimanchuk[3], Jari Haapala[4] (not onboard), Andrea Haase[5] (not onboard), Jennifer Hutchings[6] (not onboard), Phil Hwang[7] (not onboard), Nikolay Kolabutin[3] (not onboard), Ruibo Lei[8] (not onboard), Mikko Lensu[4] (not onboard), Annu Oikkonen[4] (not onboard), Chris Polashenski[2] (not onboard), Victor Smirnov[3] (not onboard)

[1]UiT/CSU
[2]Dartmouth
[3]AARI
[4]FMI
[5]HSVA
[6]Oregon SU
[7]UHud
[8]PRIC

4.8.1 Objectives

An overall objective of ice dynamics research at MOSAiC is to deepen the understanding on how pack ice moves and deforms over over a full annual cycle. In particular, we are examining spatial and temporal scales of motion and deformation and how those vary regionally and seasonally. We also aim to establish a relationship between deformation scales and physical characteristics of pack ice (in connection with data from IMB buoys, DTC, ice cores etc). The seismic stations obtain data on waves on ice and fracturing of the pack ice for a development of forecast methods for sea ice breaking.

Ice dynamics research is based on the local measurements at the Central Observatory, ice drift observations from the Distributed Network and large scale satellite products. For a collection data on local scale, we established a MOSAiC Small scale Ice Dynamics Observing System (SIDOS) on the Central Observatory. The system includes following components :

- Laser strain observatory - LSO (DC)
- GNSS (Uhud) and DGPS stations (DC)
- Seismic stations (AARI)
- Stress gauges (DC, FMI)
- Stress panels (HSVA)
- Ice radar (FMI)

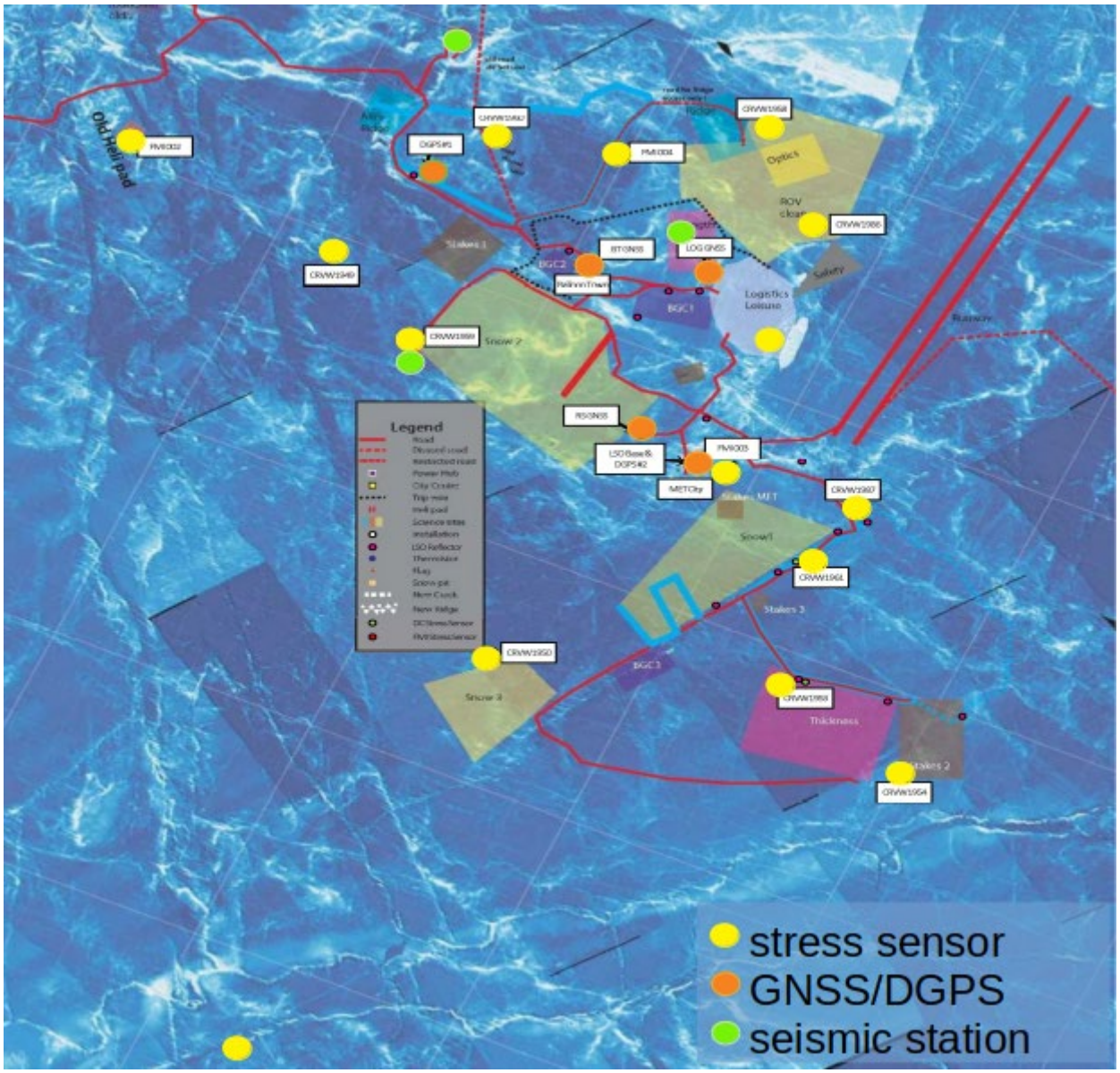

Fig. 4.8.1: Schematic figure of the MOSAiC Small scale Ice Dynamics Observing System (SIDOS) during leg2. LSO is not marked as it was not operational.

4.8.2 Work at sea

On leg 2 of MOSAiC we maintained the SIDOS (**Fig. 4.8.1**) established during leg 2. In addition, we deployed 3 stress sensors in the northern part of the CO, relocated the seismic stations, so that they span over a larger distance, deployed an additional seismic station in the DN and relocated one GNSS station. Most of the time allocated to the dynamics task was used for data download and service (battery exchange) in the existing network.

Laser Strain Observatory (LSO)

LSO provides high-precision plastic and elastic ice strain data. The observatory is composed of an array of retroreflectors (currently 14) fixed in the ice on metal posts, and an autonomous laser theodolite that tracks the displacement of the reflectors over time with mm-precision. This displacement measurement can be used to determine strain rate. The base station is accessible via the PackIce WLAN network through which data can be viewed in real-time from *Polarstern*.

The Leica TM50 base station was inoperable throughout Leg 2 due to low ambient temperatures. After troubleshooting and discussing with Leica, we decided to build a heater cover for the unit, to be shipped with the Leg 2/3 transfer. After installing the cover during the handover, we discovered that the cover severely limits the effective range of the unit, and the TM50 continues to be inoperable at the beginning of Leg 3. We will consider further solutions and wait for warmer temperatures.

GNSS and DGPS stations

The GNSS and DGPS stations measure ice motion on high precision and high sampling rate (1 and 2 s) as well as a constant reference frame for floe-relative coordinate transformations. Leg 1 deployed 3 GNSS stations in the CO: in the logistic area (S1), at the remote sensing hut (S2) and at the ROV site (S3). Since the ROV site experienced deformation during handover from leg 1 to leg 2, we relocated S3 to the Balloon Town at the beginning of leg 2. At low temperatures it is important that majority of the stations have a nearby shelter where data can be downloaded regularly. GNSS stations have large and heavy battery packs that are difficult to transport, but can at temperatures between -20 to -30 C last for 3 weeks. At temperatures bellow -30 C, they only provide power for about 1 week. Another problem with GNSS power was caused by a polar fox that chewed through the power cables of S1 at the beginning of leg 2. In general, power cables are the week point of GNSS stations as they get damaged easily at the low temperatures.

We installed two Trimble NetRS DGPS units within the CO (one at MET City and one at the Big Block on the Northern Transect) at the beginning of Leg 2. The station at the Northern transect requires regular battery exchange and data download, while the station at the MET city is connected to the line power and data can be accessed via PackIce WLAN network. For location overview see **Fig. 4.8.1**.

Seismic stations

Each of the three seismic stations (Alfa, Beta, Gamma) includes seismometer CME 4311, tiltmeter ИН-Д3-360, autonomous recorder “Baykal-8” for logging signals, GPS-antenna, antenna for signal transmission to the base and battery for powering station. Measurements were recorder to the “Baykal-8” datalogger with 100 Hz frequency. Data of the seismic stations were also transmitted by the wireless connection to a laptop deployed onboard the *Polarstern for a* continuous visual monitoring of seismic observations.

The stations were deployed close to the logistic area during leg 1, and in leg 2 we distributed them over larger distances in the CO. Gamma remained close to the logistic area (close to the new ROV site and at the sampling site for mechanics experiments), Beta was deployed at the northern end of Snow2 sampling area and Alfa was deployed north of the Alli’s Ridge. Another station (Delta?) was deployed in the DN at the L1 on 2 February 2020. All stations require regular battery service. Delta also requires regular data download. Unfortunately, L1 could not be revisited since deployment due to limited helicopter activities at the end of leg 2 (poor weather). For station location overview see **Fig. 4.8.1**.

Stress gauges

We installed eight Dartmouth College/CRREL vibrating-wire stress gauges during Leg 1, in addition to five identical sensors from FMI. One DC/CRREL sensor was destroyed in mid-November, leaving twelve intact sensors. The sensors measure local horizontal ice stress by measuring the change in frequency of three internal, actively vibrating wires. Using a network of stress sensors, the DGPS/GNSS stations, and the LSO, we will approximate the stress field

and responding strains within the local floe. The sensors are installed primarily within and around the CO, though some were installed as far as 2.5km from Polarstern (for detailed locations see **Fig. 4.8.1**). All gauges from leg 1 were installed in the remnant/second-year ice. During Leg 2, we installed three more DC/CRREL sensors in the CO (one in the remnant ice of the N transect loop and two in the FYI of the ROV observatory) , making fifteen operational sensors at the end of Leg 2. They required infrequent battery exchange and data download, but otherwise operated unattended. All gauges were deployed on level pans of ice of diameter at least 100 m.

Stress panels

Stress panels deployed in the logisitc area during leg 1 and the stress and temperature sensors delpoyed in the ship hull in void 92 were all operating unattended during leg 2. At the end of the leg data form both was downloaded. During handover between leg 2 and 3 (first observed on 5 March 2020) a small crack ran right between two stress panels and towards the ship.

Ice radar

In order to obtain data of local ice dynamics in high temporal and spatial scale, we used a system which digitizes the raw analogical ship radar data in a manner that echoes from the sea ice features, which normally are considered as a noise in marine applications, are digitized in high resolution. The radar signal digitizing unit, developed by the Imagesoft ltd., was connected to the antenna of the WAMOS radar. The set-up of the system is similar than used for the N-ICE2015 campaign (Oikkonen et al, 2017).

During the MOSAiC, processed images of every radar loop have been stored. Interval of those images is about 2 seconds. Digitizing area covers 20 x 20 kilometers area with 8.3 meters horizontal resolution. Continuous recordings begin on 25th October 2019. On leg 2 we continued with the collection and processing of the data. Images from the ship radar have been used daily for activity planning (events, scouting etc.). At strong deformation weekly animations were produced for the evening meetings.

Sea ice strength/mechanics measurements

Aim of the ice streght measurements is to determine local strength of different ice types and their seasonal variations. Measurements of vertical and horizontal ice strength were carried out according to a methodology developed in Ice Physics Laboratory of the AARI (patent №2348018) and described in “Methodic manual for studying physical-mechanical characteristics of ice formations as initial data for calculation of ice loading on shores, bottom and sea constructions” (SPb, AARI, 2011, p. 179).

For these measurements, a 50 meters x 50 meters area named ‘seismics’ was reserved. The site contains level second-year ice and it is located just next to the ROV site, next to the seismic station at the logistic area (**Fig. 4.8.1**). Local ice strength measurements were conducted with an automatic hydro complex “ЛГК 131-01” borehole probe-indenter “ЛГЦ095.055.0050.002”.

Measurements were carried out in the following way. Firstly, point of measurements was cleaned from snow and air, snow and ice surface temperatures were measured. Then at this point a hole with diameter 250 mm is drilled throughout ice cover. After that the hole was cleaned from brash ice and probe-intenter was deployed on a tripod over the hole. After testing of the system, the probe-indenter was oriented to the seflected direction and lowered down into hole on 30 cm depth and first measurement was made. For the second measurement probe-indenter is lowered down to the 60 cm depth if the thickness of ice was larger than 75 cm.

The measurements were carried out on 18. January and 5. February 2020. Each time, four holes were made and measurements were done at 30, 60, 90 and in February also at 90 cm depth. For results we refer to **Tab. 4.6.1**.

In addition, NTNU also provided a borehole jack that can ,measure ice strengths at vertical increment of 10 cm from 10 to 60cm. The instrument was used three times, each time on a different ice type. On 3. February on FYI at the dark Site, on 17 February on SYI at the Dark Site and on 24 February in the mechanics area next to the ROV hut.

Unaxial compressive strength measurements were conducted on December 5th 2019. The ice cores for vertical ice strength measurements were taken with the "Kovacs" 14 cm ice corer. For the horizontal strength measurements, first a block of ice with dimension of ~ 40 cm x 50 cm x 66 cm were taken and then horizontal ice cores at 30 cm depth was taken from that block. The samples were then transported to the ship and cut with the circular saw on 29-30 cm long pieces before compressive strength measurements.

Additional ice cores were taken for temperature, salinity and texture analysis.

4.8.3 Preliminary results

The leg2 was characterized by relatively stable ice conditions in the CO. Here the chronological overview of events important for the sea ice dynamics:

- 13. and 14. December: new cracks at the RS site and MET city. Possibly caused by arrival of Kapitan Dranitsyn.
- 15. December: the November shear zone some 100 m ahead of the PS bow was still active. There was open water in a small lead running through the main access road towards MET City and RS site. The crack at the MET City was unconsolidated and full or slush. There was regular motion where the road crossed the shear zone on the way to the old ROV site. A small crack through the northwestern corner of the logistics area and tripwire opened then quickly reconverged.
- 17.-18. December: The old ROV site breaks up (relocation of the ROV site). The crack comes from the port side of Kapitan Dranitsyn and makes a right angle right inside the ROV hole. From there is exits into the S transect loops where it narrows and disappears. At the same time there was an active lead (Alli's lead) just north of the N transect loop that prevented visits of the Dark site.
- 18. December: Departure of Kapitan Dranitsyn.
- 19. December recovery of GNSS station S3 at the old ROV site. The cracks widens and makes a new continuation straight on along the road. The ROV hole looks like a lake. The side crack into the S loop is visible, but it did not change. The lead is a couple meters wide – Nansen sled was just long enough to use a make-shift bride to rescue the station. The lead is covered by very thin layer of ice and is not active anymore.
- 29. -30. December: Alli's lead froze over and ridged. Alli's Ridge was created.
- Unknown date: small crack in the logistic area with branches towards Ocean City and ROV site.
- 31. December: Strong pressure in the ice leans the ship. High values in the stress panels.
- 29. December – 4. January: Deformation at the Dark site connection road and creating of the N lead. N lead remained active for weeks. These deformations are not visible on the ship radar due to shadowing from the ship's mast.
- 6. January: Runway becomes visible on the ship radar images
- 6. January: N lead shears on 5. January (lonely by meters, locally half meter), but access to the FYI coring site still possible. Allie's ridge got even bigger and skidoos had a few meters of steep slope to conquer.

- 8. January: Crack along the runway (port side of the ship, ~1km away), opened earlier today, at 18UTC reached by skiers, closing, ~5m wide
- 10.-12. January: lots of shear at all new leads at the port side of the ship (~1km and ~5km distance)
- 11. Jan: Michael ‘falls off the met tower’.
- 12. Jan: occurrence of first large snow dunes in Snow 1.
- 12.-15. January: deformation in rectangular shape all around the ship (distance 1-5km, not in the CO)
- 21.-26. January: A lot of motion in the sector 9-12 o clock. New leads, ridges, shear zones. A lot of sampling activity (event) from the MOSAiC teams, including a long transect towards L2 (on 23. Jan) and event sampling on the lead junction (26. Jan).
- 27. Jan: New crack perpendicular to the access road to Snow 3. The crack runs past MET City and Snow 2 towards the Dark site N lead. The crack opened in the afternoon during our visit at to Snow3 for snow pits. On our return we found two cracks, the widest was about 40 cm wide and slowly widening.
- 3.-9. Feb: New crack the old ROV site and parallel to the access road to Snow 3 (occurred on 3. Feb), on 4. Feb started to refreeze, but still full of slush, safe to cross by ski. After few days a small ridge formed there (on 9. Feb). This ridge is visible on the ship radar.
- 6. Feb: Micro crack observed across the S transect loop (running from Stakes 2 towards the Runway) at about 60 degrees angle to the wider crack along the road passing the old ROV site.
- 10. Feb (and earlier): again deformation along the N lead at the Dark site. Small deformation in the previous day, road still drive-able, but since today SYI is inaccessible again: several active cracks. FYI was available, but shrank again due to widening of the N lead.
- 10. Feb: Thin crack running across the access road to MET City and RS site (after the junction with the bypass road and just before the fork of both access road). The crack ran though Snow 1, next to the rocket traps. On the other end it ran between Ocean City and ROV site and from there into the N transect loop. This could be reactivation of old crack that was first reported on 14. December in the MET city (by M. Shupe).
- 11. Feb: Active ridges on the way to the bow stress sensor
- 13.-14. Feb: power outage on the ship and in the central observatory. Ship radar server, stress panels and stress sensors in the ships hull could be affected.
- 18. Feb: Crack at the emergency runway (1-2m wide) prevents return of one of the pisten bullies. The crack continues into the S transect loop. This crack stays open for several days. Then it finally closes.
- 20. Feb: the crack known from the runway is in the S transect loop at places 5 m wide, filled with slush. The transect loop needs a slight detour in the N part. The crack is still active at the runway, at places 1m wide. Covered by snow by pisten bullies.
- 20.-26. Feb: The same crack at the southern part of the S transect starts to develop into a ridge. In the following days it shears by a couple of meters (visible by a small shift in the road). By 26. Feb the ridge is about 1 m high, stable by crumbly.
- 28. Feb: Arrival of Kapitan Dranitsyn.
- 4. Mar: Crack in the MET City during handover.

Tab. 4.6.1 Results of the ice strength measurements from AARI borehole jack.

Point	H_snow (cm)	H_ice (cm)	H_raft (cm)	LocStr30 (MPa)	LocStr60 (MPa)	LocStr90 (MPa)
t1	16	105	97	28,166	25,281	23,099
t2	14	106	98	32,22	31,287	22,717
t3	14	105	98	32,769	28,8	21,812
t4	15	104	97	30,694	25,96	-

18.01.2020

Point	H_snow (cm)	H_ice(cm)	H_raft (cm)	LocStr30 (MPa)	LocStr60 (MPa)	LocStr90 (MPa)	LocStr120 (MPa)
t1	15	127	118	30,187	25,962	24,948	-
t2	16	130	121	30,467	25,06	20,886	-
t3	16	129	121	29,247	28,216	24,778	-
t4	14	133	125	31,388	31,216	27,336	23,116

05.02.2020

4.8.4 Data management

All data are handled, documented, archived and published following the MOSAiC data policy (see APPENDIX). All device operations were logged in the AWI sensorweb portal and all sensor raw data files are stored in platform section of MCS.

4.8.5 References

Oikkonen A, Haapala J, Lensu M, Karvonen J, Itkin P (2017), Small-scale sea ice deformation during N-ICE2015: From compact pack ice to marginal ice zone, J. Geophys. Res. Oceans, 122, 5105–5120, doi:10.1002/2016JC012387.

4.9 Ridge studies

Polona Itkin[1], Dmitry V. Divine[2], Christian Katlein[3], Martin Schneebeli[4], Daniela Krampe[3], Matthias Jaggi[4], Ian Raphael[5], Egor Shimanchuk[6], Mats Granskog[2] (not on board), Knut Vilhelm Høyland[7] (not on board), Glen Liston[8] (not on board), Don Perovich[5] (not on board), Mario Hoppmann[3] (not on board), Yusuke Kawaguchi[9] (not on board)

[1]UiT/CSU
[2]NPI
[3]AWI
[4]SLF
[5]Dartmouth
[6]AARI
[7]NTNU
[8]CSU
[9]U Tokyo

4.9.1 Objectives

Pressure ridges are formed by pilling up of crushed ice blocks during sea ice convergence. Often the features also shear. While the ridge sail is the obvious surface part of the ridge, the submerged part – ridge keel, is typically much larger and voluminous, taking up to 90% of the ridge volume. Both sails and keels are important surface roughness features that cause turbulence in atmosphere and ocean. Leg 2 of MOSAiC established a 'Ridge Observatory – Fort Ridge' with the purpose of investigating the following research questions:

- The ridge consolidation: The body a new pressure ridges is composed with ice blocks and air and water pockets between them – voids. The water-filled will gradually freeze

during cold season and the ridge will eventually consolidate. Since the winter observations of the ridges are rare, MOSAiC offers a unique opportunity to observe the ridge consolidation with direct observations (drilling and coring) and remotely (electro-magnetic induction)

- Redistribution of snow in the deformed ice: Ridges are taps for snow and MOSAiC gives an opportunity to observe seasonal development of snow thickness and stratigraphy in the ridge and its surroundings.
- Ridge-associated ecosystems: Pressure ridges remain the least studied Arctic ice-associated ecosystem, with a basic lack of data for the winter season and limited studies from other seasons. Neither are ridges represented in ecosystem models, they neglect the complex structure of ridge habitats, which is quite different from the level ice described in models. It is expected that pressure ridges will become an increasingly important component of the new Arctic sea ice regime dominated by FYI where the largest portion of the level ice melts completely in summer.

4.9.2 Work at sea

We established Sea Ice Ridge Observatory ('Fort Ridge') on the Eastern flank of the main floe of the CO. The ridge is located within the operation range of the new ROV site that was moved in the beginning of leg2. The ridge is about 80-90 m long with 1.5-2 m sail elevation over the level ice surface. The keel depth varies within 4-10 m according to ROV multibeam surveys. Coring on the ridge have demonstrated that its western flank (directions towards CO) is comprised more of SYI types, while the eastern flank is built mainly of FYI. We tentatively attributed the timing of the ridge formation to late September, early October, prior the establishment of the MOSAiC CO.

As a second component of the Ridge Observatory, we also conducted studies on the young unconsolidated ridge (aka "Alli's Ridge") that formed on the northern flank of the CO during the major deformation event in early January. The area north the CO floe was subject to a divergence event in mid-December that led to formation of a some 30-100-m wide lead that by early January was covered with 30-40 cm thick young ice. The ridge northern flank is mainly built of the blocks of this young ice while its southern flank includes more thicker SYI of the CO floe. The ridge sail at the time of formation was as high as 2-3 m over the level ice surface.

4.9.2.1 Buoy deployments in the Ridge Observatory

During MOSAiC leg 2 we deployed the following buoys:

1. Five ice mass balance buoys at Fort Ridge and Alli's Ridge that includes two SRSL SIMBA buoys and three DTC chains studying a temporal evolution of ridge consolidation
2. Two ADCP+CTD pairs on both flanks of Fort Ridge at 2 m depth below ice surface to study ridge-driven turbulence and the associated mixing process underneath ice surface.
3. Four GPS buoys on the flanks of the Fort Ridge to track potential geometric changes of the ridge and time evolution of its drift, more specifically a ridge orientation relative to the drift direction.
4. Three light string buoys of ENVIPOPE type to study a light climate underneath ice surface – all deployed on level ice in vicinity of Fort Ridge

5. Two AFZP (Acoustic Fish and Zooplankton Profiler) buoys, one upward- and one downward-looking studying the temporal variability in the occurrence of zooplankton, sea ice macrofauna and ice algal aggregates. Also deployed not directly at Fort Ridge, but in its vicinity.

Summary of major buoy parameters and details on buoys deployment locations is presented in the **Tables 4.3.1** and **4.3.2** below and also shown in **Figures 4.3.1** and **4.3.2** and **4.3.3**.

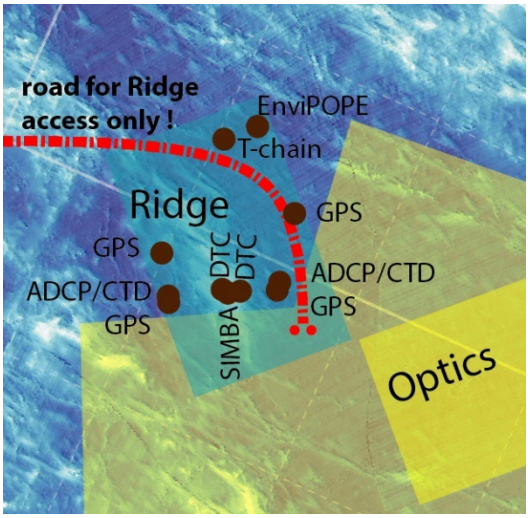

***Fig. 4.9.1**: Map of Fort Ridge showing locations of the deployed buoys per 21.02.2020: two ADCP+CTD pairs, SIMBA HAVOC 0101, DTC-24, DTC-25, ENVIPOPE-2 and four GPS buoys. Detailed sketch of the observatory is displayed on Figure 4.3.2. Surface topography is from the ALS scan flight from 21.02.2020.*

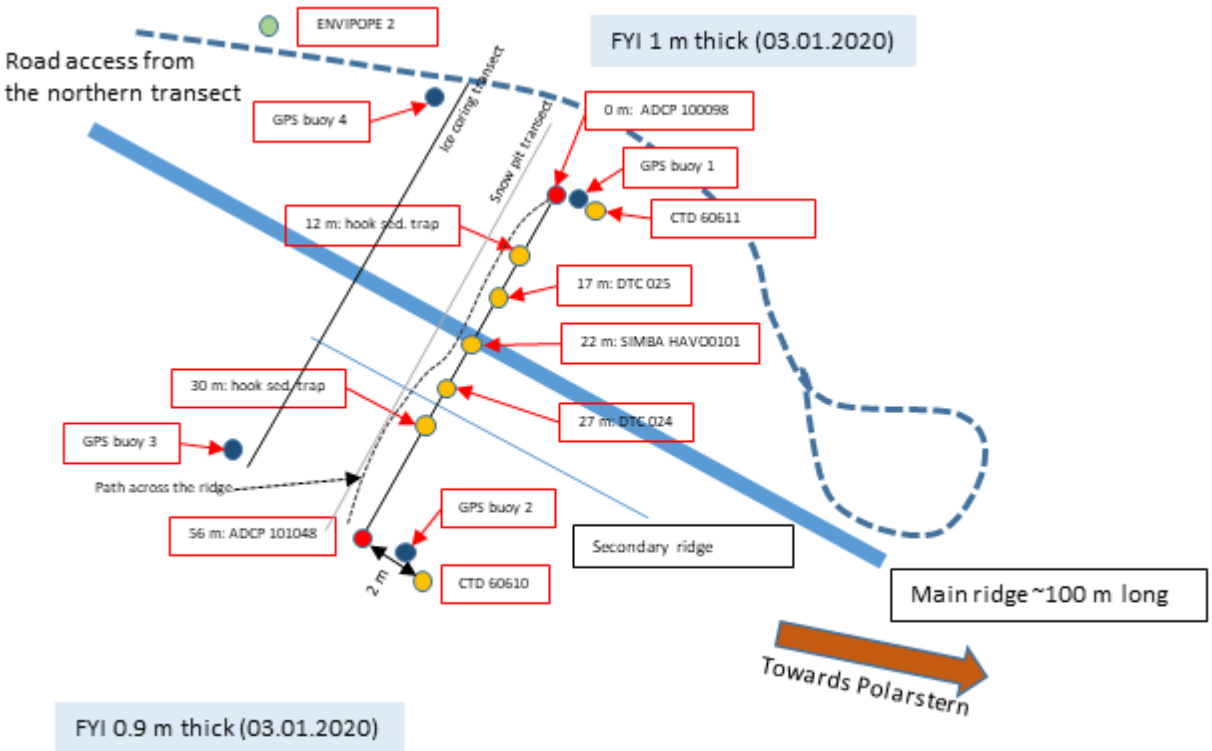

***Fig. 4.9.2**: Sketch of the Fort Ridge showing details on locations of specific buoys per 20.02.2020. Distances are given along the established instruments transect.*

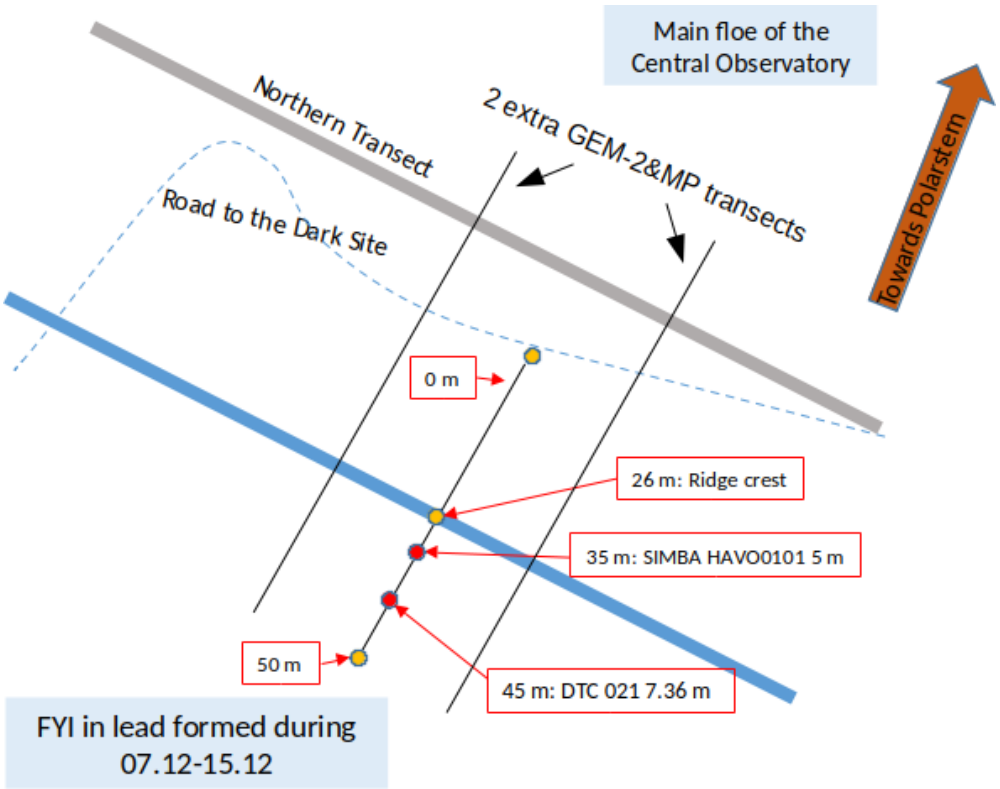

***Fig. 4.9.3**: Sketch of the Alli's Ridge formed in early January on the northern flank of the CO floe showing details on locations of specific buoys per 20.02.2020. Distances are given along the established transect.*

<u>*Deployment of SIMBA buoys and DTC chains*</u>

The SIMBA buoys and DTC chains measures the air–snow-ice–ocean temperature profile at a high vertical resolution of 0.02 m (Jackson et al., 2013). There is a pulsing heating energy given to each sensor daily. Using the measurements of the vertical temperature profile of air-snow-ice-ocean and the measurements of temperatures before and after the pulsing heating, we can obtain the interfaces among air, snow, sea ice and ocean, sequentially the mass balance of snow and sea ice. SIMBA transmits data via Iridium.

The DTC is powered by regular lead batteries and controlled by an affordable, commercially available microcontroller, the units will send their temperature and heating profiles in fixed intervals (e.g. 1 h) or on request to a central receiving unit on the ship via a direct communication link.

At the MOSAiC SIRO, we deployed one SIMBA buoy and two DTC along the established "instruments transect" (see Figure 4.3.2). One SIMBA buoy and one DTC were deployed at a young unconsolidated ridge ("Alli's Ridge") that formed on the northern flank of the CO during the major deformation event in early January (see Figure 4.3.3).

Tab. 4.9.1 Deployment information of SIMBA buoys and DTC chains at SIRO and young unconsolidated ridge ("Alli's Ridge")

Deployment time and coordinates	Buoy num. /short name	H_i (m)	H_s (m)	Chain length, m	Description of the deployment site and DSHIP operation number
08.01.2020 N87°06.974' ; E 15°12.770'	SIMBA HAVOC0101\ 2020t60:v7_klon1	6.10	0.1	9	SIRO, top of the ridge; PS122/2_14-319 2020T60
08.01.2020	DTC-024	4.1	1.0	7.5	SIRO, FYI flank; PS122/2_14-321 DTC24_416
08.01.2020	DTC-025	6.05	0.5	7.5	SIRO, SYI flank; PS122/2_14-320 DTC25_416
05.02.2020 N 87.553; E 94.597	SIMBA UIT0206\ 2020T61	7.05	0.05	5.0	Alli's Ridge, FYI flank; PS122/2_14-333
05.02.2020	DTC-021	5.35	0.01	7.36	Alli's Ridge, FYI flank

Deployment of ADCP, CTD and GPS buoys

Two ADCP+CTD pairs of instruments were deployed on both flanks of SIRO. Details are presented in Table 4.3.2 below. See also sketch of the SIRO in Figure 4.3.2

***Table 4.9.2**: Deployment information of ADCP and CTD buoys deployed in SIRO*

Deployment time and coordinates	Buoy num. /short name	H_i (m)	H_s (m)	Deployment depth, m	Description of the deployment site and DSHIP operation number
03.01.2020 N 86.9164; E 115.6908	ADCP Nortek Signature 1000 S/N 100098	1.05	0.15	1.5	SIRO, FYI flank of the ridge;Distance to the sail top of the ridge 21 m; PS122/2_14-308 nortek_100098
03.01.2020 N 86.9168; E 115.6794	ADCP Nortek Signature 1000 S/N 101048	0.85	0.12	1.65	SIRO, SYI flank; Distance to the sail top ridge: 30 (14) m, number in parenthesis stands for the distance to the secondary smaller ridge next to the main ridge PS122/2_14-307 nortek_101048

					(mistakenly registered as PS122/2_14-307 nortek_101408)
03.01.2020 N 86.9163; E 115.6910	CTD RBR Concerto S/N 60611	-	-	2.0	SIRO, FYI flank; 2 m away of ADCP 100098; PS122/2_14-310 rbr_60611
03.01.2020 86.9168; E 115.6798	CTD RBR Concerto S/N 60610	-	-	2.0	SIRO, SYI flank; 2 m away of ADCP 101048; PS122/2_14-309 rbr_60610

ADCP should be visited on a regular (at least monthly) basis to have the data downloaded. RBR CTD store the data internally; the data will be recovered upon recovery of the instruments.

In order to track the Fort Ridge ridge orientation and potential deformations four GPS buoys with Iridium data link were deployed on 14.02.2020 both flanks of the ridge, two on each side (***Fig. 4.9.1)***. On the FYI section of Fort Ridge (***Fig. 4.9.1***) we deployed in collaboration with team OCEAN a T-chain that measures temperature through ice and ocean. PI of ridge ocean instruments is Y. Kawaguchi (University of Tokyo). For more details we refer to Section 5.

Deployment of light string buoys (ENVIPOPES)

In order to study light climate underneath the ridged an level ice three ENVIPOPE type buoys consisting of a 50-m light string (string with light sensors in the PAR band) and a data transmitting (via Iridium) surface unit were deployed in various locations around the CO. These included:

ENVIPOPE-1: Ridged area of the main floe of the CO; next to AFZP-1 buoy (Figure 4.3.4)

ENVIPOPE-2: Ridged area next to SIRO (Figure 4.3.1). Due to a potential interference with the ROV operations, deployment on the ridge itself was not possible.

ENVIPOPE-3: Dark Site SYI to establish baseline values on level ice.

Tab. 4.9.3 *Deployment information of ENVIPOPE buoys*

Deployment time and coordinates	Buoy num. /short name	H_i (m)	H_s (m)	Chain length, m	Description of the deployment site and DSHIP operation number
14.02.2020 N 88.029 ; E 80.206;	ENVIPOPE-1/ envipope1	1.23	0.2	50	CO floe, north of Northern Transect; PS122/2_14-342 envipope1
14.02.2020 N 88.031; E 80.259	ENVIPOPE-2/ envipope2	1.35	0.2	50	On level ice north of SIRO; PS122/2_14-341 envipope2
16.02.2020 N 88.065; E 79.205	ENVIPOPE-3/ envipope3	1.34	0.17	50	Dark Site SYI; PS122/2_14-357 envipope3

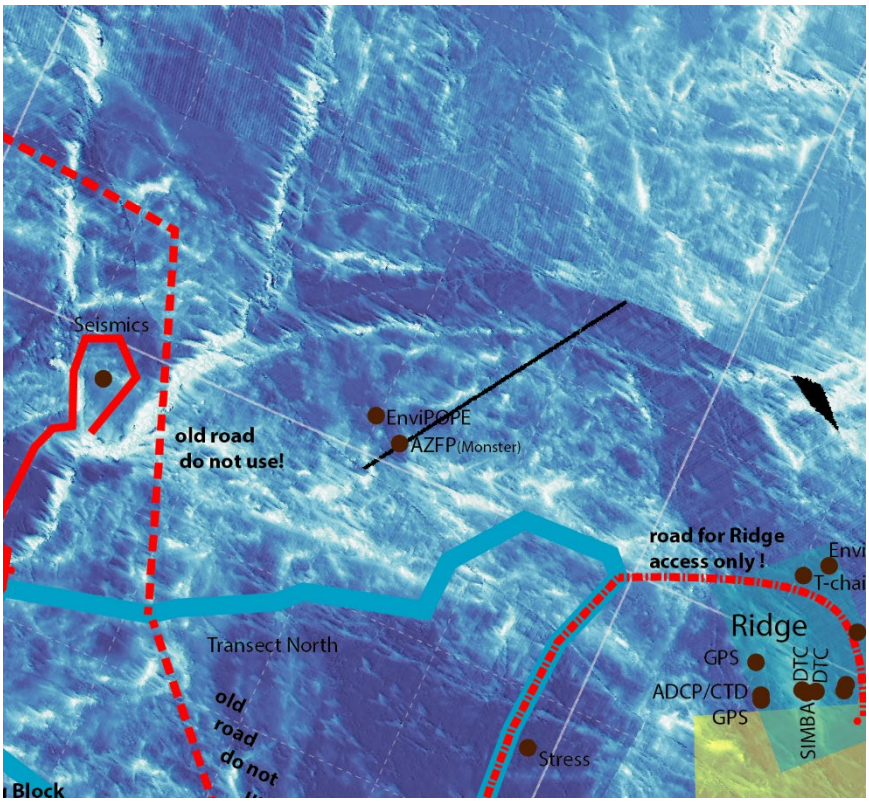

***Fig 4.9.4**: Locations of AFZP-1 and ENVIPOPE-1 buoys north of the Northern Transect (shown thick blue line). Surface topography is from the ALS scan flight from 21.02.2020.*

<u>Deployment of Acoustic Zooplankton and Fish Profilers (AZFP POPE buoys)</u>

Two AZFP-POPE buoys were deployed during leg 2:

AZFP-1 upward looking with transducers at 15 m depth and a surface unit POPE-308.

Buoy deployed on 29.01.2020 at N 87.477; E 95.058; H_ice=0.95 m,

DSHIP device operation: PS122/2_14-330 AZFPPOPEup

The buoy is placed some 80m north of the transect line in between the transect and ice ridge surrounding main floe edge on a 20-m wide area of level ice surrounded by SYI old ridges of the main floe. AZFP-1 is located some 20 m away of the ENVIPOPE-1 buoy (Figure 4.3.4)

AZFP-2 downward looking with transducers at 5 m depth and a surface unit POPE-306.

Buoy deployed on 16.02.2020 at N 88.067; E 79.189; H_ice=1.45 m, H_snow=0.13 m,

The buoy is located on Dark Site Second Year Ice, level ice area next to the main road along the first coring transect line. Access to the buoy via the road to the Dark site SYI.

Mention here the T-chain and GPS buoy deployments.

4.9.2.2 Ridge transects

The ridge ice thickness and snow depth transects were done by a combination of a broadband electromagnetic induction sensors (Geophex GEM-2) and a Magnaprobe. The Magnaprobe snow depth measurements are taken along the surveyor's tape every meter. Where the snow depth exceeded 120 cm, measurement was done by an avalanche probe. For ridge transects GEM-2 is operated without the pulk. Measurement is discrete, every 1 meter (along surveyor's tape). The ski of the instrument should be hold as horizontal as possible. This is a two person task, where first person holds the instrument, while the second person operates the field computer. The device is recording for 5-10 seconds at every measurements point and then logged off - in a very similar fashion as for the calibration.

Ridge transects were done at three transect lines at Fort Ridge: radiation transect, installation transect and coring transect. And at 3 lines spaced ~10 m at the Alli's Ridge. The transects are planned to be repeated at about 3 week intervals or at least once per leg.

Most of the transect lines were also drilled by 2'' auger. These measurements will be valuable for interpretation of the GEM-2 transects and should show some seasonal development of the ridge consolidation.

4.9.2.3 Snow Transects

See Section 4.2.

4.9.2.4 Ridge Coring

For more details on Ridge coring events please see Section 4.1.

4.9.2.5 Borehole Jack

Although borehole jack was only used on level ice, we used the time allocated to ridges and seismics tasks to perform these ice mechanics measurements. More about the measurements is described in Section 4.8.

4.9.3 Preliminary (expected) results

In total there were 10 working days with ridge transect work on leg 2. We did 3 different repeated transects at Fort Ridge and 3 at Alli's Ridge (in total 6 different lines). We drilled 32 drill holes to corroborate GEM-2 and MP transect studies.

We took 4 cores from the SIRO ridge during 2 coring events and six more cores on level ice on the flanks of this ridge. **Table 4.9.4** give an overview of all ridge transect activities; **Figure 4.9.2** shows an example of transect data.

Date	Location	Ridge transect with GEM-2	Ridge transect with MP	Ridge drilling	Ridge coring
3. Jan	Fort Ridge	-	-		Installation l. PS122_2-18-61
8. Jan	Fort Ridge	Installation l. PS122_2-19-101	Installation l. PS122_2-19-107	installation l. PS122_2-19-147	-
10. Jan	Fort Ridge	Coring line PS122_2-19-111	Coring line PS122_2-19-113	-	Coring line PS122_2-
17. Jan	Fort Ridge Alli‘s Ridge	Central line AR PS122_2-20-96	Central line AR PS122_2-20-98	Coring line PS122_2-20-81 central line PS122-2-20-82	-
24. Jan	Fort Ridge	-	-	Optical line PS122-2_21-102	Coring line PS122_21-124
31. Jan	Fort Ridge	Optical line Central line AR PS122_2-22-94	Optical line Central line AR PS122_2-22-94	Optical line PS122-2_22-124	-
5. Feb	Alli‘s Ridge	-	-		-
12. Feb	Fort Ridge Alli‘s Ridge	Coring l. 2 side lines at AR PS122_2-25-121	Coring l. 2 side lines at AR P122_2-24-69	Coring line PS122/2_24-104	-
21. Feb	Fort Ridge	Installation l. PS122_2-25-120	Installation l. Coring line PS122_2-25-122	-	-
28. Feb	Alli‘s Ridge	All 3 lines PS122_3-29-72	All 3 lines PS122_3-29-73	-	-

Tab 4.9.4: Overview of all ridge transect activities at Fort Ridge and Alli’s Ridge

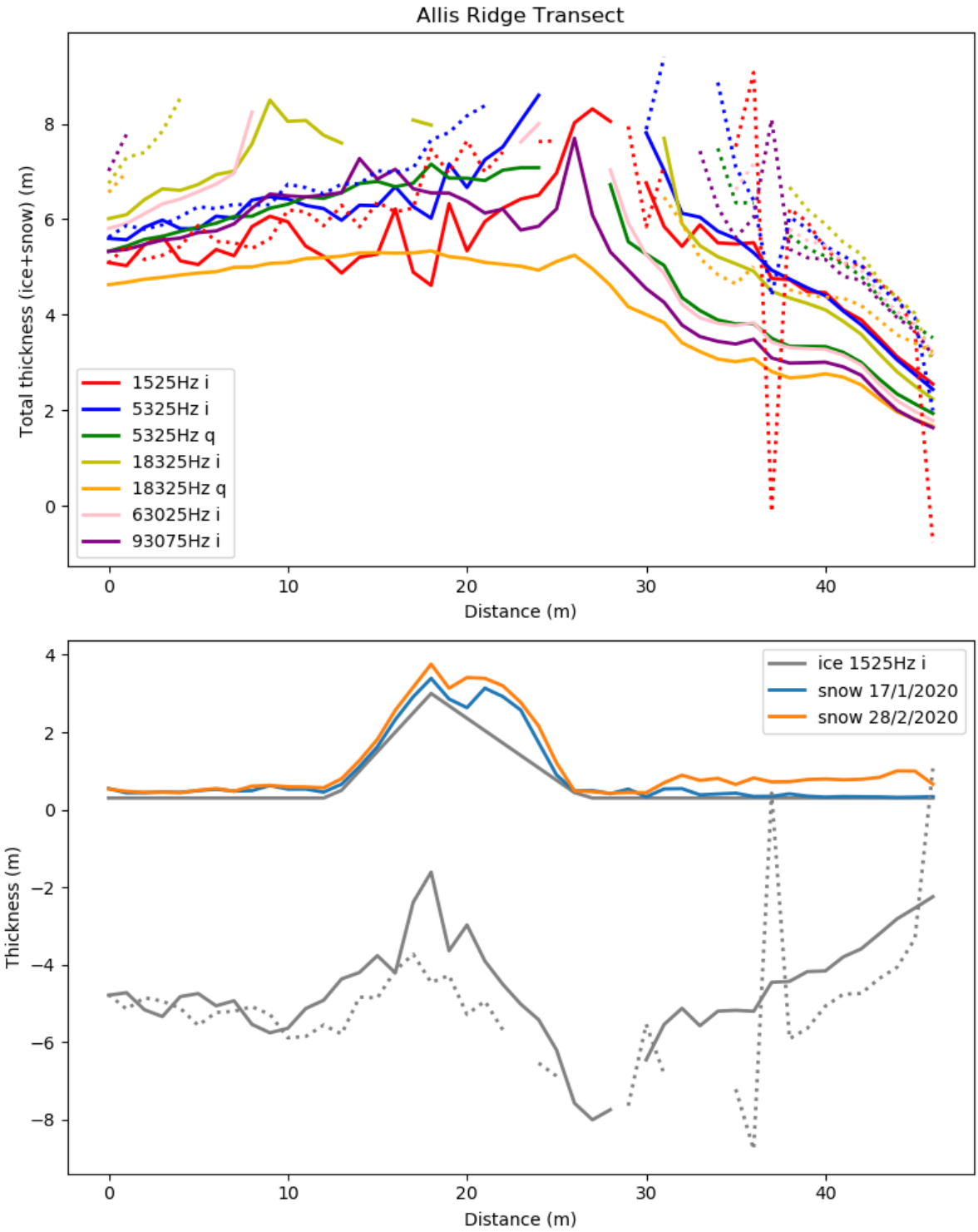

***Fig. 4.9.5**: Example of the total ice thickness from GEM-2 (top panel) and approximate surface elevation, snow depth and ice thickness at the beginning (all solid lines) and at the end (all dash lines) of the leg 2.The transect is at the Alli's Ridge (central transect). These quick-looks show thickening of the ice (or in reality consolidation) and at the same time accumulation of snow around the ridge. The surface elevation is approximated. The low thicknesses at the end of the leg at 38 and 45 m distance are artifacts due to SIMBA and DTC installation on that transect. Both objects contain large metal pieces that interfere with the GEM-2 signal. The example also shows how asymmetric ridge sail and keel are.*

On the same transects we also did a limited number of drill holes with detailed notes on ice hardness and occurrence of the dry and wet voids. In total there were 7 days when we drilled

the ridge. We drilled once at the installation line at Fort Ridge, twice at the optic transect at Fort Ridge, twice at the coring transect at Fort Ridge and twice at the central transect at Alli's Ridge.

Both ADCP buoys on SIRO ridge were visited three times during leg 2 in order to recover data and shift ADCP batteries. The list of events is presented below.

17.01.2020. Data recovery for the period 03.01.2020-17.01.2020

07.02.2020. Data recovery for the period 17.01.2020-07.02.2020.

07.02.2020. Batteries shifted on both ADCPs.

21.02.2020. Data recovery for the period 07.02.2020-21.02.2020

Preliminary analysis of the data have demonstrated the range of the instruments to be of about 10-12 m of a high quality data.

For both AFZP-POPE buoys the data is to be transmitted via the radio link. The dish plate antenna for communication was set up on A-Deck of *Polarstern*. However, it was revealed that due to programming errors, buoy AFZP-1 can not send the data, though the data are logged and stored on the internal memory of the buoy. The data are to be recovered later together with the instrument in the end of the campaign.

Buoy AFZP-2 has been sending the data successfully during the two data communication sessions in the second part of leg 2.

19.02.2020 Data recovery for the period 16.02.2020-19.02.2020

29.02.2020 Data recovery for the period 19.02.2020-29.02.2020

4.9.4 Data management

All data are handled, documented, archived and published following the MOSAiC data policy (see APPENDIX). All the instruments have been added into the system of SENSOR.awi.de and all the data has been or will be added to the MCS. The data will be submitted according the data policy of MOSAiC.

4.10 Remote Sensing Measurements

Julienne Stroeve[1,2], Vishnu Nandan[1], Rasmus Tonboe[3], Marcus Huntemann[4,5], Gunnar Spreen[5] (not on board), Estel Cardellach[6] (not on board), T. Casal[7] (not on board), Oguz Demir[8] (not on board), Claude Duguay[9] (not on board),

[1]UK.UCL
[2]CA.UMANITOBA
[3]DK.DMI
[4]DE.AWI

Friederike Fohlmeister[10] (not on board), Carolina Gabarró[6] (not on board), Stefan Hendricks[4] (not on board) Joel Johnson[8] (not on board), Nathan Kurtz[11] (not on board) Ruibo Lei[11] (not on board), Steen Savstrup Kristensen[13] (not on board), Randall Scharien[14] (not on board), Mike Schwank[15] (not on board), Maximilian Semmling[16] (not on board), Wei Wan[17] (not on board), John Yackel[18] (not on board)

[5]DE.UBREMEN
[6]ES.ICM-CSIC
[7]INT.ESA
[8]EDU.OSU
[9]CA.UWATERLOO
[10]DE.DLR
[11]GOV.NASA
[12]CN.PRIC
[13]DK.DTU
[14]CA.UVICTORIA
[15]CH.WSL
[16]DE.GFZ
[17]CN.PU
[18]CA.UCALGARY

4.10.1 Objectives

Satellite remote sensing is the ideal tool to obtain Pan-Arctic and long-term observations of the snow-covered sea ice cover, underlying ocean and overlying atmosphere. Remote sensing datasets can be used to extend observations from the MOSAiC Floe to a larger scale and set them in context with preceding environmental conditions, like the history of the ice floes MOSAiC will be established on. MOSAiC provides ideal conditions for validation of satellite remote sensing observations: (a) it is a rare case to observe the complete, annual seasonal thermodyamic cycle of sea ice growth, formation and decay. Especially, winter observations from the central Arctic are basically absent. (b) The MOSAiC concept to not only have one central measurement site but a distributed grid of measurements that cover the typical satellite footprint scales make meaningful comparisons feasible. (c) Furthermore, the combined MOSAiC airborne campaigns will allow to bridge the gap between in situ and satellite observations.

One scientific goal of MOSAiC for remote sensing is the ground validation of various satellite products and to develop novel retrieval methods for critical snow and sea ice state variables from satellites. Research questions for Leg 2 are:

- How well do satellite algorithms perform in the Central Arctic when multiyear ice is replaced by first-year ice for parameters such as sea ice thickness distribution, snow depth, ice type, floe sizes, ice concentration, and ice drift and deformation?
- Can co-located ground-based sea ice/snow and microwave measurements help to develop improved satellite retrieval methods for ice area, thickness, type, and snow depth and lead to better understanding and forward models of the emission and scattering processes in snow and sea ice?
- What is the prospect to retrieve additional physical parameters with satellite remote sensing to expand the observational capability of processes at the ice/atmosphere interface like surface roughness?
- How can the High Priority Copernicus Candidate Missions CIMR, CRISTAL, and Rose-L extend our sea ice observation capabilities in the future?

Most observed changes of the Arctic climate system are based on results from satellite remote sensing, which is one of the most important and reliable tools for Arctic monitoring. However, most satellites do not directly measure the geophysical parameters that are needed for research and monitoring. Sea ice concentrations, for example, are typically derived from passive microwave brightness temperatures or high-resolution radar images. Both methods make use of the characteristic difference between surface properties of open water and sea ice, which can be complicated by a variety of seasonal and conditional factors. Sea ice thickness is derived from microwave brightness temperatures (for thin ice) or from altimeters (ice thicker than 50cm). Altimeters measure the ice or snow freeboard, which is then converted

to ice thickness based on critical assumptions, such as snow depth and snow/ice densities. Continuous development of methods and algorithms to analyze satellite measurements is necessary to improve observational capabilities, reduce uncertainties, and ensure consistency of satellite data sets.

4.10.2 Work at Sea

MOSAiC Central Observatory

Several remote sensing (RS) instruments were deployed and operated on the ice inside the Central Observatory (CO), in addition to those deployed on the ship itself. A unique advantage of the instruments deployed is that it provided for the first time a complete set of passive and active microwave observations collected over the same snow and ice types spanning frequencies from 1.4 to 89 GHz. Table 4.10.1 gives an overview on all instruments operating during Leg 2, the responsible person maintaining the instruments during Leg 2, and the responsible PI on land.

When Leg 2 arrived to the CO, none of the on-ice remote sensing instruments were measuring. This is because they were threatened by large cracks on three sides of RS city, and were moved closer to the hut. The Leg 2 remote sensing team started to redeploy the instruments on 21 December nearby the old site. By the end of December, the team had six instruments operational (Elbara, SSMI, GNSS-R, KuKa, L-SCAT, VIS/TIR camera). The remote sensing site 3 (RS3) was maintained throughout Leg 2 and successfully handed over to the Leg 3 remote sensing team.

Tab. 4.10.1: List of remote sensing instruments deployed/redeployed Leg 2 Remote Sensing Site 1 (18.10. to 16.11.2019) and Remote Sensing Site 2 (29.11.2019 to 13.12.2019). Refer to Leg 1 Cruise Report for detailed descriptions on location description, instrument setup and activities of Remote Sensing Sites 1 and 2.

Instrument	Details	PI	Institution	Leg 2 responsible
On the ice				
Ku/Ka-band radar	Dual-frequency scanning radar: 12-18 GHz (Ku) and 30-40 GHz (Ka)	J. Stroeve	U Manitoba	J. Stroeve
L-band Scatterometer	1.26 GHz scanning radar	R. Scharien	U. Victoria	V. Nandan
C-band Scatterometer	C-band (~5 GHz) scanning radar	J. Yackel	U Calgary	V. Nandan
X-band Scatterometer	9.6 GHz scanning radar	C. Duguay	U Waterloo	V. Nandan
MW Radiometer UWBRAD	Ultra-wideband 0.5 – 2 GHz radiometer (P to L-band)	J. Johnson	Ohio State University	J. Stroeve
MW Radiometer ELBARA	1.4 GHz (L-band)	M. Schwank/ T. Casal	WSL/ESA	R. Tonboe
SSMI Radiometer	19, 37, 89 GHz (K, Ka, W-band)	J. Stroeve	U Manitoba	J. Stroeve
MW Radiometer Balamis ARIEL	1.4 GHz (L-band)	C. Gabarro	ICM-CSIC	M. Huntemann

GNSS-R	reflected GNSS signals from snow/ice	E. Cardellach/ T. Casal	ICE-CSIC/ESA	M. Huntemann
Infrared Camera	Surface temperature	G. Spreen	U Bremen	M. Huntemann
Video Camera	Visual overview of RS site	G. Spreen	U Bremen	M. Huntemann
On Polarstern				
GNSS-R	reflected GNSS signals from snow/ice	W. Wan	Peking U.	Hailong Liu (Ocean Team).
GNSS-R & atmosphere	reflected GNSS signals from snow/ice and GNSS for atmospheric water vapor	M. Semmling	GFZ	D. Divine
GNSS Ionosphere	Ionospheric scintillations for GNSS measurements	F. Fohlmeister	DLR	D. Divine
MW Radiometer EMIRAD2	1.4 GHz (L-band)	S. Savstrup Kristensen/ T. Casal	DTU/ESA	R. Tonboe

Remote Sensing Site 3 (start: 21.12.2019)

On Friday, 13 December, when the Leg 2 team arrived with the Kapitan Dranitsyn, cracks appeared at the Remote Sensing Site 2 and the Leg 1 team retreated most of the instruments to the RS hut, on 14 December the last instruments were retreated and only Visual/IR cameras were left operational. The site was handed over to the Leg 2 team on 15 December. After Leg 1 left, Leg 2 evaluated the stability and feasibility of the site, and it was determined the instruments would be redeployed a bit further east of the previous site. The Remote Sensing Site 3 (RS3) was established on 21 December, and setup in an 'L-shaped' geometry near the old RS2 site sharing about 60% of the previous RS2 area. This site primarily consisted of a refrozen melt pond on second year ice. The first instrument redeployed was the KuKa radar and it collected data starting at 19:30 UTC. By 22 December, 6 out of 9 remote sensing instruments were operating (KuKa, SSMI, Elbara, GNSS-R, L-Scat and the Visual/IR Cameras). However, since the new RS3 site was located a bit further form the hut than the RS2 site, we decided to move the hut closer to the instruments on 30 December. This required power to be turned off to the instruments for a short period of time. After the hut move, we were unable to get Elbara working again. While Elbara became off line, other instruments were deployed, including X-SCAT (deployed 16 January), C-SCAT (deployed 3 February), and UWBRAD (deployed 6 January).

As of 23 February 2020 (DSHIP Device Operations end for Leg 2) ad 03 March 2020 (Return from Polarstern to Dranitsyn), GNSS-R, SSMI and UW-BRAD Radiometer, C-Scat, L-Scat and Visual/IR Cameras are operational and measuring. The photo in **Figure 4.10.1** shows the site layout as of 19 February, acquired from the visual camera (from the University of Bremen), installed on the top of the RS hut. The GNSS-R and SSMI are on the left-hand side of the L-arm, while C-Scat and L-Scat are on the other arm of the 'L', with the visual/IR camera deployed in the intersection of the 'L'. The UW-BRAD radiometer is deployed opposite to these instruments to avoid RFI, but scans the same snow-covered sea ice type.

Fig. 4.9.1: Overview of RS3 site as of 19 Feb 2020. (Photo: Screenshot from the University of Bremen's visual camera, installed on top of the RS hut).

The ice and snow properties at RS3 site are similar to that of RS1 and RS2 sites (refrozen melt-ponded second-year sea ice). Regular snow depth measurements were taken directly in front of every instrument (without disturbing the scan area), using an avalanche snow depth probe and recorded. With frequent blowing snow and accumulation events, snow depths increased from ~ 10 cm (measured on 23 Dec) to a maximum of ~ 81 cm (measured on 22 Feb) (**Figure 4.10.2**). The ice thickness was ~90 cm during the beginning of Leg 2, which further increased to 121 cm by 15 Jan (from ice core drillings). Occasional salinity ice cores were also taken behind the instruments, with the top 15 cm were almost found to be brackish (0.8±0.2 psu), and higher salinities towards the bottom (5.2±1.2 psu).

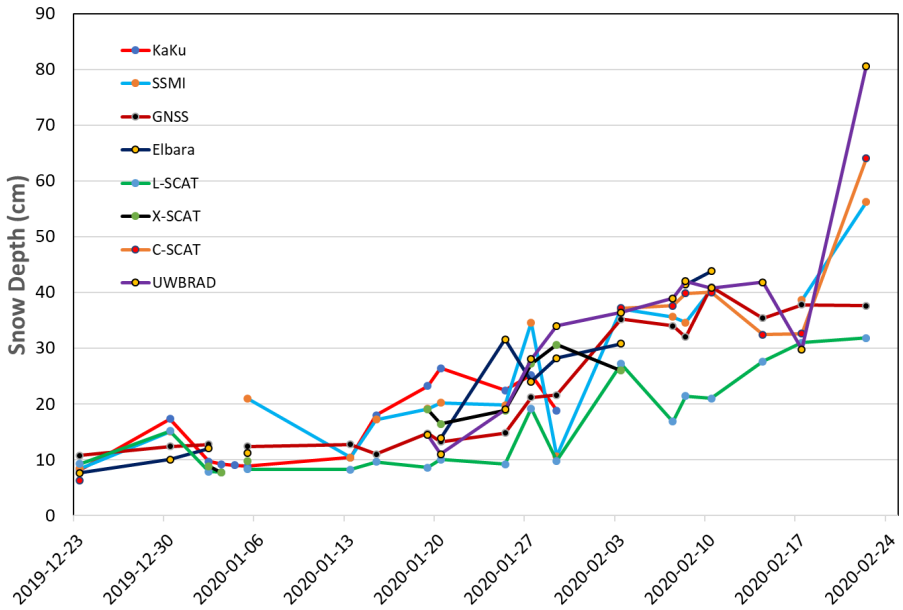

Fig. 4.9.2: Snow depth measurements recorded during Leg 2, around the instruments in the RS3 site.

Onboard Polarstern

All instruments onboard Polarstern were installed on the port side of upper and lower *Peil* deck, the highest deck of *Polarstern*. **Figure 4.10.3** gives an overview of the installations. Processing and data recording units were installed in the observation alley in front of the meteorologist's office.

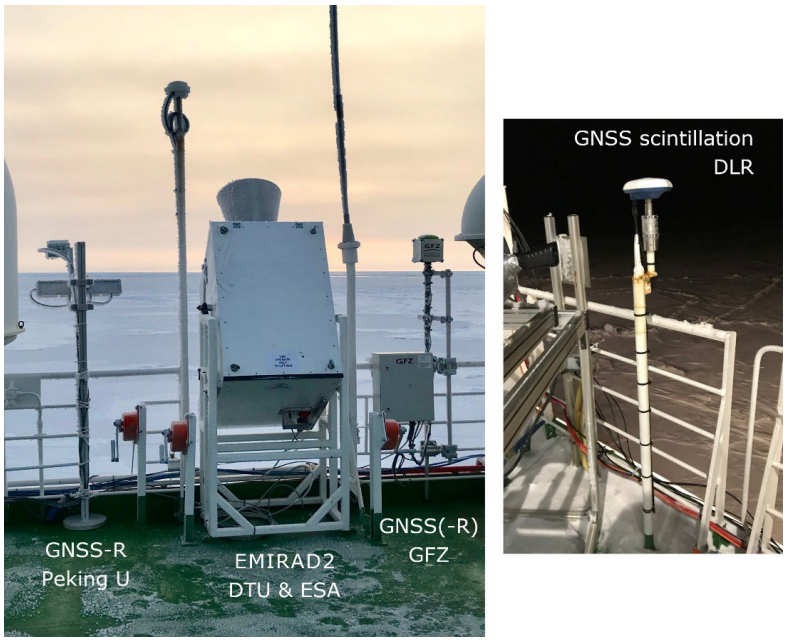

Fig. 4.9.3: Remote sensing installations on the port side of Peil

Details and Operational Status of RS Instruments (both on ice and on board)

In total 14 different instruments were operated as part of the Remote Sensing task during Leg 2, 10 on the ice and 4 onboard. All of the instruments worked at some point during Leg 2, yet all were not operational at the same time. Here we give a brief overview of the instruments and their measurement periods during leg 2.

Radar Ku/Ka-band (Not Operational – To be redeployed in Leg 4)

- Ku- (12–18 GHz) and Ka-band (30–40 GHz) radar mounted to a pedestal on a sled with flotation devices
- Nadir view for altimetry application; elevation and azimuth scanning as scatterometer
- Has additional sledge to be towed along transect in nadir configuration
- DSHIP/SensorWeb: Radar dual Ka- and Ku-band altimeter (KuKa_Radar)
- University of Manitoba
- Projects: U Manitoba Canada C150 Chair Program, NERC MOSAiC funding, and ESA MOSAiC remote sensing
- Corresponding satellite observations: CryoSat-2, Sentinel-3, AltiKa, ERS-1/2, Envisat, and future CRYSTAL altimeters; NSCAT, QuikSCAT, OSCAT, SCATSAT1, CFOSAT scatterometers

The instrument was operated in a permanent scanning mode while at the RS site (typical angle range: ±45° azimuth, 0–50° elevation) with a break of 55 minutes between the scans (30 minutes during Leg 1). One calibration was made during Leg 2 using a corner reflector. For the Transect Task (Section 4.4) the two radars were mounted on a smaller and more lightweight sledge in a nadir configuration and towed with a skidoo along the northern and southern transect loops. Additional transects were made for special events, including leads and first-year ice floe.

Scientific Objectives:

1. Better understanding of radar interface and volume backscatter in the snow layer and corresponding range biases as a function of seasonally varying snow pack properties;
2. Validation and algorithm development of satellite retrieval of snow depth on sea ice with dual-band altimetry; Better characterization of the uncertainty of freeboard retrieval in regions and periods where no validation data is currently available.

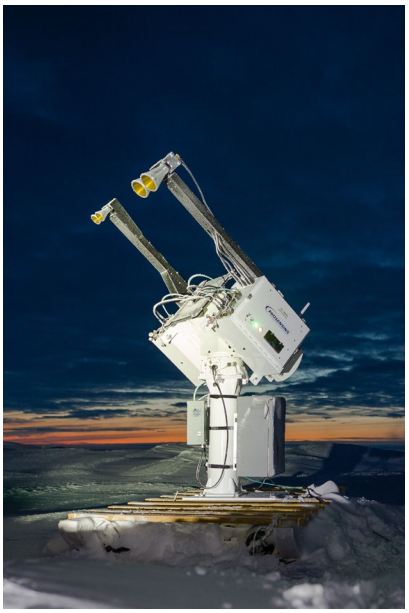

Fig. 4.9.4: Ku/Ka-band radar (photo: Stefan Hendricks)

Research Questions:

1. What is the seasonal evolution of snow backscatter at Ku/Ka-Band, especially in mid-Winter? What is the impact of snow accumulation and changes of snow properties?
2. What is the lateral variability of snow backscatter within the footprint of a satellite radar altimeter?
    a. Can potential changes in snow backscatter in both bands be constrained by auxiliary information (e.g. reanalysis data)?
    b. What is the impact of salinity on Ku and Ka-band backscatter?

Output:

- Co-located Ku- and Ka-band backscatter at cm-scale range resolution
- Tracked range distance for primary scattering horizon in nadir mode. Difference between Ku (snow-ice interface) and Ka (air-snow interface) frequency could be indicative for snow depth.

Operational Status during Leg 2: From 21 December 2019 through 31 January 2020, the instrument operated in near hourly scanning mode at the RS3 site, and weekly transects were made in nadir mode along the northern and southern transect loops (see Table 4.10.2 for list of transects made during Leg 1 and 2). After the 31st of January, the instrument was brought back to the ship to diagnose failures in the scanning mode, as the instrument would randomly shut down after a few hours of data collection. The team found that some wires from the GPS in the Ku RF unit became lose, along with a wire on the RCB board which likely caused the random shutdowns of the scanning and Ku-RF unit. The jarring of the instrument during the transects also appeared to loosen bolts that held the lid. Turning on the unit inside the ship resulted in further failures of the computer boards. Spare computer boards were sent to Svalbard and are awaiting the Polar 5/6 flights to bring them to Polarstern for Leg 4. The hope is that the instrument will be operational again before the end of Leg 3 and continue to collect data in both scanning and transect mode through advanced melt.

Since surface conditions were relatively stable through a full diurnal cycle during Leg 2, scanning mode measurements were collected every 50 minutes between -45 and + 45o azimuth and from 0 to 60o in elevation. Figure 4.10.5 depicts an example 24-hr Ka- and Ku--Scat VV-polarization channel dataset, acquired on 20 January. The data files were copied almost daily from the instrument to the MOSAiC Central Storage (MCS). The scan files are stored under Device operation PS122/2_14-288. Weekly transect data files are stored based on their weekly time-tags under the PS122/2 directories (e.g. PS122/2_18_*,PS122/2_19_*,...).

Table 4.10.2. *Dates for when the northern and southern transects were conducted, in addition to dates when the instrument sampled lead/frost flowers as well as first-year ice at the runway site.*

Date	Northern Transect	Southern Transect	Lead/Frost Flowers	Runway – first-year ice
7 November 2019	X			
14 November 2019	X			
23 November 2019			X	
20 December 2019	X			
26 December 2019	X	X		
2 January 2020	X	X		
9 January 2020	X	X		
12 January 2020				X
16 January 2020	X	X		
19 January 2020				X
23 January 2020			X	
24 January 2020			X	
30 January 2020	X	X		

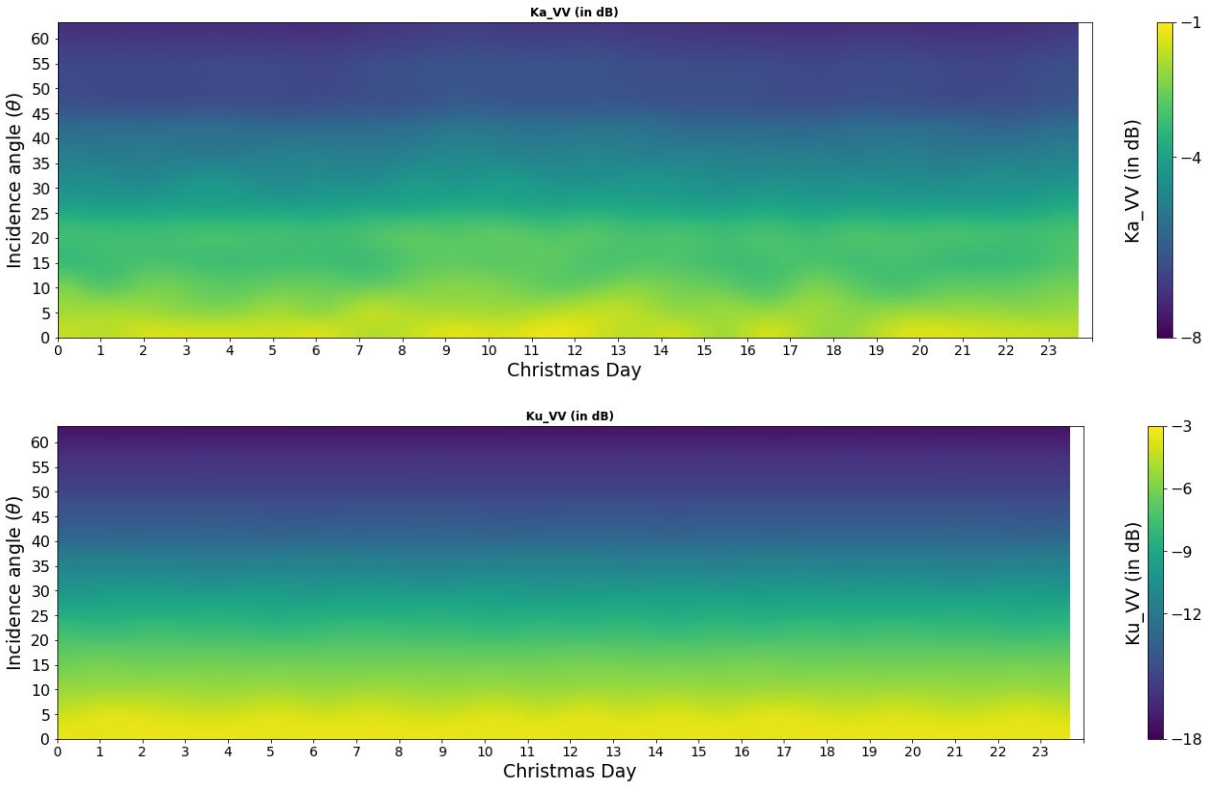

Figure 4.10.5.: Bilinear interpolated surface plot (hourly-averaged) of VV-polarized backscatter, acquired by KuKa on 25th December 2019. Time (in hours) are plotted along x-axis and incidence angle (in degrees) along y-axis. (Plot: Vishnu Nandan).

Scatterometer L-band (L-Scat) (Operational)

- L-band (Centre Frequency:1.26 GHz), fully-polarimetric scatterometer
- Bandwidth: 500 MHz, range resolution 0.3 m
- Antenna beamwidth: 14°

- Transmit power: -13.5 dBm
- DSHIP/SensorWeb: Scatterometer L-band (**Scat-L**) (IP: 192.168.3.127)
- University of Victoria, Canada; PI: Randall Scharien
- Project: CanScats supported by NSERC and EUMETSAT
- Corresponding satellite observations: L-band SAR: ALOS/PALSAR-1, -2, and -3; SAOCOM; NISAR; ROSE-L

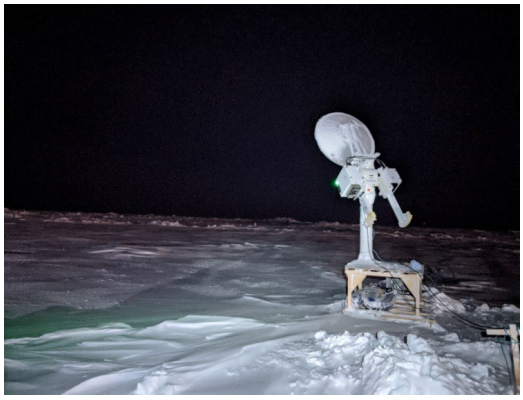

Fig. 4.9.6: L-Scat (Photo: Vishnu Nandan)

Scientific Objectives:

- Evaluation of current and future satellite missions with ground-based measurements.
- Investigation of the temporal evolution of radar backscatter and its changes caused by environmental conditions like snow accumulation and metamorphism, temperature changes, ice growth and melting, desalination, ice crusts and wind-packed snow formation, etc. for an entire annual sea ice cycle.
- Improving forward models of radiative transfer in snow and sea ice like the Snow Microwave Radiative Transfer Model (SMRT) and Microwave Emission Model of Layered Snow-packs & Active (MEMLS-A) with the goal to develop new satellite retrievals.

Output:

- Calibrated polarimetric radar backscatter data at L-band frequency

Operational Status: Throughout Leg 2, the L-Scat (**Fig. 4.10.6**) operated in a permanent scanning mode stationery at the RS3 site. The L-Scat is presently programmed to measure automatically once every 55 min between -30° to +45° azimuth-, and at 18° to 66° (at 3° steps) incidence-angle range. **Figure 4.10.7** depicts an example 24-hr L-Scat VV-polarization channel dataset, acquired on 20 January. The L-Scat scan files are automatically copied every night at 0400 hrs (ship time), from the L-Scat server to the MOSAiC Central Storage. The scan files are stored under Device operation **PS122/2_14-292** in **Scat-L** for continuous measurements, and was recommended to the Leg 3 team to use this device operation for continuous measurements.

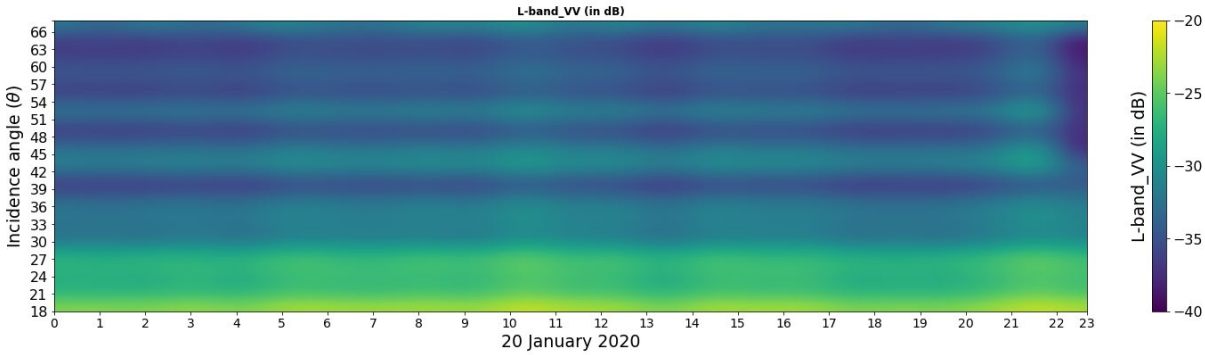

Fig. 4.10.7: Bilinear interpolated surface plot (hourly-averaged) of VV-polarized backscatter, acquired by L-Scat on 20th January 2020. Time (in hours) are plotted along x-axis and incidence angle (in degrees) along y-axis. (Plot: Vishnu Nandan)

Whenever feasible, the L-Scat sled was moved along-track either forward or backward (depending on the availability of cable slack) at least 60 cm or more (upon request by the PI), and collected measurements, to acquire more independent samples of the snow-covered sea ice than possible by one static position. The scan files in the moved position were noted as a readme text file in the MCS, as being in the modified position.

On 7 February, L-Scat calibration was successfully conducted using the L-Scat corner reflector and mounting pole. The calibration files were sent to the PI and to ProSensing, to check for calibration data quality and recommendations were made to conduct additional calibrations in Legs 3 and 4.

A standard operational procedure document for L-Scat (exclusive for MOSAiC operations) was drafted in Leg 2, and handed over to Leg 3 team, and the document is saved under 'Documentation' in the TEAM ICE Public Folder.

Scatterometer C-band (C-Scat) (Operational)

- C-band (Centre Frequency: 5.52 GHz), fully-polarimetric scatterometer
- Range resolution: 0.3 m
- DSHIP/SensorWeb: Scatterometer C-band (**Scat-C**) (IP: 192.168.3.174)
- University of Calgary, Canada; PI: John Yackel
- Project: CanScats supported by NSERC and EUMETSAT
- Corresponding satellite observations: C-band SAR: Sentinel-1 A/B, RADARSAT-1/2, RADARSAT Constellation Mission (RCM); ASCAT scatterometers

***Fig. 4.9.8**: C-Scat (Photo: Vishnu Nandan)*

Scientific Objectives:

- see under "Scatterometer L-band"

Output:

- Calibrated polarimetric radar backscatter data at C-band frequency

Operational Status: Since 3 February, the C-Scat (**Fig. 4.10.8**) operated in a permanent scanning mode stationery at the RS3 site. The C-Scat is presently programmed to measure manually 5 to 10 scans every day, between 0° to 45° azimuth-, and at 24° to 60° (at 3° steps) incidence-angle range. The C-Scat scan files are automatically copied every night at 0400 hrs (ship time), from the C-Scat ELNORA server to the MOSAiC Central Storage. The scan files are stored under Device operation **PS122-2_14-290** in **Scat-C** for continuous measurements, and was recommended to the Leg 3 team to use this device operation for continuous measurements. The data acquisition program "scatd" running on the C-Scat server stopped working and crashed after a few hours on a regular basis. No data is lost. Measurements had then to be restarted from the ship or from the RS hut via network. Data transfer were accomplished via network as well using SSH.

Instrument Repair and Refurbishments: During Leg 1, although C-Scat measured continuously, it was later found during Leg 2 that the measurements were noise, and that the tracker/positioner lost its configuration file. No usable C-Scat measurements were recorded in Leg 1. Therefore, the C-Scat was retreated back to the ship for repair on 28 December. C-Scat underwent multiple rounds of refurbishments:

Replacement of C-Scat tracker/positioner by a spare tracker from the University of Waterloo's X-Scat system. The C-Scat tracker was replaced after two tracker motor capacitors were found to be defective. Although the capacitors were replaced, we found multiple hardware failures

(including motor circuit), which led to a decision to replace the tracker with the spare X-Scat tracker. The replacement was successful. It was also found that, during the diagnosis, the power supply unit installed on the C-Scat RF unit and the oscillator generator circuit was defective. The power supply was replaced with a spare unit obtained from the ship's workshop, while a switch had to be installed to activate the oscillator circuit. Both replacements were successful.

Following extensive and successful troubleshooting, repair and refurbishments, C-Scat was redeployed on the RS site on 2 February, and started measuring from 3 February. Initial scans after redeployment were sent to the PI and ProSensing for data quality check (successful).

C-Scat corner reflector calibration is pending, planned for Leg 4.

A standard operational procedure document for C-Scat (exclusive for MOSAiC operations) was drafted in Leg 2, and handed over to Leg 3 team, and the document is saved under 'Documentation' in the TEAM ICE Public Folder.

Scatterometer X-band (X-Scat) (Not Operational – To be redeployed in Leg 4)

- X-band (9.6 GHz), dual-polarisation (H+V) scatterometer
- Bandwidth: 500 MHz, range resolution 0.3 m, sensitivity -50 dB m^2/m^2 at 15 m range
- Antenna beamwidth: 4.3° (narrow) to 5.8° (flood)
- Transmitted power: -9.5 dBm (flood) to -11.8 dBm (narrow)
- DSHIP/SensorWeb: Scatterometer Ku- and X-band (**Scat-ku_x**)
- University of Waterloo, Canada; PI: Claude Duguay
- Project: CanScats supported by NSERC and EUMETSAT
- Corresponding satellite observations: TerraSAR-X, PAZ, COSMO-Skymed;

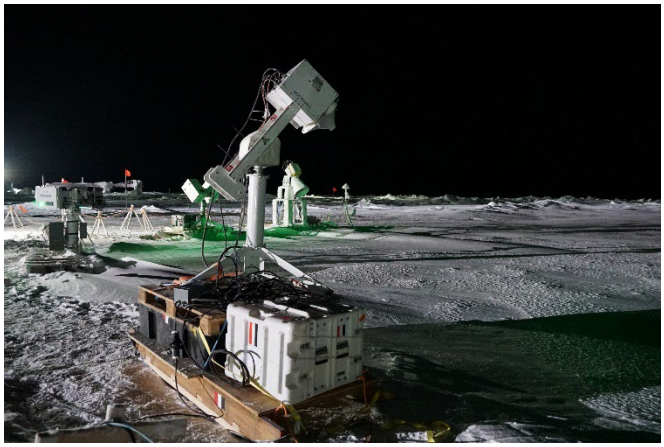

Fig. 4.9.9: X-Scat (Photo: Julienne Stroeve)

Scientific Objectives:

- see under "Scatterometer L-band"

Output:

- Calibrated polarimetric radar backscatter data at X-band frequency.

Operational Status: The X-Scat (**Fig. 4.10.9**) was in permanent scanning mode, stationery at RS3 site between 16th and 30th January. During the initial phase of Leg 2, the X-Scat system had to retreated back to the ship on 28 December, since the radar system was working but the tracker was dysfunctional. The tracker was diagnosed and it was found that the tracker loses its configuration file which led the tracker unable to respond to azimuth and incidence angle movement commands. The tracker was uploaded with new configuration file and a defective capacitor was replaced which solved the problem. Upon repair and refurbishment, the X-Scat was redeployed on 16 January and started measuring. The scans were done manually from the RS hut and downloaded and uploaded to the MCS **Scat-ku_x** sensor under **PS122-2_14-317**. No usable X-Scat measurements were recorded in Leg 1.

On 30 January, the X-Scat stopped working. The system was retreated back to the ship on 5 February and diagnosed. It was found that the X-Scat computer motherboard installed inside the data acquisition box had failed, due to presence of snow in the circuit, causing it to short

circuit the system. Since the X-Scat system did not have any spare computer, it was decided to wait until Leg 4 for the spare parts to be brought in. On 15 February, the X-Scat was packed onto respective boxes and stored in the ship's A-Deck (excluding the data acquisition box, stored inside the AWIU900-4 warm container).

X-Scat corner reflector calibration is pending, planned for Leg 4.

A standard operational procedure document for X-Scat (exclusive for MOSAiC operations) was drafted in Leg 2, and will be used by Leg 4 team, and the document is saved under 'Documentation' in the TEAM ICE Public Folder.

Microwave Radiometer UWBRAD (Operational)

- 0.5 to 2 GHz in four channels (540, 900, 1380 and 1740 MHz)
- 125 MHz bandwidth resolved in 512 sub-channels per each of the four channel
- DSHIP/SensorWeb: Ultra-Wideband Software-defined Microwave Radiometer (0.5-2GHZ) (UWBRAD)
- Ohio State University
- Project: "Ultra Wide Band Radiometer Measurements of Sea Ice" supported by NSF
- Corresponding satellite observations: SMOS, SMAP, Aquarius

***Fig. 4.9.10**: UWBRAD microwave radiometer (photo: Julienne Stroeve)*

Scientific Objectives: The UWBRAD (Ultra-Wide Band Microwave Radiometer) is a novel instrument designed to observe sea ice microwave emissions at four different channels (540, 900, 1380 and 1740 MHz) over the spectrum range 0.5–2 GHz in real-time. Each channel occupies 125 MHz bandwidth resolved into 512 sub-channels, and the medium rate data samples are generated approximately every four seconds after integration over 100 ms acquisition. The lowest channel of UWBRAD is more sensitive to the emissions from deeper layers of the ice compared to the space-borne radiometers operating at L-band, so it will contribute to the estimations of thicker ice floes. In addition, its advanced sampling features allow the instrument to detect the spectral and temporal changes of ice properties with a high precision. The UWBRAD also performs an advanced RFI mitigation algorithm over each channel to clear the acquired data from unwanted signals which allows it to operate at a large bandwidth.

Output:

- Integrated brightness magnitudes for both the ice surface and the sky before the calibrations and RFI mitigations.

Operational Status: This instrument was the most difficult to deploy and maintain during Leg 2. Power and Network cables were destroyed by a polar fox, the UPS had trouble powering up in the cold, cables attached to the rotation box broke, and network connection would randomly shut down. Data were mostly continuous during the last two week of January through the handover to Leg 3.

Microwave radiometer ELBARA

- L-band (1.4 GHz)
- Swiss Federal Institute WSL
- DSHIP/SensorWeb: Microwave Radiometer ELBARA L-band (ELBARA)

- Project: ESA MOSAiC remote sensing
- Corresponding satellite observations: SMOS, SMAP, Aquarius

Scientific Objectives:

- The large penetration depth of electromagnetic waves at L-band provides good sensitivity to thickness of ice up to approximately 0.5 meter.
- Volume scattering from snow microstructure and brine and air inclusions in the ice is negligible in the microwave L-band. This means that microwave emission models for L-band do not need to include volume scattering.
- Coincident measurements of L-band microwave emission and in-situ sea ice profiles of e.g. dielectric properties are used for the development and improvement of sea ice microwave emission models and corresponding retrieval schemes.
- Better understanding of the emissivity for improved satellite retrieval of sea ice parameters or assimilation of brightness temperatures in ocean-ice forecast models.

Output:

- Calibrated microwave brightness temperature data at L-band frequency

Operational Status: The sampling goal was to have ELBARA operating continuously at a constant incidence of 40°, with once per week sky calibration at 130° incidence angle to be performed. The instrument was redeployed during Leg 2 on 21 December. Data was downloaded daily to the MCS by manually using ftp to transfer files. However, while the instrument functioned properly upon initial deployment, once the hut was moved and the power was turned off, Elbara stopped working. One reason may be a fuse that was blown during the power instability, as well as moisture inside the computer. Spare computer was brought with Leg 3 and the instrument was redeployed until ice breakup caused the power to be shut off again at RS3.

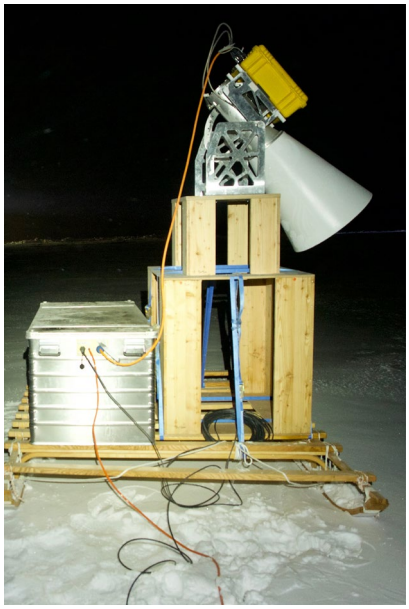

Fig. 4.9.11: ELBARA microwave radiometer (photo: Gunnar Spreen)

Microwave radiometer 19-37-89-GHz

- Dual-polarization microwave radiometers
- 19 GHz, 1 GHz bandpass, 0.04 K sensitivity for 1 second delta T, direct detection (AC1900)
- 37 GHz, 2 GHz bandpass, 0.03 K sensitivity for 1 second delta T, direct detection (AC3700)
- 89 GHz, 4 GHz bandpass, 0.08 K sensitivity for 1 second delta T, double-sideband downconvert (AC8900)
- Manufacturer: Radiometrics Corporation
- Kipp & Zonen 2AP positioner
- DSHIP/SensorWeb: Microwave Radiometer 19, 37, 89 GHz (SSMI type) (SSMI_radiometer_SN002)
- University of Manitoba
- Projects: U Manitoba internal
- Corresponding satellite observations: NIMBUS-5 ESMR, NIMBUS-7 SMMR, AMSR-E/2, SSM/I, SSMIS, MetOp SG MWI, CIMR, MWR

Scientific Objectives:

- Evaluation of satellite microwave radiometers with ground-based measurements. While the point-measurements do not fully cover the footprint of the satellite observations, they will allow investigation of the temporal evolution of signals caused by environmental changes like snow accumulation and metamorphism, temperature changes, ice growth and melting, desalination, ice crusts and wind-packed snow formation, etc. These environmental changes are effective on a satellite footprint scale, which will allow to compare the temporal evolution of the ground-based and with current satellite radiometers like AMSR2 and SSMIS measurements and preparation for MWI and CIMR.
- Develop a better understanding of the electromagnetic wave interaction with snow and sea-ice and thus the brightness temperature measured by satellite radiometers. To develop retrieval methods of snow and ice properties from these measurements, improved forward models of the radiative transfer in the snow and sea ice are needed. To develop and validate such models joint ground-based microwave radiometer measurements with in-situ measurements of all relevant variables are needed.
- The measurements at 19, 37, and 89 GHz will be analyzed in conjunction with the lower frequency microwave radiometer measurements by ELBARA, EMIRAD2, Balamis ARIEL, and UWBRAD. Together the full frequency range from P to W-band will be covered.

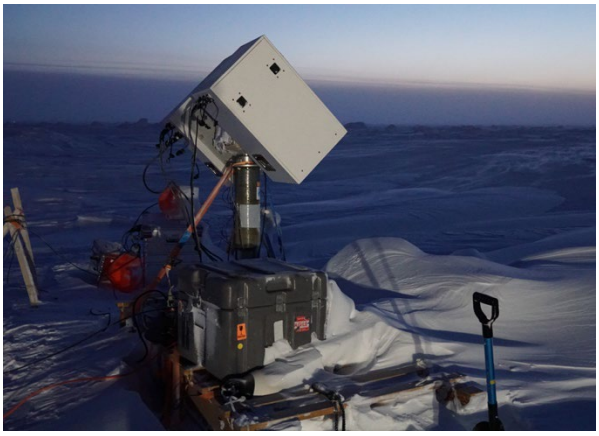

Fig. 4.9.12: 19-37-89-GHz microwave radiometer after snow drift event (photo: Julienne Stroeve)

Output:

- Calibrated microwave brightness temperature data at frequencies 19, 37, and 89 GHz.
- Photographs of the field of view of the radiometers in regular intervals

Operational Status: In contrast to Leg 1 where the 19, 37 and 89 GHz channel radiometer was operating only periodically (i.e. scans were obtained at least weekly for a duration of several scan cycles together with periods of fixed incidence angle (45o) at other times), during Leg 2 we ran the radiometer continuously, scanning from 30 to 60o in increments of 5o. These measurements are supported by a visual camera that takes an image for each scan. While no calibration was made during Leg 1, Leg 2 team performed both a sky calibration (December 23, 2019) and an absorber calibration (February 8, 2020). During Leg 2 we had time to evaluate the data collected during Leg 1 and also during Leg 2. During this evaluation we found that there was RF interference (see Figure 4.10.13) and we further found there was a problem with the 37 GHz channel, which would have large erroneous fluctuations in brightness temperature. The instrument was brought inside on 5 January to diagnose the problem, and after our evaluation and conversations with Radiometrics, it appeared that the 37 GHz channel had failed. Since Radiometrics no longer supports this old instrument, we decided to redeploy the instrument on 9 January as the 19 and 89 GHz channels were functioning as expected. It should be noted that at times the 37 GHz would still give good data values, but mostly the data was unstable until it was fixed permanently on 27 January. The fix happened after a storm that caused the instrument power/computer box to become filled with snow. All components were taken apart and dried inside the hut and later remounted. After this, the 37 GHz channel provided brightness temperatures in the expected range.

Note on January 18, 2020 a polar bear visited the RS3 site and moved the 89 and 37GHz feedhorn at 21:00 UTC. This was corrected the following day and the instrument was turned

back on at 13:22 UTC. Leg 2 continuous data are stored in PS122-2_14-163. We additionally moved the instrument to a second year ice floe on 10 February 2020 until 13 February 2020, and on 14 February 2020, we performed a hair-dryer experiment, where the snow surface was heated with a heat gun and brightness temperatures were collected prior, during and after. Snow and ice samples were taken. Instrument was moved back to the refrozen melt pond location on 14 February 2020. Finally, we attempted one northern loop transect with the SSMI instrument but found the pedestal was not stable enough to handle the vibrations of the towing with skidoo.

Note the GPS gives the wrong dates in all the data files, while the UTC times are correct. Readme files contained in the directories provide information that can help reconcile the dates.

Instrument was functioning as expected during the handover to Leg 3 and continued making 5o increment scans from 30 to 60o incidence angle. Data should be downloaded once every 2 weeks by removing the USB and placing into a computer to download and transfer to the MCS.

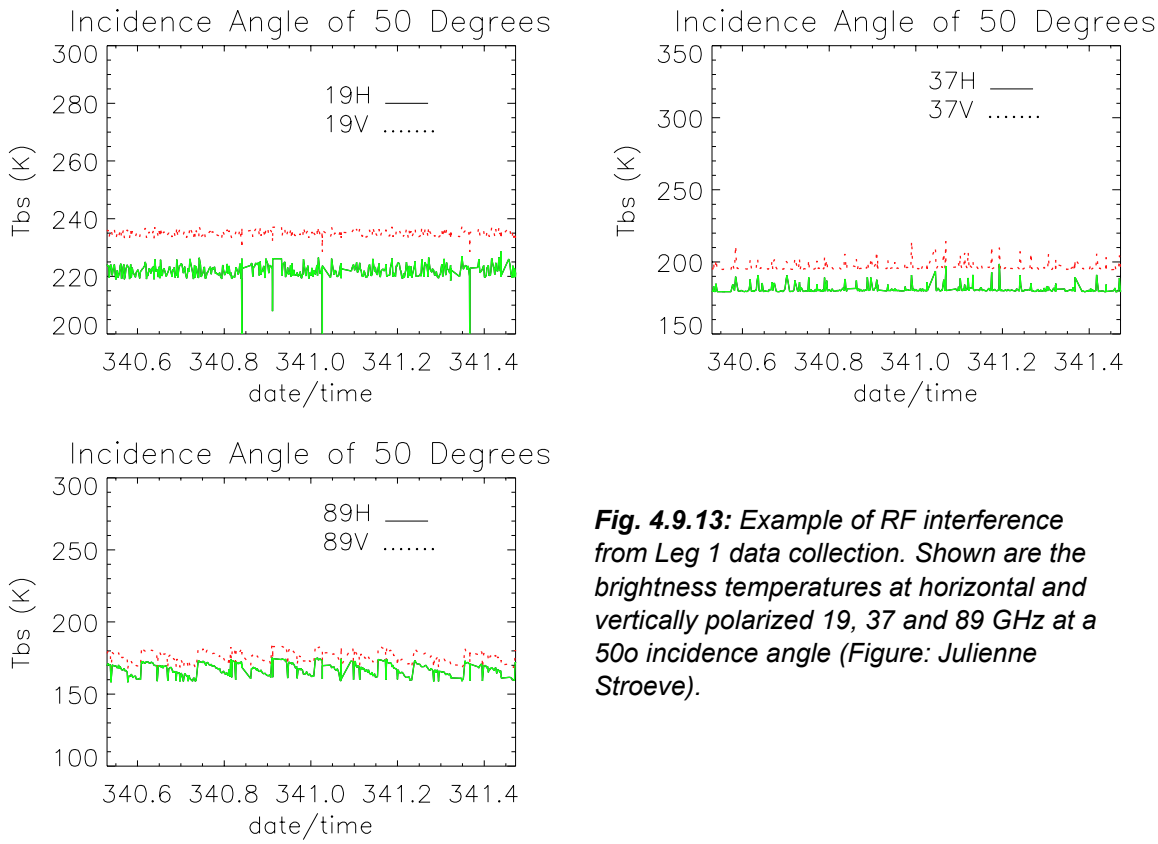

Fig. 4.9.13: *Example of RF interference from Leg 1 data collection. Shown are the brightness temperatures at horizontal and vertically polarized 19, 37 and 89 GHz at a 50o incidence angle (Figure: Julienne Stroeve).*

Microwave radiometer Balamis ARIEL

- L-band (1.413 GHz), dual-polarisation (H+V)
- Bandwidth 20 MHz, 0.7 K radiometric accuracy at 1 Hz
- Beamwidth: ~ 37°
- Manufacturer: Balamis

- Operated on a sledge to be pulled along transects; sledge parked at remote sensing site
- Institut de Ciències del Mar - CSIC
- DSHIP/SensorWeb: BALAMIS_Radiometer (BALAMIS_Rad)
- Project: “Improving emission models for sea ice low-frequency microwaves” supported by Spanish MOSAiC funding (MINECO)
- Corresponding satellite observations: SMOS, SMAP, Aquarius

The Balamis ARIEL radiometer was only operated during transects. See description in Section 4.4.

Scientific Objectives:

- Measurements of brightness temperatures at L-band frequencies for snow covered ice across a long period of time under varying environmental conditions.
- Spatial and temporal variability of 1.4 GHz brightness temperatures by combining measurements from two radiometers, i.e. ARIEL and ELBARA, and comparison against satellite measurements.
- Validation of microwave emission models across frequencies using collocated remote sensing and in-situ measurements.
- The data collected will be the basis for improved sea ice emission / radiative transfer models, for improved retrieval algorithms of key sea ice parameters

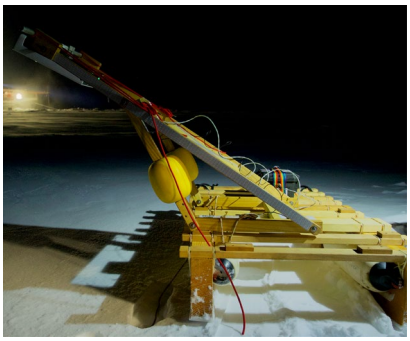

Fig. 4.9.14: Balamis ARIEL microwave radiometer (photo: Gunnar Spreen)

Output:

- Calibrated microwave brightness temperature data at L-band frequency.

Operational Status:

Balamis ARIEL leg 1 measurements were diagnosed with severe RFI affecting all measurements which compromised all collected data so far during leg 1 and leg 2. During Leg 2 several tests were made to finally find the RFI to be internal to the ARIEL box. Several attempts guided by Roger Jove from Balamis were made to reduce RFI contamination by isolation of unused cable openings within the ARIEL box. On later transects during leg 2 ARIEL was operated solely to see the influence of temperature on the RFI contamination issue. No operation temperatures were found where the ARIEL had reduced or no RFI.

Microwave radiometer EMIRAD2 (ONBOARD)

- Location: upper Peil deck, port side
- L-band (1.400–1427 GHz)
- Full polarimetric
- Retrieved geophysical variables: ice thickness up to 1 m
- Technical University of Denmark
- DSHIP/SensorWeb: Microwave Radiometer L-band EMIRAD2 (EMIRAD2)
- Project: ESA MOSAiC remote sensing
- Corresponding satellite observations: SMOS, SMAP, Aquarius

EMIRAD was operated continuously at 45° incidence angle from the time we left the Russian EEZ on leg 1 and it has been measuring continuously throughout leg 1 and leg 2. About twice per week a sky calibration at 150° and additional measurements at 35° and 55° were done.

Occasionally, housekeeping data were processed for one day and sended back to the PI SSK for evaluation. According to SSK the instrument was operating nominally. Sampling of snow and ice properties (snow depth, density, salinity and ice salinity and microstructure of the upper part of the ice were done near the EMIRAD2 footprint on the following dates 2020/01/29, 2020/02/09, 2020/02/16, 2020/02/22.

Scientific Objectives:

- See under “Microwave radiometer ELBARA”

Output:

- Calibrated microwave brightness temperature data at L-band frequency

GNSS reflectometry on ice

- DSHIP/SensorWeb: GNSS Reflectometry equipment on MOSAiC Sea Ice Floe (GNSS-R_IceFloe)
- Sub-device: GNSS Reflectometer at dual linear polarizations on MOSAiC sea ice floe (GNSS-R_LinPol)
- Instituto de Ciencias del Espacio (ICE-CSIC/IEEC)
- Project: ESA MOSAiC remote sensing
- Corresponding satellite observations: UK TDS-1, future: ESA PRETTY, China FY-3E and Taiwan FS-7R

The three GNSS antennas are installed on a tripod and are controlled by the GNSS receivers and instrumentation in a Zarges box located close by. The installation is meant for continuous operation. However, the powering and recharging of the internal battery did not work during leg 1 and the beginning of leg 2. Therefore, in the beginning of leg 2 the measurement periods were limited to the length the battery could power the instrument (typically 1-2 days). The batteries were exchanged during each visit to the RS sites. This issue was fixed by installing a different battery charger into the battery box and disconnecting the external 220V cable from power. After that the instrument was running without interruptions.

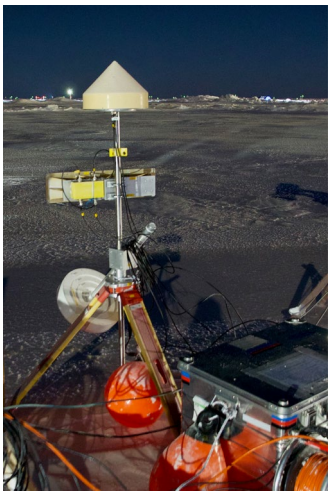

Fig. 4.10.15: GNSS Reflectometer (photo: Gunnar Spreen)

Scientific Objectives:

- GNSS signals reflect off the sea ice
- The delay, amplitude and polarization of the reflected signals can provide information about:
    - Sea Ice thickness
    - Sea Ice concentration
    - Snow layer on the Sea Ice
    - Sea Ice age

Output:

- Reflected GNSS data from the sea ice in four polarizations of LHCP, RHCP, Vertical, and Horizontal.

GNSS sea ice reflectrometry (ONBOARD)

- Location: upper Peil deck, port side
- Retrieved geophysical variables: snow depth, thin ice thickness
- Peking University
- Project: Chinese contribution to MOSAiC

- Corresponding satellite observations: UK TDS-1, future: ESA PRETTY, China FY-3E and Taiwan FS-7R

This GNSS system is used to observe the reflected GNSS signals from the snow and ice. No user interaction is needed. Only a regular daily check if the data is recorded was performed. When the software is interrupted, we have to restart the software. There are some temporary interruption (~several hours) for the recording program occurring on 28 Oct., 1 Nov., 7 Nov., 16 Nov., 27 Nov., 1 Dec., and 13 Dec. By the end of Leg 1, this system is handed over to Hailong Liu (Ocean Team).

Scientific Objectives:

- GNSS signals reflect off the sea ice
- The delay, amplitude and polarization of the reflected signals can provide information about:
    - Sea Ice thickness of thin ice
    - Snow depth
    - Moisture of snow layer over the ice

Output:

- Reflected GNSS data from the sea ice in four polarizations of LHCP, RHCP, Vertical, and Horizontal.

GNSS atmosphere and sea ice reflectrometry (ONBOARD)

- Location: upper Peil deck, port side
- Retrieved geophysical variables: atmospheric water vapour, sea ice properties like thin ice thickness
- Helmholtz Centre Potsdam GFZ, German Research Centre for Geosciences
- DSHIP/SensorWeb:
- GNSS-receiver for multi-GNSS observations (GNSS-receiver-TINY)
- GNSS-receiver for Occultation Reflectometry and Scatterometry measurements (GNSS-receiver-GORS)
- Corresponding satellite observations: UK TDS-1, future: ESA PRETTY, China FY-3E and Taiwan FS-7R

The GNSS system to observe reflected GNSS signals from the snow and ice and measure atmospheric water vapor from GNSS delay is a fully automatic system. No user interaction is needed. Only a regular weekly check if the data is recorded was performed. The system daily sends an email with a data report back to GFZ on land.

Scientific Objectives:

- The refractive delay of GNSS signals can be measured to estimate atmospheric parameters, for example, the atmospheric water vapor content.
- Reflected GNSS signals can be used to sense surface parameters including, for example, water or ice surface heights or the permittivity or amount of sea ice.
- Collect data of GNSS reflections over the Arctic ocean and sea ice. Delay and amplitude of these signals are used to investigate L-band reflectivity and penetration depth for different sea ice conditions. Dependencies on sea ice thickness, conductivity (brine content) and concentration will be in focus.

Output:

- Precipitable water vapor with accuracy of about 1 mm
- Reflected GNSS data from the sea ice

GNSS ionospheric scintillation (ONBOARD)

- Location antenna: lower Peil deck, port side
- Location processing unit: observation alley, in front of meteorologist's office
- Global Satellite Navigation Systems (GNSS) recording
- DLR, Germany
- DSHIP/SensorWeb:
- GNSS_NTlab_FE (GNSS_NTlab_FE)
- GNSS_navX_MBANT (GNSS_navX_MBANT)

The GNSS ionospheric scintillation installation is an autonomous instrument that does not require operator interaction. The operation and data acquisition were checked on a weekly basis. Some instrument problems lead to small manual changes of the data processing and acquisition software running on the instrument server, which was accomplished by the instructions from. The system daily sends an email with a data report back to DLR on land.

Scientific Objectives:

- Different distortions can severely degrade the GNSS accuracy and availability. One of these distortions are ionospheric scintillations, which occur mainly in equatorial and polar regions.
- The goal of this research is to record pre- and post-correlation samples of polar ionospheric scintillations to evaluate the impact of scintillations on GNSS and to develop new signal processing algorithms to mitigate scintillation from the received signal.

Infrared thermography system and visual camera

- VarioCAM HDx head 625
- Manufacturer: Infratec
- 7.5-14 µm, 640x480 pixel
- In addition to the IR camera a visual camera is installed for monitoring purposes
- DSHIP/SensorWeb: Infrared VarioCAM HDx head 625 (IR_VarioCAM_01)
- DSHIP/SensorWeb: Camera VIS_INFRALAN_01 (VIS_INFRALAN_01)
- University of Bremen
- Project: Satellite Remote Sensing – Germany and MOSAiC microwave RS supported by DFG

The infrared and visual cameras are installed together on one tripod, which is accompanied by one Peli case with a battery and an ebox PC for operation. Thus the system is mobile and can be moved to different sites. During leg 1 the system monitored the instruments field of view at RS 1 and RS2 sites. The time between the break-up of the RS1 site and the repositioning at RS2, the IR camera was setup at two different cracks with thin ice. Sampling was set to 10 minutes for the IR and 5 minutes for the visual camera.

During Leg 2 the tripod was installed several time temporarily on the Balamis ARIEL Sledge for transect measurements interupting the time series of the continues measurement ocacionally. During the transect the acquisition rate was adjusted to be 1Hz for both, Visual and Infrared camera.

Scientific Objectives:

- Monitor the surface temperature of snow and thin sea ice in dependence of environmental parameters like incoming longwave radiation, air temperature, water temperature, snow depth, and ice thickness.
- Provide a support dataset for the microwave radiometer and scatterometer measurements about the surface temperature variability at the remote sensing sites. The visual images will in addition support the interpretation of the microwave data.
- Derive the thickness of thin ice at leads and cracks from the surface temperature measurements.
- Support transect observation of ARIEL and Ku/Ka with additional footprint information about topography and temperature.
- Output from measurements:
- Time series of infrared brightness temperatures (every 10 minutes) and visual images (every 5 minutes) of the RS sites and two cracks
- Infrared brightness temperatures and visual images of transect situation in 1s interval

Fig. 4.9.16: Infrared and visual camera systems (photo: Gunnar Spreen)

Supporting snow and ice measurements

The measurements listed in **Table 4.10.1** will be combined with detailed measurements of the snow and sea ice close to the remote sensing validation site (e.g., thickness, densities, SSA, temperature, salinity, ice stratigraphy). Within the snow task (Section 4.2) “A” snow pits were performed on comparable snow and ice conditions to RS1 and RS2 at the respective “snow1” and “snow2” sampling sites. During leg 2 B+ snow pits were done in a sampling area adjacent to RS3. In addition, sampling of the ice salinity and upper ice microstructure was done behind the instruments occasionally during leg 2. The area around the instruments was sampled to investigate the site history. During transects (Section 4.7) with the mobile Balamis ARIEL radiometer and Ku/Ka-band radar systems, 6 “C” snow pits with additional salinity measurements were taken along the remote sensing transect (one section of the Northern transect). For continuous ice and snow thickness measurements at the RS1 site five thermistor chains (Section 4.6) were deployed at the locations indicated in **Figure 4.10.1**. At RS2 site two thermistor chains were deployed. One of them was extended with three snow temperature probes (Section 4.6) to form a transect over a snow dune. In addition to these activities described in the respective task sections, snow depth measurements were taken along the RS instruments. With the help of the BGC team salinity ice cores with a higher vertical resolution of 3 cm in the upper part were taken at the BGC1 site and during leg 2 at the RS3 site. In addition, the salinity cores (5 cm sections) from the “dark site” can be used. The additional snow and ice measurements performed within the remote sensing task are listed in **Table 4.10.14**. Many measurements from the ICE and other teams are relevant for interpreting the RS measurements. Here a none exclusive list of supplementary measurements:

Important supplementary measurements for the remote sensing program

- Meteorological data acquired on the ship and at MET city (Chapter 3)
- Helicopter (Section 4.8): laser scanning and thermal imaging for characterizing the snow, ridge, lead, over-frozen melt pond, and thin ice distributions of the CO and for regional upscaling for, e.g., comparison to satellite data.
- Terrestrial laser scanning (Section 4.2): snow distribution and redistribution by wind for the RS sites and CO

- Snow (Section 4.2): snow depth, density, grain size, moisture, salinity, presence of special structures (snow crust, superimposed ice), snow structure CT
- Ice cores (Section 4.5): density & salinity sections; thick, thin sections, and CT for air bubble, brine channel distributions and ice structure
- Autonomous observation in the CO and DN (Section 4.3): snow and IMB buoys, thermistor chains (CO), and snow temperature profilers (CO)
- Ice dynamics (Section 4.6): position data from all buoys of the distributed network; ice stress measurements (direct and laser array)

4.10.3 Preliminary (expected) results

All RS instruments (Table 4.10.1) will provide a time series of the seasonal development of their measured parameters, i.e., microwave brightness temperature and backscatter at different frequencies, reflected GNSS signals, infrared temperatures and visual images. Their variability and changes will depend on the atmospheric conditions, e.g., temperature and snow accumulation. The combination of on-ice remote sensing measurements together with the comprehensive snow and ice measurements will allow to improve microwave emission and scattering models of snow and ice, which in turn will lead to improved satellite remote sensing datasets.

Data recorded and stored in the MCS during legs 1 and 2 are primarily raw, uncalibrated measurements like backscatter power from the radars and voltages from the radiometers. We here show a few exemplary early results.

KuKa

Two primary goals of the KuKa radar are to improve our understanding of radar penetration into snow at Ku- and Ka-bands so that we can improve both sea ice thickness retrievals using satellite radar altimetry and to also retrieve snow depth as the difference in freeboards. The transect mode of the instrument is the most similar to radar altimetry and thus once a week we towed KuKa along the northern and southern transects to evaluate the evolution of radar backscatter as a function of snow depth and snowpack properties. Only a small section of the northern transect includes measurement of snowpack properties, whereas both the northern and southern transects include a full suite of snow depth and ice thickness observations.

An example of nadir mode backscatter for the northern and southern transect is shown in **Figure 4.10.17** Several key features are immediately apparent. One is that at both Ka- and Ku-band, the dominant backscatter tends to come from the snow/air interface. While we expected this to be true for Ka, the Ku-band radar is very sensitive and also sees strong backscatter at the snow/ice interface. The key difference is that the return is primarily limited to the air/snow interface at Ka, while at Ku-band there is significant penetration into the snow cover. In this example the local peak at the air/snow interface is generally stronger at Ku-band than at the snow/ice interface, but this will depend strongly on snow depth, density and composition (fresh or metamorphic snow). Instances along the transect where the backscatter is greater at depth are apparent. **Figure 4.10.17** also highlights the influence of snow depth on the backscatter, with less penetration and less multiple scattering observed for the data collected along the southern transect.

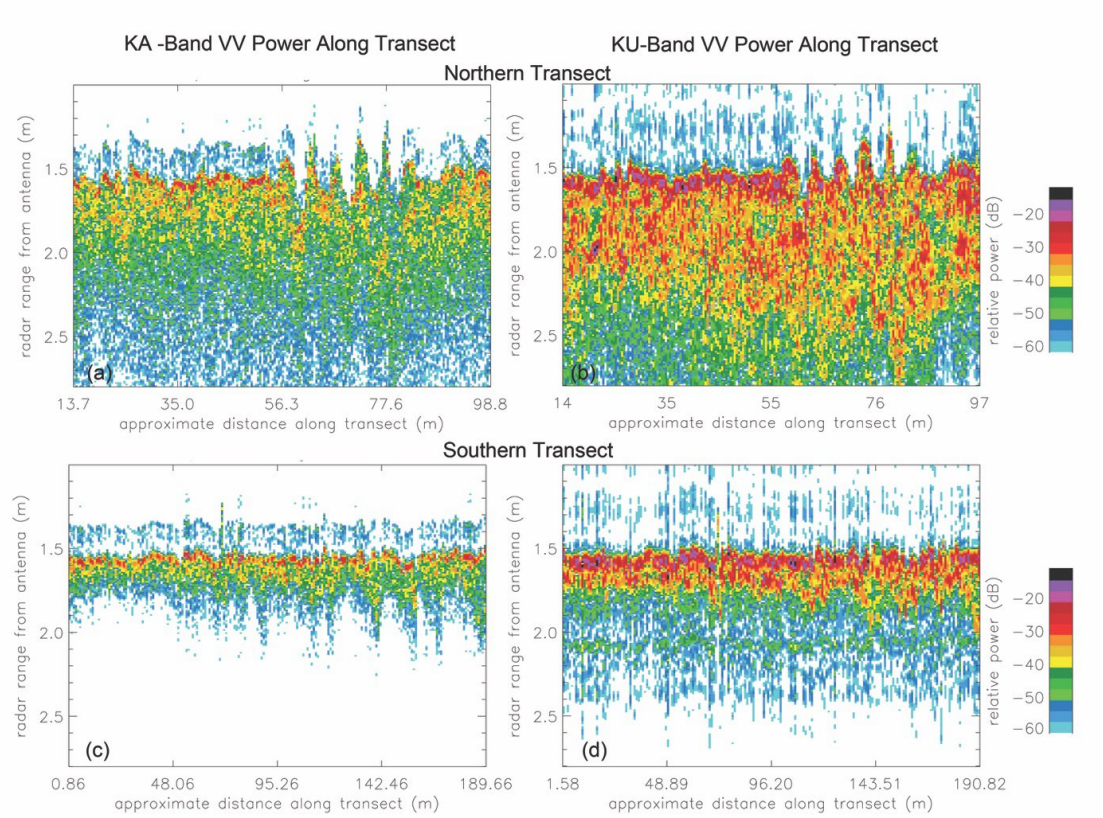

Figure 4.10.17: Ka- (a, c) and Ku-band (b, d) VV radar backscatter as a function of distance along the northern (top) and southern transect (bottom). Data acquired on 16 January 2020 at 10:52 and 12:02 UTC for the northern and southern transects, respectively. (Plot: Julienne Stroeve)

Benefits of multiple frequencies (L-Scat to Ka-Scat)

The multi-frequency aspect of the scatterometer measurements acquired from KuKa radar, X-Scat, C-Scat and L-Scat allows us to better determine the influence of different microwave scattering mechanisms from the snow-covered sea ice media on the measured signal. **Figure 4.10.18** illustrates an example of daily-averaged Ka-, Ku-, X-, C- and L-band VV-polarized backscatter measurements (as a function of incidence angle), acquired from RS site 3 on different days (since many instruments were not able to acquire data coincidentally). The scatterplot shows higher backscatter from Ka-band (possibly from the air/snow interface and upper snow layers) and lower backscatter from L-band (possibly from the sea ice volume).

19-37-89 GHz Radiometer

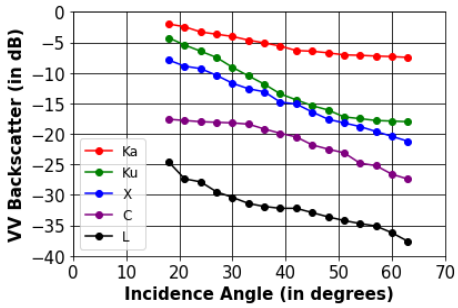

***Fig. 4.9.18**: Scatterplot of daily averaged Ka-, Ku-, X-, C- and L-band VV-polarized backscatter (y-axis) against incidence angle (x-axis). Note that Ka-, Ku- and L-band data are from 8 Jan, while X-band data is from 17 Jan and C-band data is from 6 Feb. Ka-, Ku-, and L-band data are calibrated. Markers represent the mean backscatter and joined by a cubic spline interpolation.*

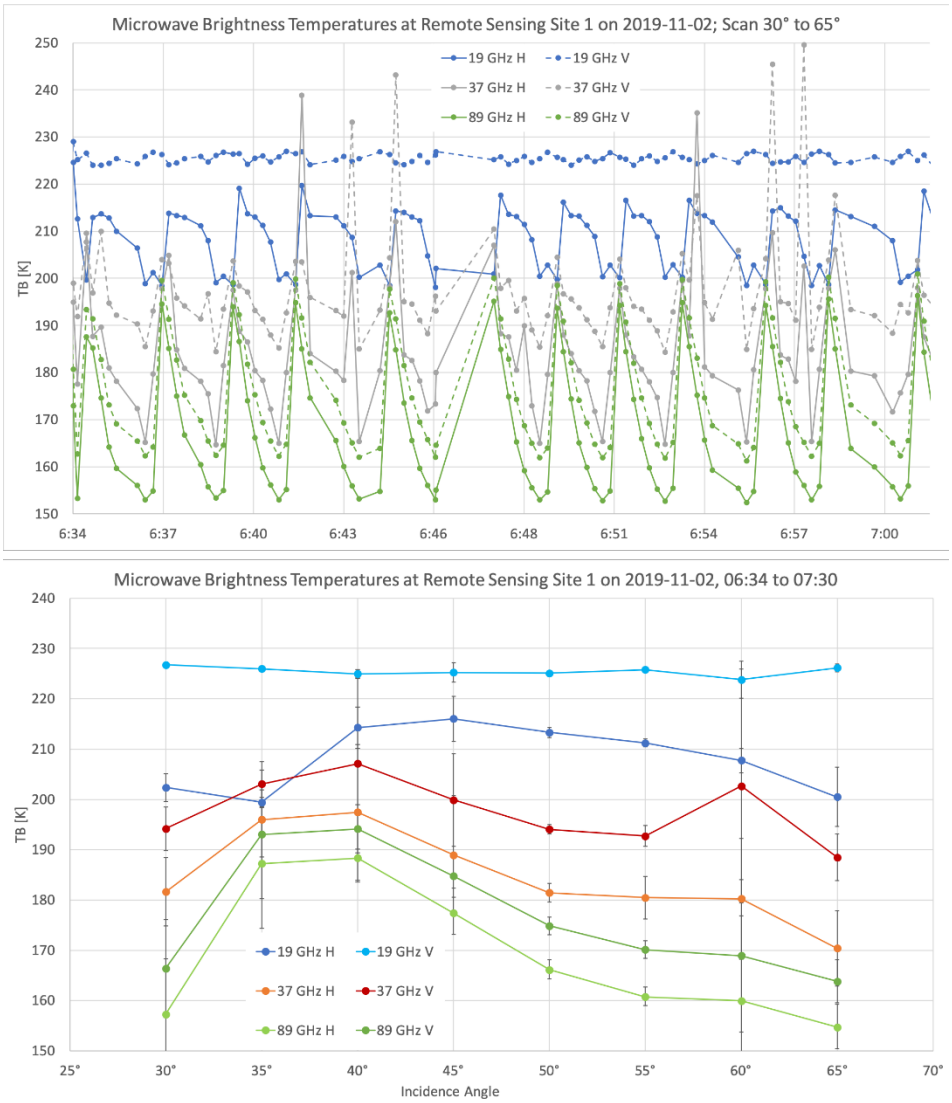

Fig. 4.10.19: Exemplary, uncalibrated microwave brightness temperatures (TB) from the 19-37-89-GHz radiometer measured during about one hour on 2 November 2019 at RS1 site. Top: time series during several scan cycles from 30° to 65° incidence angle. Bottom: TB vs. incidence angle including standard deviations (error bars) for that about one-hour long scan.

Figure 4.10.19 shows as an example the uncalibrated microwave brightness temperatures (Tb) measured by the 19-37-89-GHz radiometer on 2 November 2019 during an about one-

hour period from 06:34 to 07:30 UTC. During that time period the radiometer was scanning in elevation from 30° to 65° incidence angle. These scan cycles clearly can be seen in the time series in the upper plot. The lower plot shows the Tbs versus the incidence angle. A Tb change with incidence angle can be observed, however, not necessarily as expected with an increase of Tb. While Leg 1 thought this likely is due to missing calibration, at 30° the instrument sees the sled and thus is not a pure snow/ice signature. Also, there were problems with RF interference. Once this was fixed for Leg 2 we started to evaluate the Tbs at 50° incidence angle to match that seen by the SSMI sensor and ran various sea ice algorithms on this data. Results are shown in **Figure 4.10.20**. There is quite a bit of variability in the sea ice concentration between algorithms, with NASA Team generally giving values over 100%, though in the algorithm these are capped at 100%. On the other hand the Bristol algorithm generally gave ice concentrations slightly below 100% despite the radiometer looking at 100% sea ice cover.

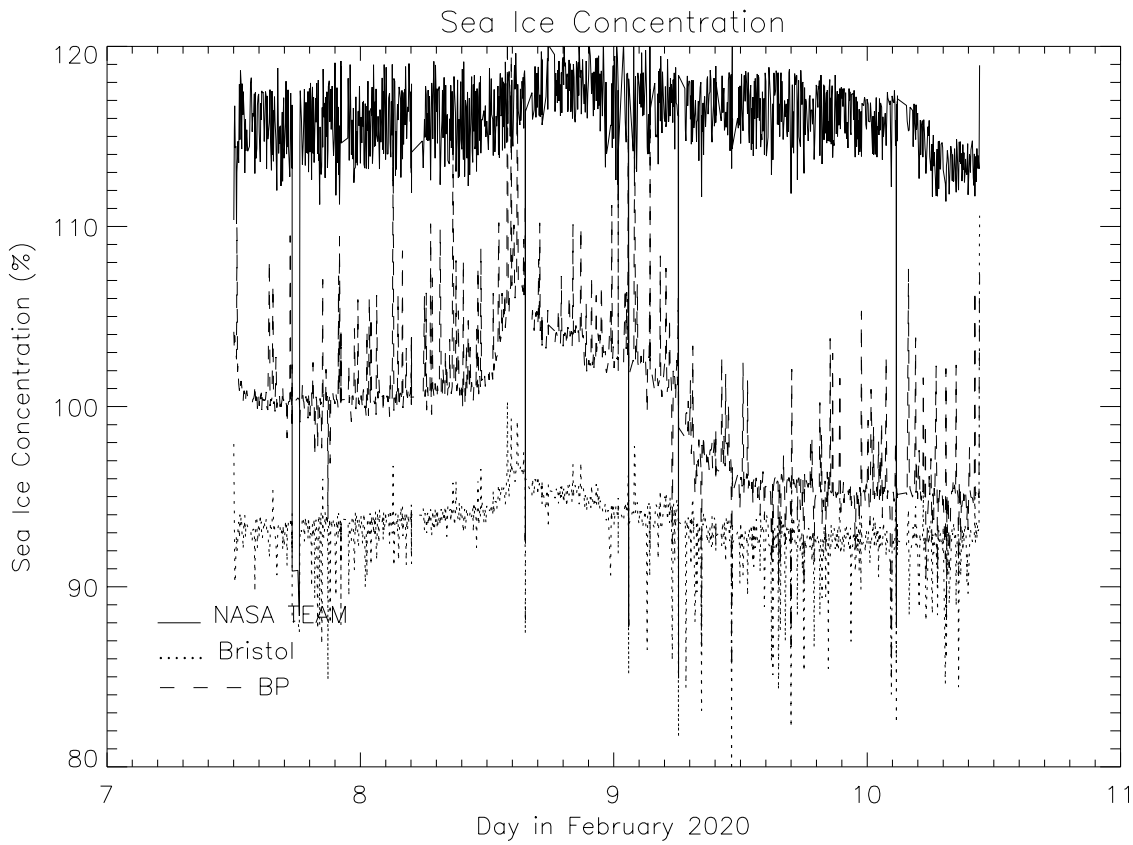

Fig. 4.10.20: Sea ice concentration from February 7 to 10 for three different algorithms using the brightness temperature from the SSMI-like radiometer.

UWBRAD

The UWBRAD processes raw data, and generates Level1 products every hour for preliminary observations. The measured power from the entire spectrum for one hour of operation is illustrated in **Figure 4.10.21**. All four channel powers drop significantly every 10 minutes due to the sky calibrations. Some portions of the spectrogram are polluted with internal or external RFI sources (the spots with extreme power levels, especially at channel 540 MHz). These will be discarded during calibration and post-processing in order to derive the true brightness temperatures of the monitored scene.

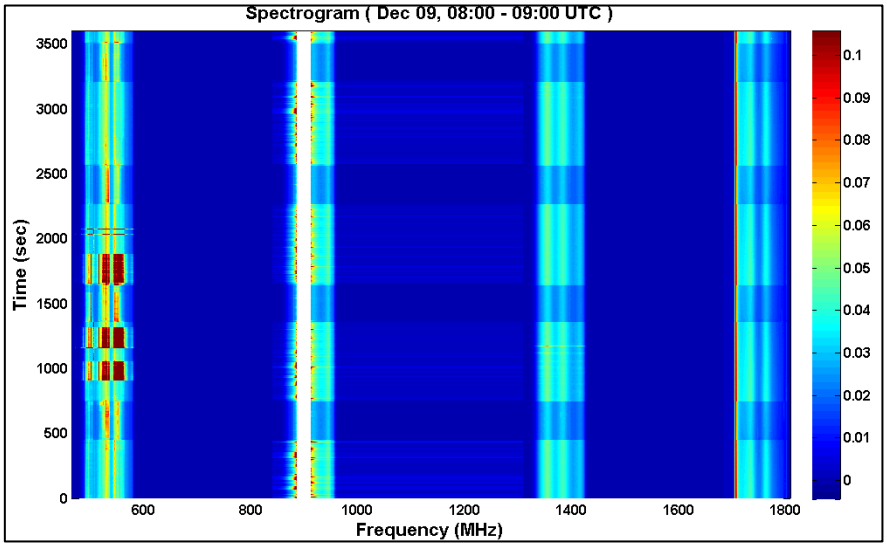

Fig. 4.10.21: Entire power spectrum for the four UWBRAD channels at 540, 900, 1380 and 1740 MHz measured during one hour (y-axis). For this uncalibrated data the power has an arbitrary unit.

Infrared camera

The infrared thermography system measures the surface temperature at the remote sensing site, which is influenced by the incoming longwave radiation, atmosphere and ocean temperatures, and snow and ice thickness. Figure 4.10.22 shows to example images from the IR camera a snowpit and a lead during the new established transect mode.

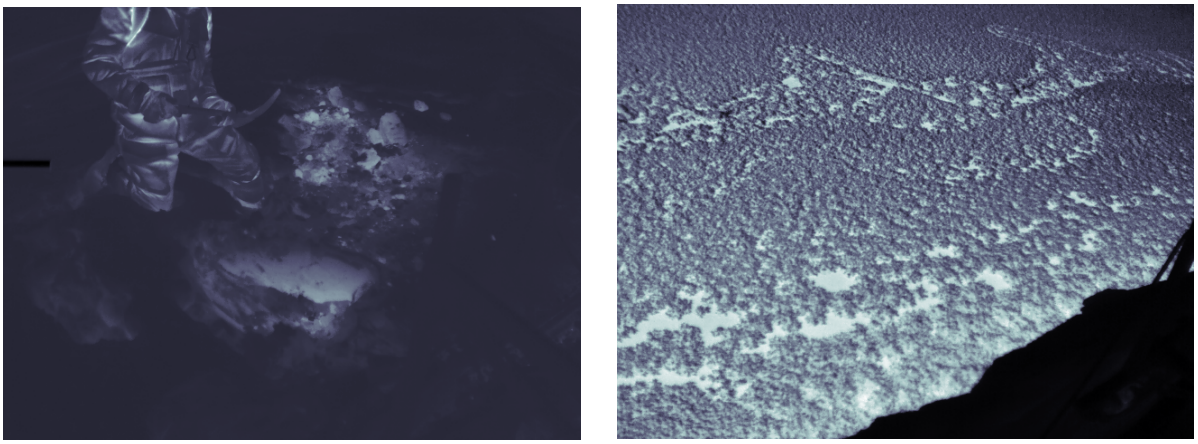

Fig. 4.10.22: Relative temperature difference images, brighter is warmer. Left: experiment with a snowpit to observe temperature gradient within the snow column. Expected temperature gradient is visible, cold at the top, warmer at the bottom. Right: frost flowers on a lead from observations during a lead transect from 2020-01-23

4.10.4 Data management

All data are handled, documented, archived and published following the MOSAiC data policy (see APPENDIX). All final data of all on-ice and onboard remote sensing instruments will be stored at the MOSAiC Central Storage (MCS) and at PANGAEA (World Data Center PANGAEA Data Publisher for Earth & Environmental Science (www.pangaea.de)) after post-processing and quality checks. Storage and release of data follow the MOSAiC data policy.

All data are handled, documented, archived and published following the MOSAiC data policy.